# Energy Efficient Press and Sinter of Titanium Powder for Low-Cost Components in Vehicle Applications

# Final Scientific Report

Department of Energy NETL – DE-FC26-08NT01913

June 29th, 2011

Dr. Thomas M. Zwitter – Webster-Hoff Corp (Project Director)

Prof. Philip Nash – Illinois Institute of Technology

Xiaoyan Xu – Illinois Institute of Technology

Chadwick Johnson – Oshkosh Corporation

DISCLAIMER

**INDEX**

## I. – Executive Summary

This is the final technical report for the Department of Energy NETL project NT01931 "Energy Efficient Press and Sinter of Titanium Powder for Low-Cost Components in Vehicle Applications.

Project Objective: Titanium has been identified as one of the key materials with the required strength that can reduce the weight of automotive components and thereby reduce fuel consumption. Working with newly developed sources of titanium powder, Webster-Hoff will develop the processing technology to manufacture low cost vehicle components using the single press/single sinter techniques developed for iron based powder metallurgy today. Working with an automotive or truck manufacturer, Webster-Hoff will demonstrate the feasibility of manufacturing a press and sinter titanium component for a vehicle application. The project objective is two-fold, to develop the technology for manufacturing press and sinter titanium components, and to demonstrate the feasibility of producing a titanium component for a vehicle application.

The lowest cost method for converting metal powder into a net shape part is the Powder Metallurgy Press and Sinter Process. The method involves compaction of the metal powder in a tool (usually a die and punches, upper and lower) at a high pressure (up to 60 TSI or 827 MPa) to form a green compact with the net shape of the final component. The powder in the green compact is held together by the compression bonds between the powder particles. The sinter process then converts the green compact to a metallurgically bonded net shape part through the process of solid state diffusion.

The goal of this project is to expand the understanding and application of press and sinter technology to Titanium Powder applications, developing techniques to manufacture net shape Titanium components via the press and sinter process. In addition, working with a vehicle manufacturer, demonstrate the feasibility of producing a titanium component for a vehicle. This is not a research program, but rather a project to develop a process for press and sinter of net shape Titanium components. All of these project objectives have been successfully completed.

The authors wish to acknowledge the following individuals and their respective companies for their contributions to this project:

1) Adrienne Riggi and Jeff Kooser - Department of Energy – NETL – for their help, support, and guidance on this project
2) Jack Webster – Webster-Hoff Corporation for initiating this project.
3) Hon. Peter Roskam – Member of Congress – for believing in the project and supporting our efforts
4) Adam Benish (in Memoriam) – Illinois Institute of Technology and International Titanium Powders for his pioneering work.
5) Dennis Hammond – APEX Industrial Technologies for his contribution to lubrication systems
6) Yingjie Yan and Kerem Araci – Illinois Institute of Technology for their dedication to the project
7) Kamal Akhtar and Brian Fuller – International Titanium Powder for their support
8) Mike Carollo and Liaquat Babul – Webster-Hoff Corporation for their support
9) Matthew Schmink – Global Titanium for his support
10) Colin McCracken – Reading Alloys for his support

The authors wish to acknowledge many others from the various conferences and technical discussions that have helped and encouraged us.

Papers published as a result of this project are:

1) "Energy Efficient Press and Sinter of Titanium Powder for Low-Cost Components in Vehicle Applications" – Dr. Thomas M. Zwitter Webster-Hoff Corp., Prof. Philip Nash, IIT, and Xioyan Xu, IIT. – MPIF PMTech Conference, June 2009.
2) "Cost Effective Press and Sinter of Titanium and Ti6Al4V [powder for Low-Cost Components in Vehicle Applications" – Dr. Thomas M. Zwitter Webster-Hoff Corp., Prof. Philip Nash, IIT, and Xioyan Xu, IIT. – MPIF PMTech Conference, June 2010.
3) "Densification and Micro-structural Behavior on the Sintering of Low Cost Ti and Ti6Al4V Powder Metallurgy Components. – Dr. Thomas M. Zwitter Webster-Hoff Corp., Prof. Philip Nash, IIT, and Xioyan Xu, IIT. – MPIF PMTech Conference, May 2011.

## II. Titanium Powders and their Properties

There are a wide variety of Titanium Powders available today. Because the nature of our project is low cost vehicle components, we focused on the lower cost Titanium Powder production methods that yield powder amenable to the press and sinter process. So the primary drivers in our powder selection process were cost and powder morphology.

For the cost target, we eliminated all powders that were higher than $15/lb. This cost target eliminated Gas Atomized powders (GA powders), plasma rotating electrode powders (PREP powders), and plasma atomized powders (PA powders). We were left with the commercially available powders produced from the Hunter-Kroll reduction processes (sponge fines); the powders produced by the Hydride De-Hydride process from wrought or sponge fines, and the powders manufactured by the Armstrong process.

We will analyze two basic Titanium Chemistries, commercially pure Titanium (TiCP) and the Titanium-Aluminum-Vanadium alloy (Ti64 – 90%Titanium, 6%Aluminum, and 4%Vanadium). The Ti64 chemistries are derived in 2 methods, one from pre-alloyed powder, and the other from blended elemental and master alloy powders.

As we proceed through our analysis and the development of the press and sinter process, we have developed a mnemonic system to identify the source and nature of powders for our use. The powder definition we will use is **AAAA-BBBB-C** where the first 4 alpha-numeric define the powder chemistry, the second 4 alpha-numeric define the manufacturing process, and the last alpha-numeric defines the manufacturer. The details of these code definitions are shown in the glossary.

The measurable key characteristics of the powders that will affect the press and sinter properties are:

A. Morphology
B. Chemistry
C. Mesh Distribution
D. Apparent Density
E. Hall Flow Rate
F. Compressibility
G. Green Strength of the powder compact

The results of our tests are shown in sections that follow.

A. Powder Morphology

All of the measurable key powder characteristics except the powder chemistry are derivatives or related to the powder morphology (structure). Generally speaking, the powder forms are as follows:

1) Spherical – Gas Atomized, Plasma Atomized and PREP
2) Sponge – Sponge fines and Armstrong Powders
3) Angular – Hydride De-Hydride Powders

The morphologies of the powders we tested are shown below:

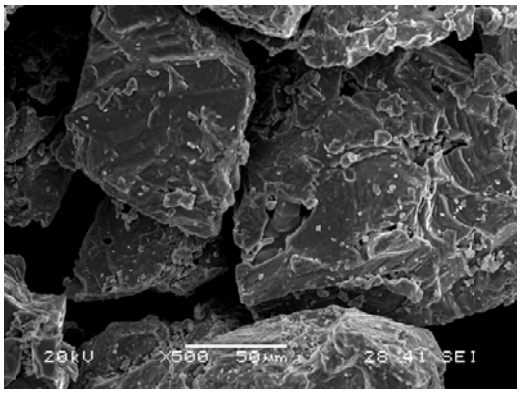


Figure II-1 - **TiCP-HdHW-T** – Hydride De-Hydride powder manufactured from Wrought by TIPRO.

Note this HdH powder is angular, almost like crushed rock, with a very controllable mesh distribution.

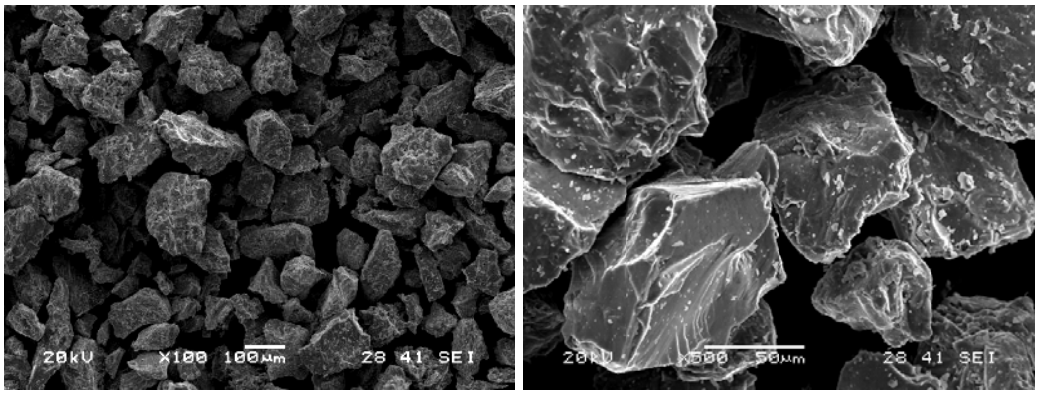


Figure II-2 - **TiCP-HdHW-R** - Hydride De-Hydride powder manufactured from Wrought by Reading Alloys.

Note this HdH powder is angular, almost like crushed rock, with a very controllable mesh distribution.

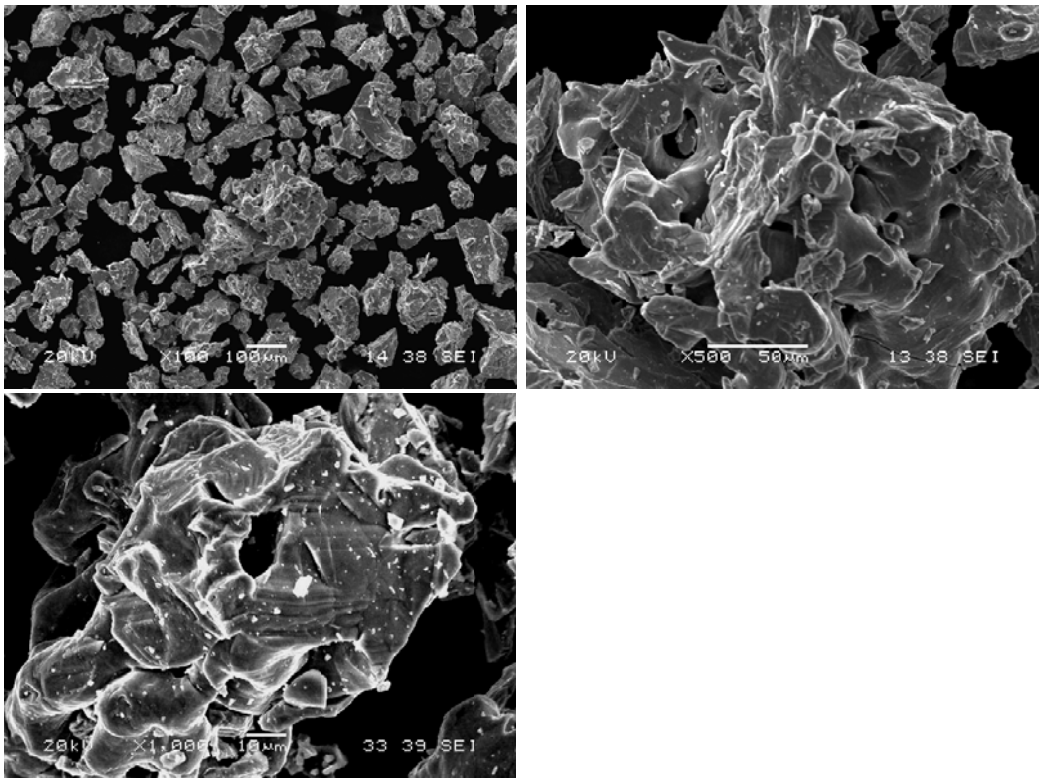


Figure II-3 - **TiCP-HdHS-G** - Hydride De-Hydride powder manufactured from Sponge Fines by Global Titanium.

Note this powder is sponge like in nature but the rough edges have been smoothed out via the hydride de-hydride process.

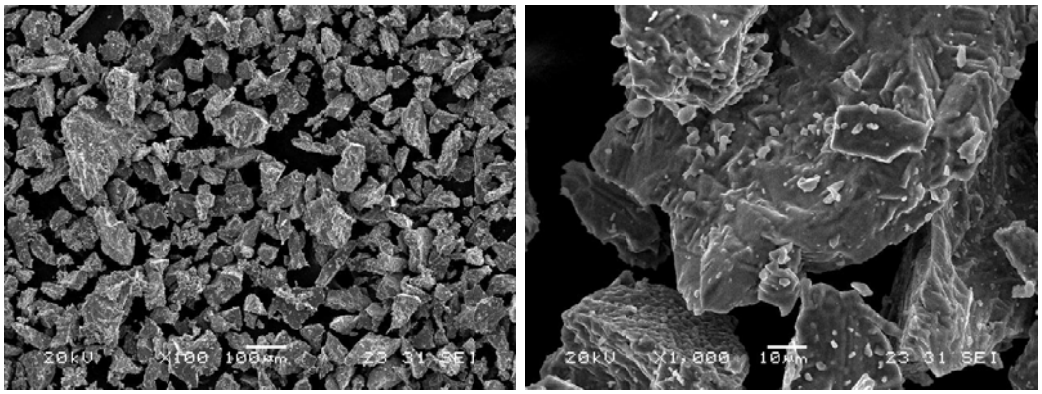


Figure II-4 - **TiCP-HdHP-G** - Hydride De-Hydride powder manufactured from wrought Scrap by Global Titanium.

Note this HdH powder is angular, almost like crushed rock, with a very controllable mesh distribution.

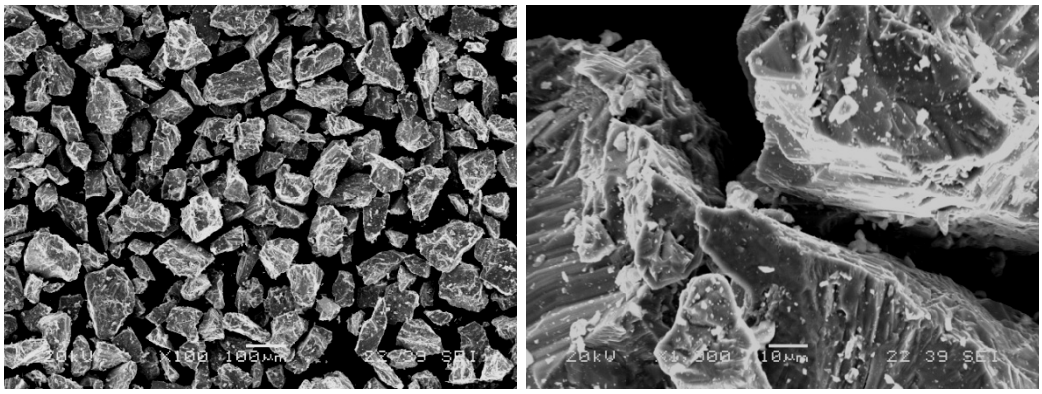

Figure II-5 - **TiCP-HydW-R** – Hydrided powder manufactured from Wrought by Reading Alloys.

Note this Hyd powder is angular, almost like crushed rock, with a very controllable mesh distribution. It retains hydrogen because it has not been de-hydrided.

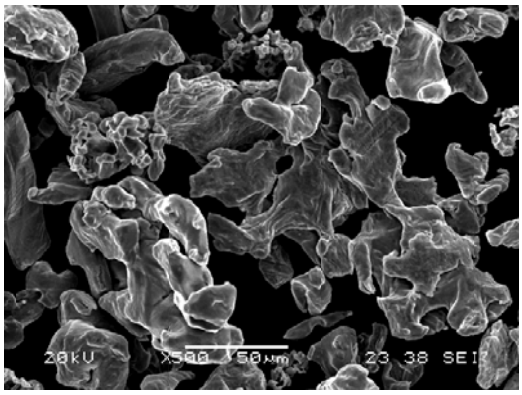

Figure II-6 - **TiCP-SoRC-D** – Sponge powder produced by sodium reduction by DuPont.

Note this powder is sponge like in nature, and has not been through the HdH process.

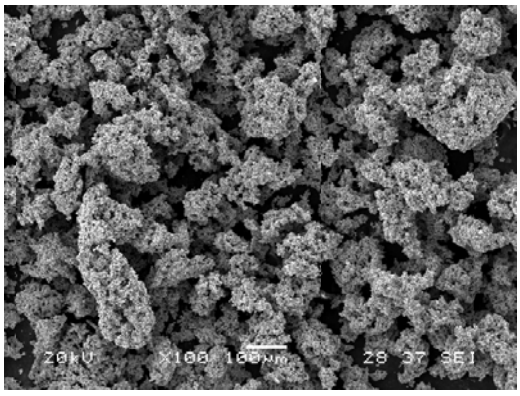

Figure II-7 - **TiCP-ArmC-I** – Sponge powder produced by the Armstrong Process from Chlorides by International Titanium Powders.
Note this powder has a dendritic-sponge-cake like structure formed from drying the sodium reduced chlorides. The powder has a very large surface to volume ratio.

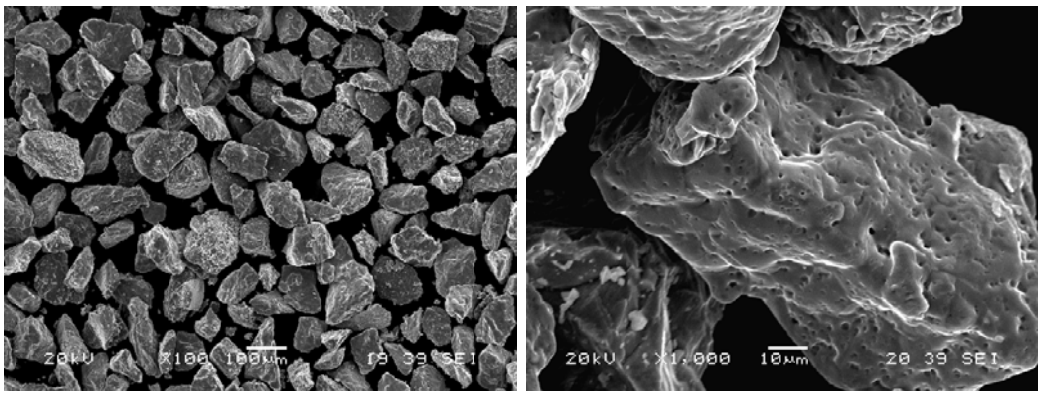


Figure II-8 - **Ti64-HdHW-R** – Hydride De-Hydride powder manufactured from Wrought Ti64 alloy by Reading Alloys.

Note this HdH powder is angular, almost like crushed rock, with a very controllable mesh distribution.

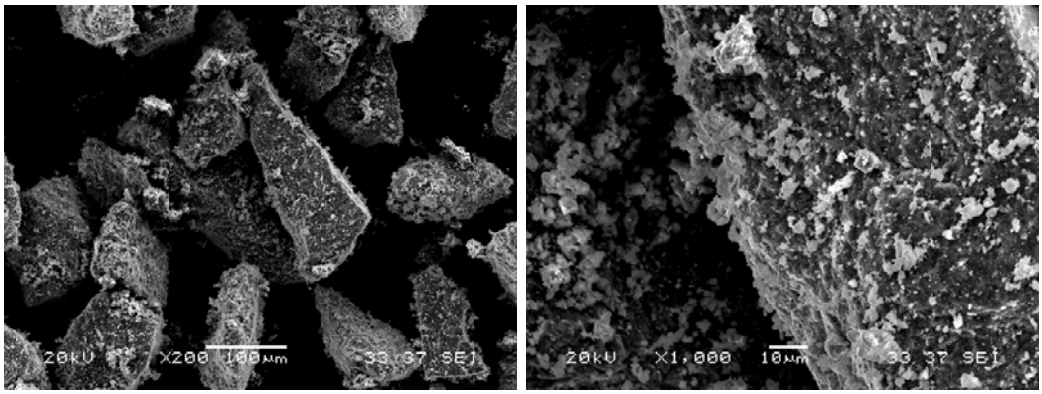


Figure II-9 - **Ti64-HydW-R** – Hydrided powder manufactured from Wrought Ti64 by Reading Alloys.

Note this Hyd powder is angular, almost like crushed rock, with a very controllable mesh distribution. It retains hydrogen because it has not been de-hydrided.

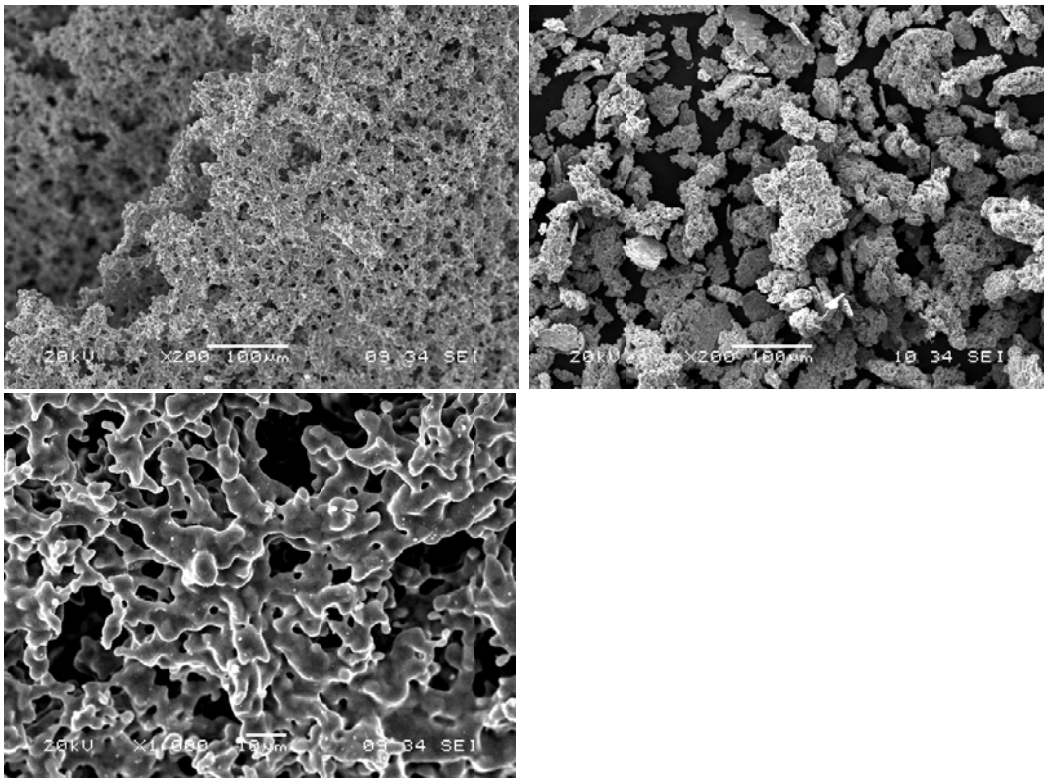

Figure II-10 - **Ti64-ArmC-I –** Sponge powder produced by the Armstrong Process from Chlorides by International Titanium Powders.

Note this powder has a dendritic-sponge-cake like structure formed from drying the sodium reduced chlorides. The powder has a very large surface to volume ratio.

B. Powder Chemistry

The chemistry of Titanium Powders is defined in terms of the impurities present in the powder. These impurities are a derivative of the manufacturing process used to produce the powder. For example the Kroll process uses magnesium reduction to produce the sponge fines, so one would expect to find magnesium as an impurity in powders produced via the Kroll process. Powders produced using the hydride de-hydride process will contain the impurities of the original source (wrought or sponge fines), with added hydrogen left over from the hydride process.

In Table II-1 Chemical composition of TiCP powders, we have included the results of our analysis of the chemical composition of the powders.

Table II-1 Chemical composition of TiCP powders in parts per million (ppm)

| | TiCP-SoRC-D | TiCP-HdHW-T | TiCP-HdHW-R | TiCP-HydW-R | TiCP-HdHP-G | TiCP-HdHS-G | TiCP-ArmC-I |
|---|---|---|---|---|---|---|---|
| Oxygen | 990 | 2200 | 2800 | 1100 | 1650 | 1340 | 2070 |
| Nitrogen | 44 | 100 | 170 | 60 | 100 | 50 | 100 |
| Carbon | 208 | 130 | 130 | 200 | 1260 | 200 | 250 |
| Total Oxygen Equivalence (O+2N+0.67C) | 1217.4 | 2487.1 | 3227.1 | 1354 | 2694.2 | 1574 | 2420 |
| Hydrogen | 61 | 140 | 90 | 35400 | 200 | 270 | 45 |
| Sulfur | 86 | | | | 50 | 50 | |
| Sodium | 960 | | | | | | 470 |
| Surface Chloride | | | | | | | |
| Total Chloride | 1100 | <100 | | | <100 | 330 | 125 |
| Magnesium | | | | | <50 | 160 | |
| Aluminum | <50 | | | | 0 | 0 | |
| Iron | 83 | 370 | 390 | 100 | 300 | 300 | 155 |
| Silicon | <50 | 150 | | | 80 | 50 | |
| Tin | <100 | | | | | | |

**TiCP-SoRC-D** is powder produced by the Hunter sodium reduction process, so we see that the powder has a very high level of Sodium (960 ppm) and Chloride (1100 ppm). The hydride de-hydride powders HdHW and HdHS powders all show slightly higher hydrogen content (90 to 270 ppm). The hydride powders HydW and HydS show very high hydrogen content (35,000 ppm) because the hydrogen is not removed via the de-hydride process. The **TiCP-ArmC-I** powder is produced by the continuous sodium reduction of Titanium chlorides, the residual sodium is moderately high (470 ppm).

Because Titanium is a very high "getter" for oxygen, carbon, and Nitrogen, these impurities are present in all Titanium powders. The term Total Oxygen Equivalency was developed (O + 2N + 0.67C) to define the total level of these impurities in Titanium [1]. These elements will tend to reside in the grain boundaries (interstitial) affecting the mechanical properties of the Titanium. A low value of Total Oxygen Equivalency is desirable. From Table I We see that **TiCP-SoRC-D** has the lowest Total Oxygen Equivalency, while **TiCP-HdHW-R** has the highest Total Oxygen Equivalency.

In Table II-2 Chemical composition of Ti64 powders and Master Alloy Powder, we have the results of our analysis of the pre-alloyed and master alloy powders.

Table I-2 Chemical composition of Ti64 powders and Master Alloy Powder

| | Ti64-HdHW-R | Ma64-AtmM-R | Ti64-HydW-R | Ti64-ArmC-I |
|---|---|---|---|---|
| Oxygen (1) | 1700 | 1100 | 3600 | 2400 |
| Nitrogen(2) | 280 | 10 | 210 | 300 |
| Carbon(.67) | 270 | 380 | 230 | 170 |
| Total Oxygen Equivalence (O+2N+0.67C) | 2441 | 1375 | 4174 | 3114 |
| Hydrogen | 90 | 60 | 47500 | 60 |
| Aluminum | 59900 | 573900 | 65800 | 57000 |
| Iron | 170 | 120 | 200 | 40 |
| Silicon | | 140 | | |
| Tin | | | | |
| Vanadium | 39200 | 421100 | 44200 | 41000 |
| Manganese | | 30 | | |
| Molybdenum | | 180 | | |
| Nickel | | 190 | | |
| Chromium | | 170 | | |
| Sodium | | | | 20 |

**Ti64-HdHW-R** and the **Ti64-HydW-R** powders were produced from wrought Ti64 material. The HydW powder shows a significantly higher hydrogen content 47,500 ppm because the powder was not de-hydrided. The **Ti64-ArmC-I** powder was produced by the continuous reduction of Titanium, Aluminum, and Vanadium chlorides, and does not show any significant sodium or chlorides. This indicates the process was well controlled, and the powder was properly cleaned. The master alloy of Aluminum and Vanadium **Ma64-AtmM-R** shows other metal impurities that are part of the production process.

The Total Oxygen Equivalency of **Ma64-AtmM-R** is the lowest at 1375 ppm, and **Ti64-HydW-R** powder has the highest oxygen equivalency at 4174 ppm.

C. Powder Mesh Distribution

The powder Mesh Distribution is one of the key characteristics that define the compaction characteristics of the powders [2]. The tooling used for uni-axial compaction of the powders must have tool clearances between the punches and the die, so that the punches can move smoothly in the die. These tool clearances are typically about .0005" or 12.7 microns. If a large portion of the powder particles are smaller than 12.5 microns, then the powder will wedge between the punch and the die jamming the tool. This can be a catastrophic failure for the tool. The typical powder specification for press and sinter applications is +325 mesh (45 microns) up to -100 mesh (150 microns) in size.

Table II-3: Mesh distribution of TiCP powders

| Mesh Distribution | TiCP-SoRC-D (%) | TiCP-HdHW-T (%) | TiCP-HdHW-R (%) | TiCP-ArmC-I (%) after ball milled for 10 min |
|---|---|---|---|---|
| +100 | 32.70 | 1.00 | | 62 |
| -100 + 200 | 37.30 | 65.00 | 97.50 | 15 |
| -200 + 325 | 15.60 | 32.00 | | 18 |
| +325 | 14.40 | 2.00 | 2.30 | 5 |

We see that the hydride de-hydride HdHW and HdHS powders have a mesh distribution that lies primarily in the range of -100/+325. The **TiCP-SoRC-D** and the **TiCP-ArmC-I** powders have a large fraction above +100 in size. This is due to the morphology of these powders (sponge like in nature), which makes it difficult to reduce the size of the particles to the preferred range (-100/+325).

Table II-4 Mesh Distribution of Ti64 Powders

| Mesh Distribution | Ti64-HdHW-R (%) | Ti64-ArmC-I (%) after ball milled for 10 min |
|---|---|---|
| +100 | | 68 |
| -100 + 200 | 83 | 19 |
| -200 + 325 | 17 | 7 |
| +325 | | 5 |

We see that the hydride de-hydride pre-alloyed HdHW Ti64 powders have a mesh distribution that lies primarily in the range of -100/+325. The **TiCP-ArmC-I** powders have a large fraction above +100 in size. This is due to the morphology of these powders (sponge like in nature), which makes it difficult to reduce the size of the particles to the preferred range (-100/+325).

D. Powder Apparent Density

The powder Apparent Density is one of the key characteristics that define the compaction characteristics of the powders [2]. For the compaction process, it is desirable to achieve the highest green density possible. The apparent density of the powder defines the starting density prior to compaction, thereby defining the necessary volume of powder required to compact to the final green density. In the Powder Metallurgy world the apparent density defines the compaction ratio necessary to compact the part to the desired green density.

If the final green density of the TiCP compact is 3.8 g/cc (85% dense), and the apparent density is 1.5 g/cc, then the compaction ratio is 2.53. This ratio 2.53:1 defines the fill height (depth of powder in the die) to achieve the desired green density (3.8 g/cc). If the part is to be 1” tall in the green state, then you will need 2.53” of powder fill in the die.

Table II-5 Apparent density of TiCP powders with and without internal lubrication (EN-I)

| Apparent Density (g/cc) | TiCP-SoRC-D | TiCP-HdHW-T | TiCP-HdHW-R | TiCP-HdHS-G | TiCP-ArmC-I |
|---|---|---|---|---|---|
| CP Ti powder (no lube) | 1.34 | 1.58 | 1.56 | 1.62 | 0.68 |
| CP Ti powder +0.4% EN-I lube | 1.17 | 1.51 | 1.42 | 1.58 | 0.65 |

The apparent density of the hydride de-hydride powders HdHW and HdHS are in the range of 1.56 g/cc to 1.62 g/cc. This apparent density is well within the range of acceptability for conventional press and sinter powder metallurgy. The **TiCP-SoRC-D** powder has an apparent density of 1.34 g/cc, which is lower than the HdH powders, but still acceptable. The **TiCP-ArmC-I** powder has an apparent density of .68 g/cc, which will require a fill ratio of 5.6:1, which will require special pressing tooling and techniques to form taller parts.

Table II-6: Apparent density of Ti64 Powders

| Apparent Density (g/cc) | Ti64-ArmC-I | Ti64-HdHW-R |
|---|---|---|
| Ti6Al4V powder (no lube) | 0.67 | 1.93 |
| Ti6Al4V +0.4% EN-I lube | 0.60 | 1.66 |

The apparent density of the **Ti64-HdHW-R** powder (1.93 g/cc) is significantly higher than the **Ti64-ArmC-I** powder. To achieve a green density of 3.8 g/cc, the fill ratio of the HdH powder would be 1.96:1, whereas the fill ratio of the Armstrong powder would be 5.7:1. This is a very significant difference and we will discuss this later in our report.

E. Powder Hall Flow Rate

The powder Hall Flow Rate is one of the powder key characteristics that define the die filling process. The Hall Flow Rate is defined as the time it takes in seconds to empty a volume of powder through a fixed diameter nozzle [2]. The lower the Hall Flow Rate, the faster and more evenly the powder will fill the die from a feeder shoe.

Table II-7 Hall Flow Rate of TiCP powders

| Hall Flow (sec./50g) | TiCP-SoRC-D | TiCP-HdHW-T | TiCP-HdHW-R | TiCP-HdHS-G | TiCP-ArmC-I |
|---|---|---|---|---|---|
| CP Ti powder (no lube) | 40 | 33 | 30 | 34 | Non-flow |
| CP Ti powder +0.4% EN-I lube | 49 | 39 | 37 | 41 | Non-flow |

The Hall Flow Rates of the hydride de-hydride powders HdHW and HdHS are in the range of 30 to 34 seconds. This Hall Flow Rate is well within the range of acceptability for conventional press and sinter powder metallurgy. The TiCP-SoRC-D powder has a Hall flow Rate of 40 seconds, which is higher than the HdH powders, but still acceptable. The TiCP-ArmC-I powder has a Hall Flow Rate defined as Non-Flow. This means that the powder will not flow through the standard nozzle, and a larger diameter orifice is used.

Table II-8: Hall Flow Rate of Ti64 powders

| Hall Flow (sec./50g) | 90% TiCP-HdHW-T + 10% Ma64-AtmM-R | 90% TiCP-HdHW-R + 10% Ma64-AtmM-R | Ti64-ArmC-I | Ti64-HdHW-R |
|---|---|---|---|---|
| CP Ti powder (no lube) | 30 | 24 | Non-flow | 23 |
| CP Ti powder+ 0.4% EN-I lube | 34 | 33 | Non-flow | 36 |

The Hall Flow Rates for the blended HdH powders are in the range of 24 to 34 seconds, very acceptable for traditional PM die filling. The **Ti64-ArmC-I** powder has a rating of Non-Flow, which is not good for die filling.

F. Powder Compressibility

The powder Compressibility defines the relationship between the green density (g/cc) of the powder compact and the pressure (tons per sq. in. (TSI) or MPa) required for that green density. The compressibility of a powder is determined by the powder morphology and the particle hardness [2]. The Compressibility curves are prepared using die wall lubrication to reduce the effect of die wall friction on the compressibility curves.

Figure II-11: Compressibility of TiCP powders.

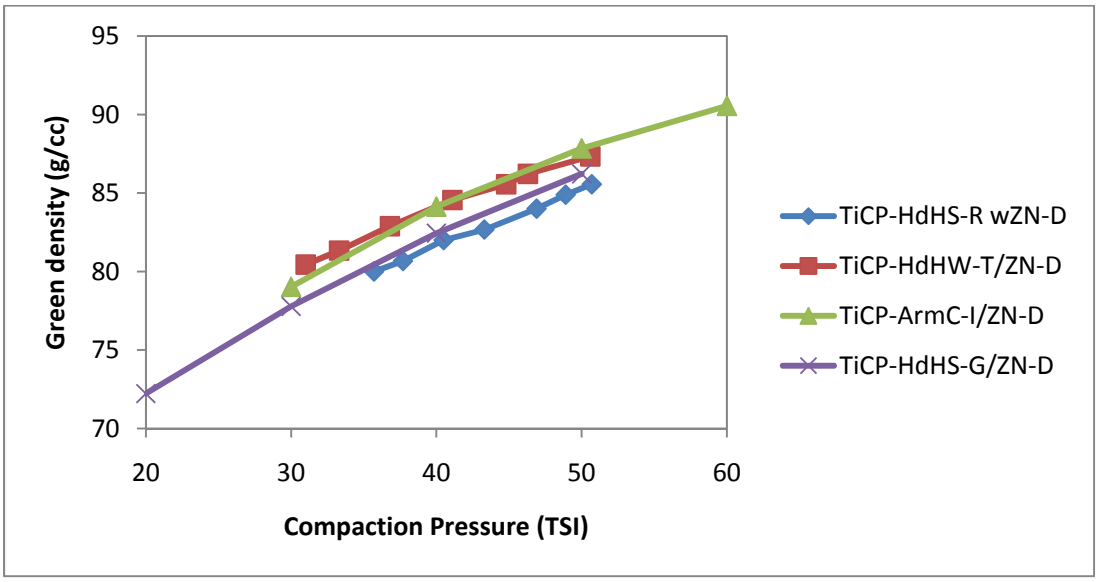


The compressibility curves for the TiCP powders show that the powders have very similar compressibility curves. **TiCP-ArmC-I** and **TiCP HdHW-T** show the highest compressibility whereas **TiCP-HdHS-R** and **TiCP-HdHS-G** have slightly lower compressibility.

Figure II-12: Compressibility of Ti64 powders.

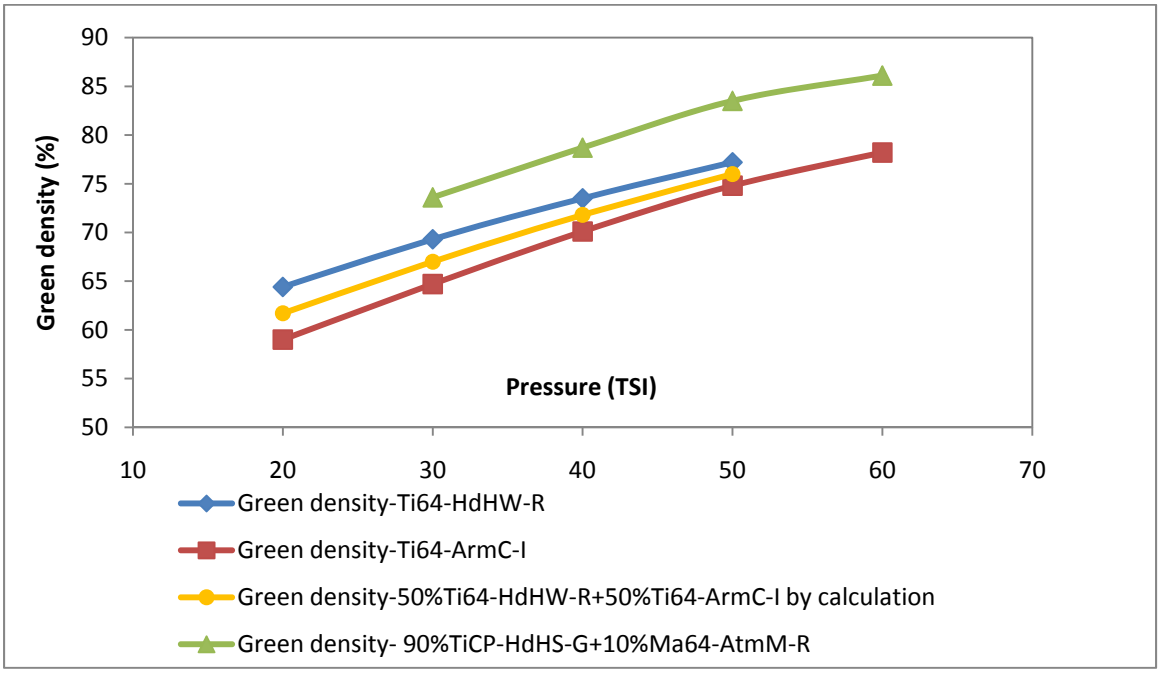


Comparing the compressibility of **Ti64-HdHW-R** and **Ti64-ArmC-I**, we see that **Ti64-HdHW-R** has a slightly higher compressibility (will achieve a higher green density at the same compaction pressure).

G. Powder Green Strength

The powder green strength is defined as the Transverse Rupture Strength of a green compact (TRS bar shape) at a specific compaction pressure (TSI or MPa). Green Strength is important for Press and Sinter processing because it is the determining factor in the type of handling that is required for further processing the parts prior to sintering.

Figure II-13: Green Strength of TiCP powders.

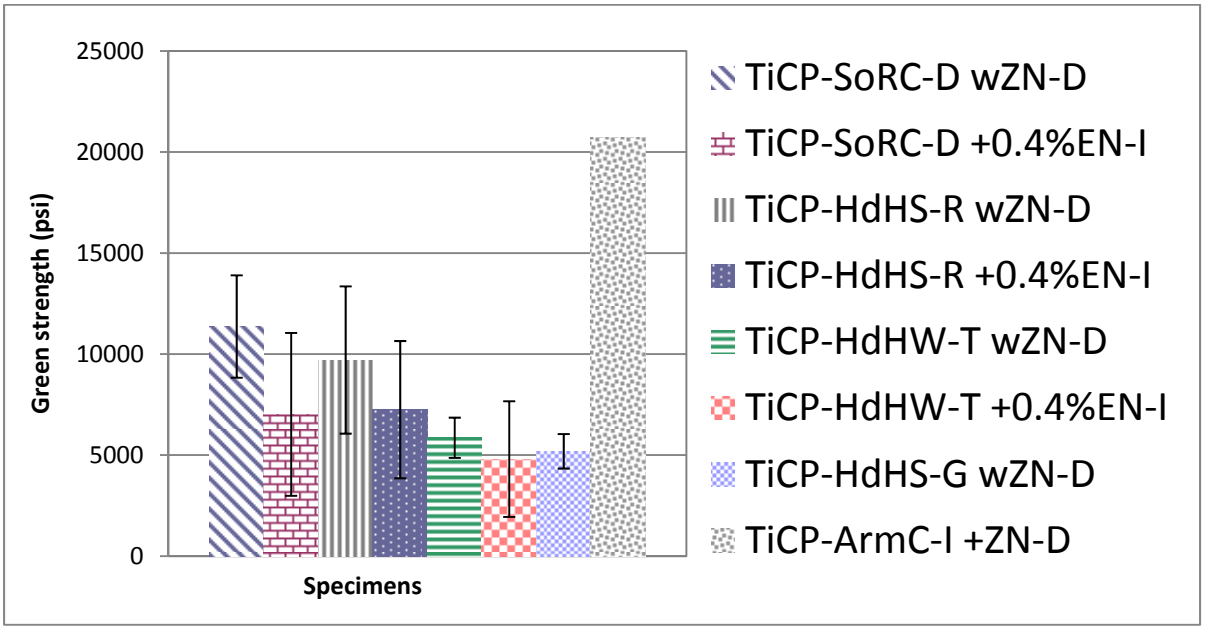


Note that the Armstrong Sponge Powder has the highest green strength (21,000 psi), followed by the DuPont Sponge powder with 11,000 psi. The HdH powders have the lowest green strength due to their rocky powder morphology.

Figure II-14: Green Strength of **Ti64-ArmC-I** powders.

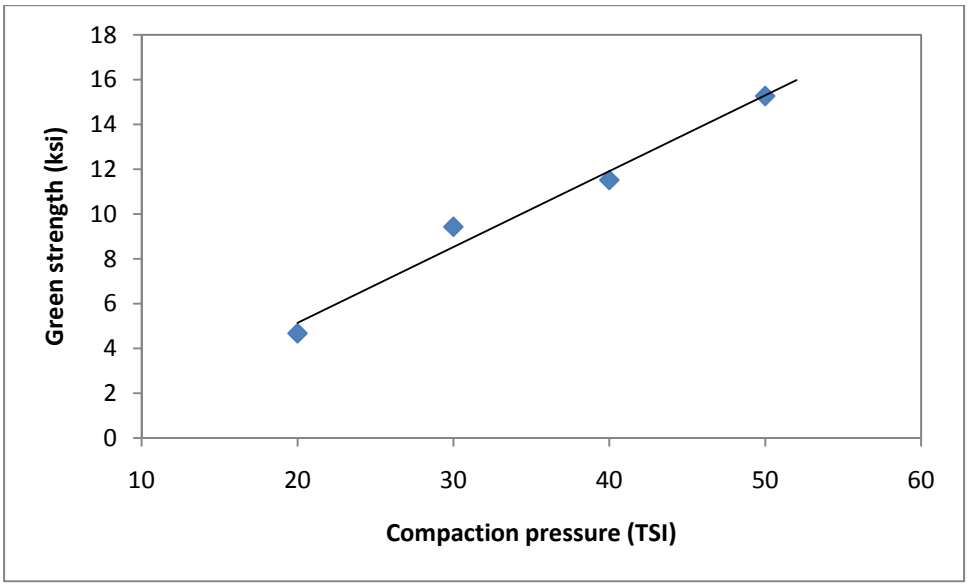


Note that the green strength of the **Ti64-ArmC-I** powder is a linear function of compaction pressure.

## III. Lubrication Systems

For traditional Powder Metal compaction processes, lubrication systems have always been used to provide the necessary lubrication to be able to eject the compact from the die, and to assist with the re-alignment of powder particles during the compaction process. Without some form of lubrication, the compact will weld itself to the die and the tool will be destroyed very quickly. There are 2 basic kinds of lubrication systems to accomplish this, die wall lubrication and internal lubrication.

1) Die wall lubrication – in the case of die wall lubrication systems, the die cavity is coated with a lubricant prior to filling the die cavity with powder. The typical forms of die wall lubrication used in the compaction process are Zinc Stearate, Lithium Stearate, Electrostatic Hydrocarbon Powders, high density polyethylene, and moly disulfide. These techniques can work quite well to provide the necessary lubrication for ejection of the green compact from the die, but they do nothing to enhance the re-arrangement of the powder particles within the compact, particularly for high hardness powder particles (pre-alloyed powders). Die wall lubrication systems can be automated by using an electrically charged powder which is sprayed into the die cavity just before die filling, which allows for a fast cycle for compaction of green parts.
2) Internal Lubrication – in this case a lubricant (usually a powder) is blended with the metal powder prior to compaction. After compaction, the lubricant is removed from the green compact by boiling off the lubricant in a de-lube process. The amount of lubricant (%) added is usually a compromise between sufficient lubrication for ejection and minimizing the amount of lubricant that must be removed prior to sintering. Internal lubricants also increase the apparent density of the powder reducing is flow and fill characteristics. Internal lubricants also aid the ejection from the die, as the lubricant will flow to the die walls during the compaction process. Internal lubrication can pose a problem for Titanium, because the lubricants are primarily hydro-carbons that can lead to increasing the impurities in the Titanium compact. Internal lubricants can also be designed to be hydrostatic in nature, where the lubricant powder converts to a liquid under heat or shear stress, allowing the powder particles to flow in a fluid slurry. The hydrostatic compaction process is designed to minimize density gradients due to the uniaxial compaction process.

We have tested a variety of die wall and internal lubrication systems, and have chosen to use Zinc Stearate Spray for our Die wall lubrication experiments and a proprietary lubricant powder for our internal lubrication experiments. For the purposes of tracking these, we have used the abbreviation of ZN-D for zinc stearate die wall lube, and EN-I for the internal lube system.

## IV. Blended Titanium Powders and their properties

Blended powders are those powders which are not a single powder type. TiCP and pre-alloyed Ti64 powders are a single type. When we add another powder to the single powder and blend the two or more powders together this becomes a blended powder (sometimes referred to as an admixed powder). The reasons for blending powders prior to compaction can vary, for example to add an internal lubricant, or to blend 2 types of powders to improve a characteristic such as apparent density. Another general category for blending powders is to create an alloy by blending elemental powders or master alloys with the base powder, in this case TiCP.

Table IV-1: Oxygen Equivalency for Blended Ti64 Powders.

| Blends of different powders | 50% Ti64-ArmC-I +45% TiCP-HdHS-G + 5% Ma64-AtmM-R | 90% TiCP-HdHS-G +10% Ma64-AtmM-R | 50% Ti64-ArmC-I + 50% Ti64-HdHW-R) |
|---|---|---|---|
| Oxygen Equivalency (ppm) | 2334 | 1554 | 2778 |

The Table IV-1 shows the comparison of the oxygen equivalency for blended powders. In the table IV-1 **90%TiCP-HdHS-G + 10%Ma64-HdHW-R** powder is a blended powder to form Ti64 from the commercially pure Titanium and a master alloy powder consisting of 60%Aluminum and 40%Vanadium. The powder **50%Ti64-ArmC-I + 50% Ti64-HdHW-R** is a blend of 2 pre-alloyed powders with very different apparent densities. The powder **50%Ti64-ArmC-I + 45%TiCP-HdHS-G + 5%Ma64-AtmM-R** is a blend of a pre-alloyed powder with a master alloy blended powder. Note that the blend **90%TiCP-HdHS-G + 10%Ma64-AtmM-R** has the lowest oxygen equivalency which is an advantage for the mechanical properties of the sintered compact.

Table IV-2: Apparent Density of Blended and Single Ti64 Powders with and without internal lube (EN-I)

| Mixtures of different powder | Lubrication type | Apparent density (g/cc) |
|---|---|---|
| 100% Ti64-ArmC-I | ZN-D | 0.67 |
| | 0.4% EN-I | 0.60 |
| 50% Ti64-ArmC-I +45% TiCP-HdHS-G + 5% Ma64-AtmM-R | ZN-D | 1.01 |
| | 0.4% EN-I | 1.00 |
| 90% TiCP-HdHS-G +10%Ma64-AtmM-R | ZN-D | 1.61 |
| | 0.4% EN-I | 1.58 |
| 50% Ti64-ArmC-I + 50%Ti64-HdHW-R | ZN-D | 1.16 |
| | 0.4% EN-I | 1.00 |
| 100%Ti64-HdHW-R | ZN-D | 1.93 |
| | 0.4% EN-I | 1.66 |

The table IV-2 and Figure IV-1 show the comparison of the apparent density for blended powders versus single pre-alloyed powders with and without internal lubrication. The powders labeled 100% are single powders, and the blended powders show the percentages of each type of powder. Having a high apparent density is a significant advantage for the compaction process.

Figure IV-1: Apparent Density of Blended and single Ti64 powders

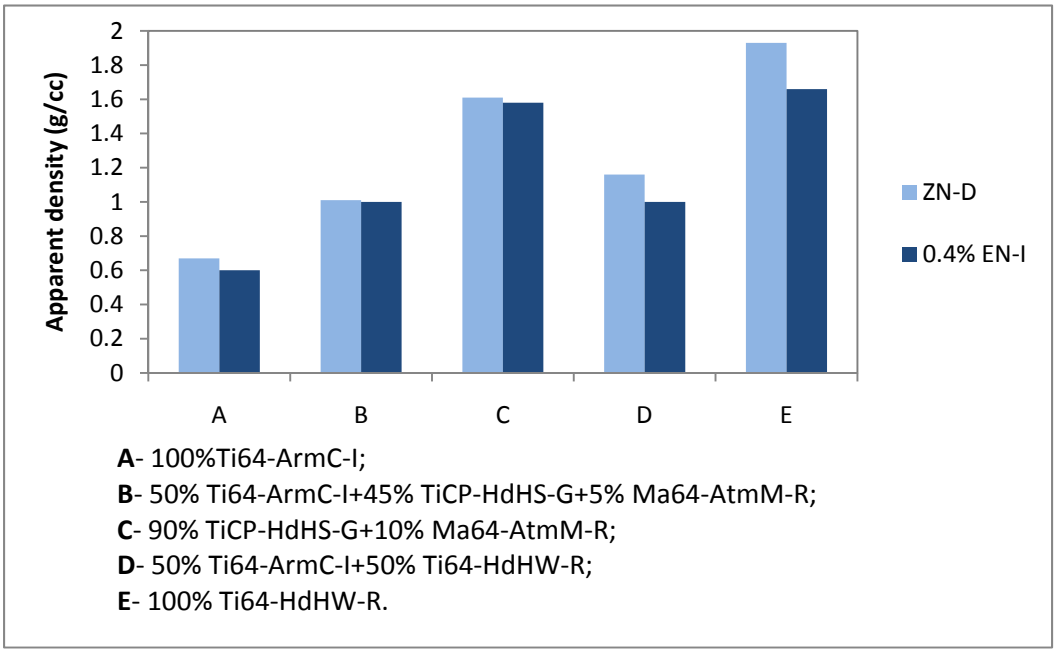


Figure IV-2: Apparent density of the **Ti64-ArmC-I** powder blended with the **Ti64-HdHW-R** powder

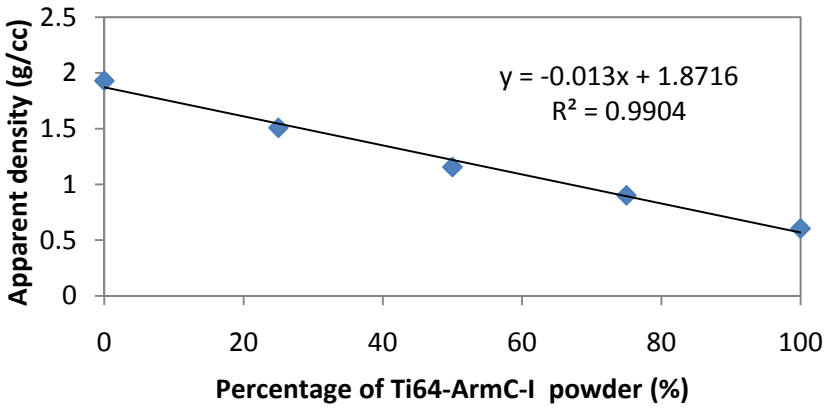


Figure IV-2 shows that the apparent density of the blended **Ti64-ArmC-I** powder with the **Ti64-HdHW-R** powder is a linear relationship. Therefore one could blend these 2 powders in a fraction appropriate to the desired apparent density. It is important to increase the apparent density for the compaction process, yet still retain the better sintering properties of **Ti64-ArmC-I** as we shall see later in this report.

Table IV-3: Green Density of Blended and Single Ti64 powders with and without internal Lubrication

| Blends of different powder | Lubrication type | Green density (%) |
|---|---|---|
| 100% Ti64-ArmC-I | ZN-D | 74.8% |
| | 0.4% EN-I | 75.8% |
| 50% Ti64-ArmC-I<br>+45% TiCP-HdHS-G<br>+ 5% Ma64-AtmM-R | ZN-D | 80.1% |
| | 0.4% EN-I | 81.7% |
| 90% TiCP-HdHS-G<br>+10% Ma64-AtmM-R | ZN-D | 86.5% |
| | 0.4% EN-I | 87.6% |
| 50% Ti64-ArmC-I<br>+ 50% Ti64-HdHW-R | ZN-D | 75.3% |
| | 0.4% EN-I | 77.9% |
| 100% Ti64-HdHW-R | ZN-D | 77.4% |
| | 0.4% EN-I | 78.8% |

Figure IV-3: Green Density of Blended and Single Ti64 powders with and without internal Lubrication.

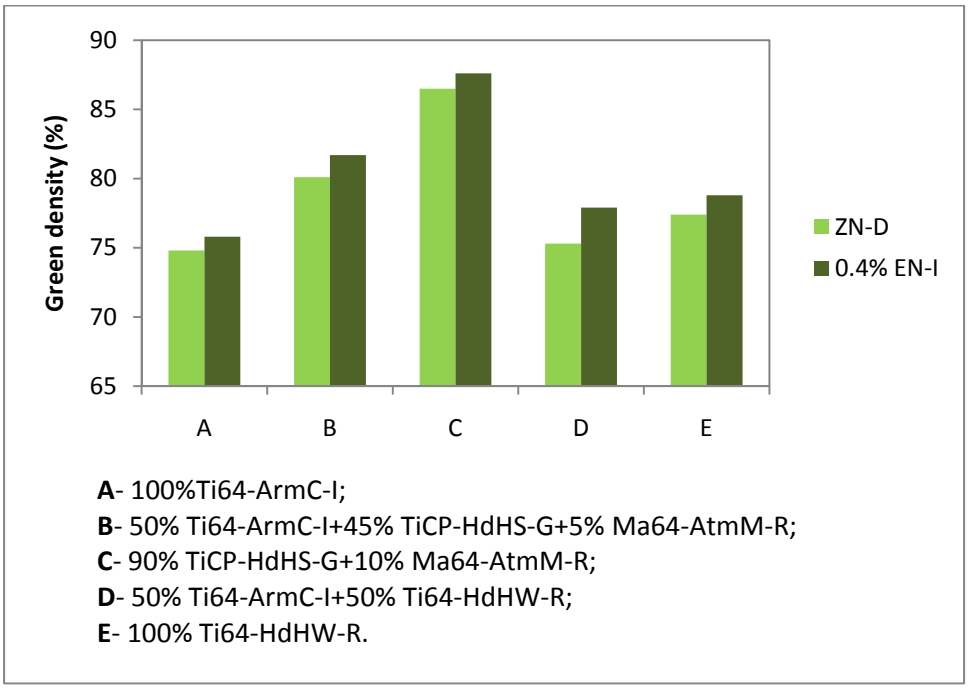

This figure IV-3 shows the increase in green density when internal lubrication is blended with the single powders. The lubrication allows for higher green density, but reduces the green strength.

In this comparison, all the powders were compacted at 50 TSI (689 MPa). We can see from the table that the highest green density is achieved by **90%TiCP-HdHS-G + 10%Ma64-AtmM-R** with 0.4%EN-I powder (87.6%). The lowest green density is achieved by **Ti64-ArmC-I** powder compacted with die wall lubrication.

## V. Compaction Process

For traditional Press and Sinter Powder Metallurgy, the compaction process is the methodology to form a green compact from the loose powder. The powder is compacted in a tool consisting of a die, with upper and lower punches. The press, which generates the compaction force may be single acting (press from one side only) or double acting (press from 2 sides or with a floating die).

The basic function of compaction is to form a green compact to a designed net shape, by pressing the powder under a very high force (up to 60 TSI, 829 MPa). The high compaction pressure will form compression bonds between the powder particles, giving the net shape green strength so that it can be handled prior to sintering. The sintering process will follow, transforming the compression bonds into metallurgical bonds forming the final net shape part.

The goal of the compaction process is to press the green compact to the highest possible green density without breaking the tool, and to eject the part from the die in one piece.

The phases of the compaction process are

1) Die filling – the tool is positioned to the fill position and the feeder shoe will fill the die cavity to the top via a shaking process over the die cavity. In the die filling process, a powder with a fast Hall Flow Rate (measured in sec.) will fill the die more quickly and evenly. For even density throughout the part, it is necessary that the powder fill over each section of the part (level) be filled to the same ratio (compaction ratio of the powder).
2) Pre-compaction – For complex tools (multi-level parts), the press motions will reposition the powder prior to applying pressure to locate each section of the powder to the final green compact shape.
3) Compaction – The compaction phase is the application of pressure between the upper and lower punches to squeeze the powder between the punches and the die, forming the compression bonds between the powder particles. The die is usually a floating die, allowing for upper and lower compaction of the part, forming a density gradient with the lowest density right in the middle on the part (top to bottom).
4) Ejection – The part is ejected from the die using the lower punches to force the green compact out of the die. To prevent lateral cracks in the part, the green part is usually held tightly between the upper and lower punches during ejection to prevent the die friction from cracking the green compact as it exits the die and springs back from its compacted shape with the release of die pressure.

The parameters that affect the compaction process are as follows:

1) Powder Characteristics
    a. Mesh Distribution – a wide mesh distribution allows for closer packing of the powder particles, forming a higher green density.
    b. Apparent Density – a powder with a higher apparent density allows for a shorter tool (die), which fills faster and more evenly than a low apparent density powder.
    c. Hall Flow Rate – a powder with a fast Hall Flow Rate will fill the die faster and more evenly than a powder with a slow Hall Flow Rate.
    d. Internal Lubrication – Internal lubrication is helpful for allowing the particles to move past each other in the pre-compaction and compaction processes, generating a higher green density. The internal lube will also allow the green compact to be ejected from the die. The green compact will not release from the die without some form of lubrication (internal or die wall).
    e. Compressibility – The powder compressibility is a determining factor on the achievable green density of the compact. The higher the compressibility, the higher the green density.
    f. Green Strength - The green strength of the powder compact determines the ability to handle the green compact prior to sintering. If the green strength is very high, certain machining operations can be completed in the green strength at significantly lower cost than machining the final sintered part. The green strength of dendritic powders is usually significantly higher than the acicular/angular powders.
2) Type of Press

a. Single or double acting (floating die) – A double acting press will generate a green compact with ½ the density gradient of a single acting press. This is important for the reduction of distortion in sintering.
b. Top Punch Hold Down – Top Punch hold down allows for the ejection of a green part without creating lateral cracks.
c. Single or Multi-level – A multilevel press allows for the compaction of more complex parts with balanced density.
d. Mechanical, hydraulic, or electric servo – Generally the method of applying force to the compact is not critical, however the control for press tolerances on height is. The Electric Servo press generates the tightest control on pressing height, followed by the hydraulic servo press, and finally the mechanical press.

3) Type of Part (single level or multi-level) – Part complexity is usually defined by the number of levels in a part. As the number of levels increase, the number and complexity of the punches increases. The control of density of a multilevel part is also more complex.
4) Tool Design – The tool design follows the type of part, with multi level tooling being the most complex and difficult to control.
5) Die Wall Lubrication – Die wall lubrication is used to minimize or eliminate the internal lubrication in the green compact. A reduction of internal lubrication increases the apparent density of the powder and increases the green density of the compact.

Summary

The design of the compaction process involves working through the complex choices regarding powder properties, part design, tool design, and press control to successfully generate the green compact at production rates (hundreds or thousands of parts per hour). Powder properties have a large influence on the design and successful operation of the compaction process. Titanium powders have very specific challenges related to their powder morphology, and the ductile nature of the powder as it compacts.

## VI. De-Lubrication Systems

For traditional Powder Metal compaction processes, internal lubrication systems have always been used to provide the necessary lubrication to be able to eject the compact from the die, and to assist with the re-alignment of powder particles during the compaction process. If an internal lubricant is used to enhance the compaction process and protect the tooling, then the lubricant must be removed (as much as possible) prior to sintering.

For traditional metal powders, nickel steel, stainless steel, etc., the de-lubrication involves boiling off the internal lubricant at a temperature well below the sintering temperature while the porosity remains open and interconnected. This can be done as a separate de-lubing operation in a separate furnace prior to sintering, or de-lubing can be the first stage of a sintering furnace where the first zone of the furnace is operated at the burn off temperature of the lubricant.

In the case of Titanium and its' alloys, it is imperative to burn off as much lubricant as possible because the remaining lubricants are hydrocarbons which will leave interstitial impurities in the Titanium matrix affecting the mechanical properties.

There have been studies that show that below 400 Deg. C., Titanium and its' alloys do not absorb oxygen very rapidly, if at all. Above 400 Deg. C., the pickup of oxygen is quite rapid. We decided therefore to de-lube our parts at a temperature of 400 Deg. C.

De-lube Methods for Internal Lubricants

1) Nitrogen Burnout – the process involves burning out the green compact in a continuous furnace with a 100% nitrogen atmosphere for at least 60 minutes.
2) Partial Vacuum Burnout – the process involves burning out the green compact in a batch furnace with a partial vacuum and a flush of Argon gas.

To check the efficiency of the de-lube process; we checked the weight loss of the samples before and after de-lubing. Since we know the weight of the lubricant added to the powder; we can determine the lubricant remaining after de-lubing. Since we always use die wall lubrication there is a small amount of die wall lube on the surface of the part, as well as the internal lube.

Table VI-1: Comparison of De-lubing Methods with 0.4% EN-I (Nitrogen Burnout and Partial Vacuum Burnout)

| Weight loss | Method A (Nitrogen) | Method B (Vacuum) |
|---|---|---|
| 90% TiCP-HdHS-G +10%ArmM-R +0.4% EN-I | 0.30% | 0.43% |

We used green compacts formed from a blended powder **90%TiCP-HdHS-G + 10%MA64-ArmM-R + 0.4%EN-I** with 0.4% internal lube added to the powder. The TRS bars were compacted at 50 TSI with addition die wall lubricant ZN-D, and then de-lubed using the 2 different methods. Based on our results, the Partial Vacuum Burnout was the most effective method for removing the internal lubricant. The weight loss of 0.43% when only 0.4% lube was added is due to the additional die wall lube which was added to assist the ejection from the die. The die wall lube was also burned off the surface of the part.

Table VI-2: Comparison of De-lubing Methods with 1.0% EN-I (Nitrogen Burnout and Partial Vacuum Burnout)

| Sample type | Weight loss |
|---|---|
| 90% TiCP-HdHS-G +10%ArmM-R +1% EN-I | 1.06%, 1.09% |
| TiCP-ArmC-I +1.0% EN-I | 0.5%, 0.48% |

To further test the de-lube process, we added 1.0% internal lube to the TRS Bars. This time we compared the Partial Vacuum De-Lube process for 2 different powders. The powders **90%TiCP-HdHS-G + 10%MA64-ArmM-R + 1.0%EN-I** and TiCP-**ArmC-I + 1.0%EN-I** were compacted at 50 TSI with added die wall lubricant ZN-D to form green TRS Bars. The green compacted bars were then de-lubed using the Partial Vacuum Method. In comparing these two results, we see that the Partial Vacuum de-lube

process worked well (1.06% to 1.09%) for the blended HdH powder, but did not work effectively for the Armstrong powder. This result shows that the closely packed dendritic green compact of **TiCP-ArmC-I + 1.0%EN-I** limited the burn off of the lubricant due to its' closed porosity. We have not found an effective de-lube process for internal lube additions to the Armstrong powders.

Based on these results, the Partial Vacuum System was chosen as the de-lubing system for our further work with HdH powders.

## VII. Sintering Process

For the traditional Powder Metal sintering process, the primary mechanism for converting the green compact to a metallurgically bonded part is to raise the temperature of the part in a controlled atmosphere or vacuum to accelerate the diffusion process of bonding the powder particles. Titanium alloys follow the same model. Titanium alloys are sintered in a vacuum or inert atmosphere at a temperature where the Titanium alloy is in the beta phase where the diffusion rate is high. The goal for sintering Titanium alloys is to achieve the highest possible sintered density while minimizing the increase in impurities and minimizing the degradation (coarsening) of the microstructure. The critical factors for the Titanium sintering process are as follows:

1) Powder Alloy and Types of Powder Blends
2) Powder Particle Size and Morphology
3) The Starting Green Density
4) Powder Impurity Types and Levels
5) Sintering Temperature
6) Heating Rate
7) Time at Temperature
8) Atmosphere and/or level of vacuum

The powder alloy types that we sintered were TiCP and Ti64.

TiCP Sintering

Our initial work on sintering TiCP was to determine the effect of Temperature on the final sintered Density.

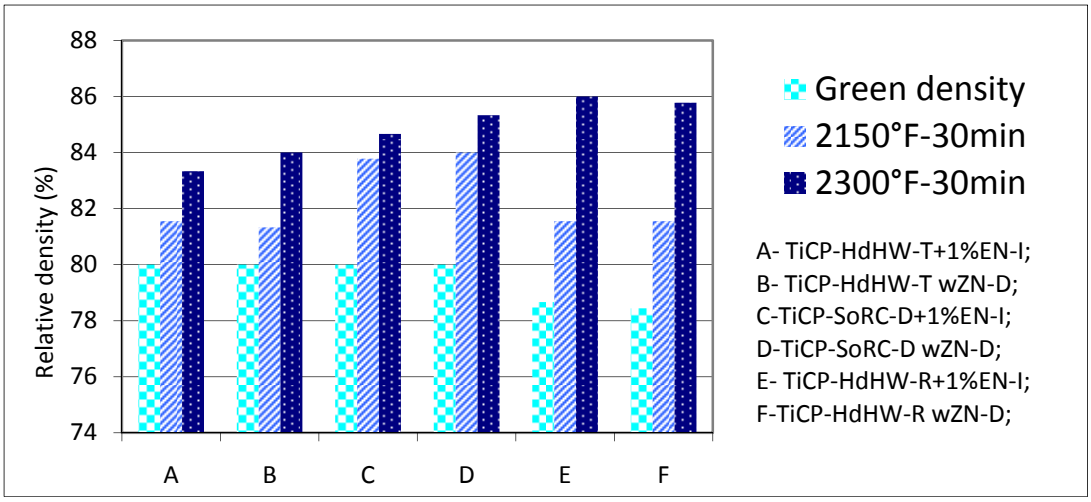


Figure VII-1 Green density (compacted at 40TSI) and sintered density of different TiCP powder compacts. Samples were sintered at 2150°F (1177 °C) and 2300°F (1260 °C) for 30 min.

The sintered density of samples sintered at 2150°F (1177 °C), and 2300°F (1260 °C) for 30 min are shown in Figure VII-1. The 2300°F (1260 °C) sintered specimens have a higher density than the 2150°F (1177 °C) specimens as expected. Figure VII-1 shows that increasing sintering temperature will increase the shrinkage of the green compact.

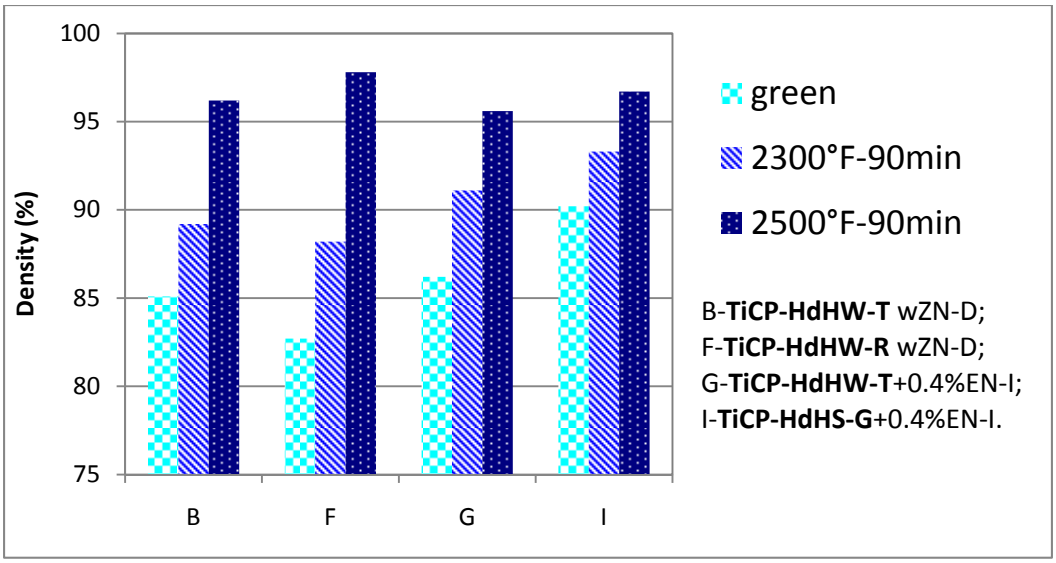


Figure VII-2 Green density and sintered density of different types of TiCP powder compact. Samples were sintered at 2300°F (1260 °C) and 2500°F (1371 °C) for 90 min.

Thermal dilation is the process of measuring the length change caused by a physical or chemical process. In the case of sintering, we use thermal dilation to measure the shrinkage versus the temperature. Figure VII-2 shows 2500°F (1371 °C) sintering temperature will provide a higher sintered density than the 2300°F (1260 °C) temperature. For the **TiCP-HdHW-R** specimen, after vacuum sintering at 2500°F (1371 °C) for 90 min., the sintered density can reach 97.8%. The other 3 samples all obtained a high density of more than 95%. Note that the addition of internal lubrication tends to reduce the final sintered density, even though the starting green density is higher.

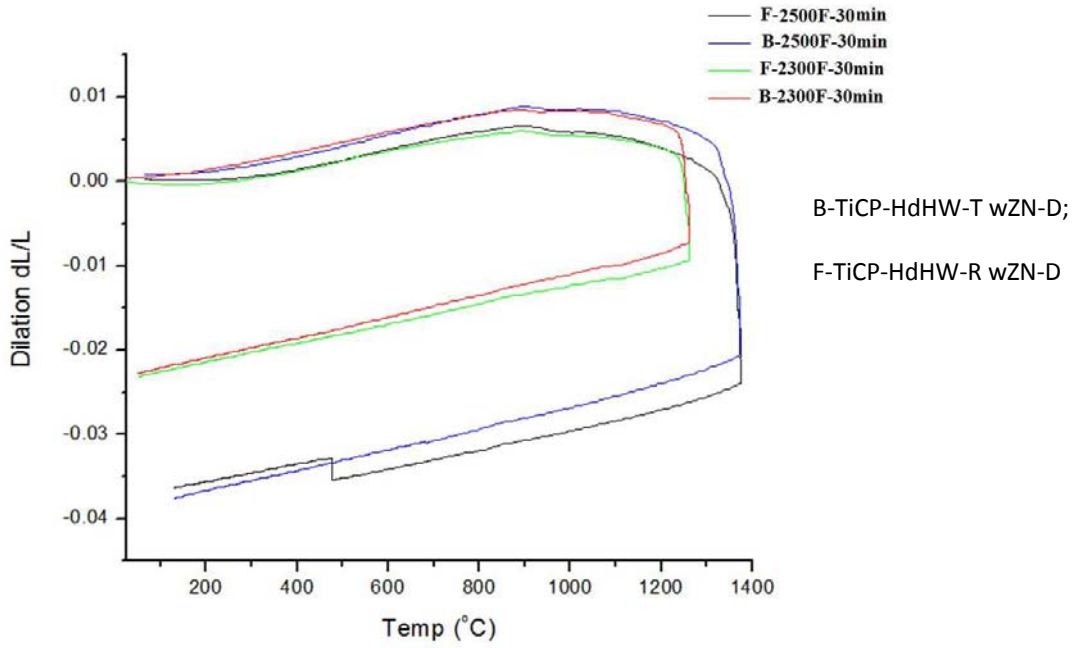


Figure VII-3 Thermal dilation curves for **TiCP-HdHW-T** and **TiCP-HdHW-R** specimens. Samples were standard transverse rupture (TRS) bars pressed at 50 TSI, sintered at 2300°F (1260 °C) or 2500°F (1371 °C) for 30 min with a heating rate of 20°C/min.

Figure VII-3 shows the shrinkage of the samples as a function of two temperatures, 2300°F (1260 °C) or 2500°F (1371 °C). From figure VII-3, we can see that the curves for material B (**TiCP-HdHW-T**) and the curves for material F (**TiCP-HdHW-R**) directly overlay each other until they depart based on the sintering temperature difference 2300°F (1260 °C) or 2500°F (1371 °C). The majority of the shrinkage occurs at the final sintering hold temperature, where the samples sintered at 2500°F (1371 °C) have a higher shrinkage than those sintered at 2500°F (1371 °C). All samples were held for 30 minutes at the sintering temperature.

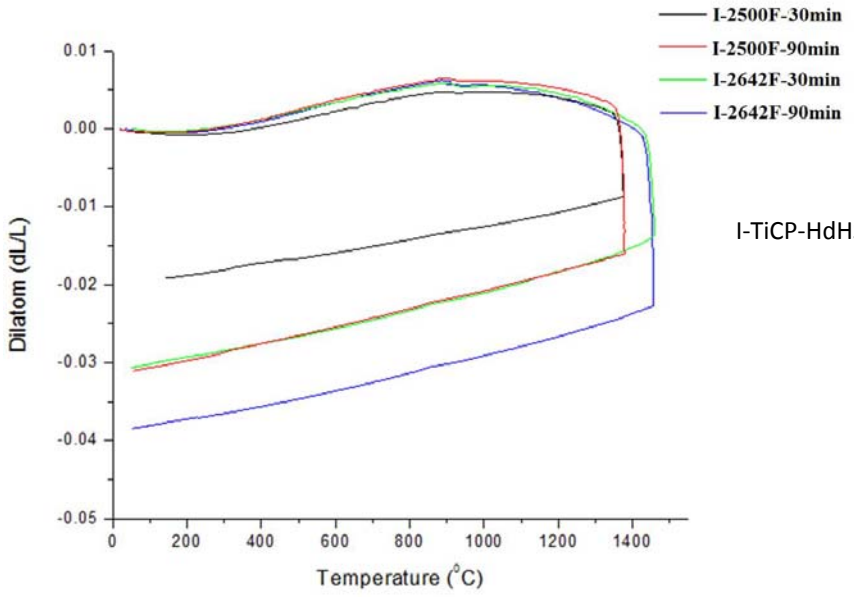


I-TiCP-HdHS-G+0.4%EN-I

2

Figure VII-4 Thermal dilation curves for **TiCP-HdHS-G** specimens. Samples were standard transverse rupture bars pressed at 50 TSI, sintered at 2500°F (1371 °C) and 2642°F (1450 °C)for 30 min or 90 min with a heating rate of 20°C/min.

These dilatometer curves of Type **TiCP-HdHS-G +0.4% EN-I** are given to show how the material behaves for different sintering profiles. In figure VII-4, we show the effect of two different temperatures 2500°F (1371 °C) and 2642°F (1450 °C) and 2 different holding times (30 min. and 90 min.). The increase in temperature from 2500°F (1371 °C) to 2642°F (1450 °C) increases the shrinkage at the same holding time. The increase in holding time from 30 min. to 90 min. also increases the shrinkage for the same temperature. It can be seen that extending the sintering time or increasing the sintering temperature results in greater densification. In terms of densification, sintering at 2500°F (1371 °C) for 90 minutes is equivalent to sintering at 2642°F (1450 °C) for 30 minutes. For these samples sintering becomes rapid around the alpha-beta transformation temperature (Approximately 1562°F (850 °C)) but most shrinkage occurs during the hold at the sintering temperature.

Impurity levels can affect the final sintered density of the part as well as the mechanical properties. Generally, the interstitials (Oxygen, Nitrogen, and Carbon) do not degrade the sintered density since they go into solution in the Titanium Matrix. There are impurities in the powder prior to processing, but it is also important to understand how the sintering process affects these impurities.

Figure VII-5 below shows the Pickup/Reduction of impurity contents during processing of a compacted dog-bone with and without internal lubrication (EN-I). The specimens were de-lubricated using a Nitrogen Burn-off at 750°F (400 °C) and vacuum sintered at 2150°F (1176 C) for 30 minutes.

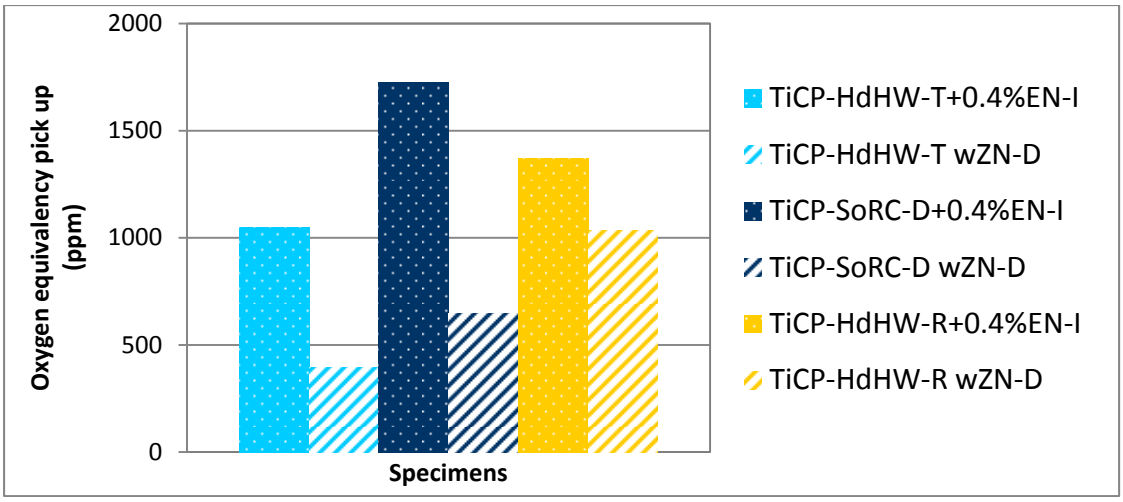


Figure VII-5 Pickup of Interstitial Impurities after compaction, Nitrogen de-lubrication, and vacuum sintering 2150°F (1177 °C), of TiCP Dog-bones, with and without internal lubrication (0.4%EN-I) The samples labeled wZN-D were compacted using die wall lubrication only.

All samples were processed through our nitrogen de-lubing furnace 750°F (400 °C), sufficient to boil off the hydro-carbon lube. Both internal lubed (EN-I) and die wall lubed parts (ZN-D) were processed through the de-lube operation. The Oxygen Equivalency pickup is shown in Figure 6. Extrapolating the data we have, we attribute 300 to 500 ppm pickup of Oxygen Equivalency pickup due to the internal (EN-I) lube system. This seems to be a reasonable tradeoff in order to achieve full automatic compaction with good tool protection and higher green densities. We must keep in mind that we added approximately 7800ppm of hydro-carbons in the lube to the powder, and a majority of the carbon was removed during the de-lubrication and sinter process.

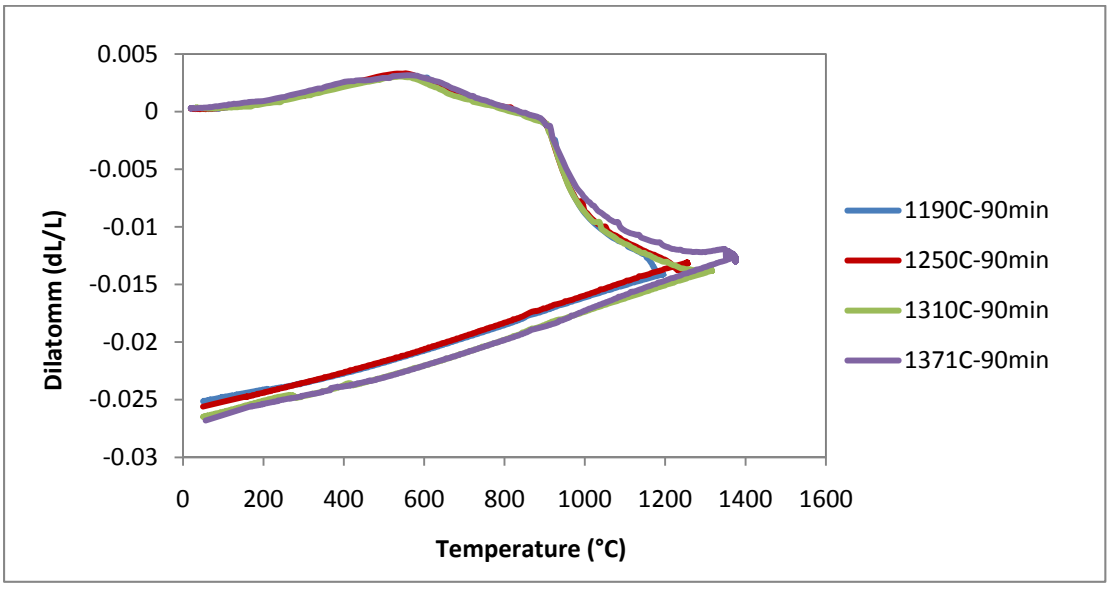


Figure VII-6 Thermal dilation of **TiCP-ArmC-I** powder compact which sintered at different temperature for 90min.

Figure VI-6 shows the thermal dilation of **TiCP-ArmC-I** powder compact sintered at 2175°F (1190 °C), 2282°F (1250 °C), 2390°F (1310 °C)and 2500°F (1371 °C) for 90 min. Compared with the HdH powder, the TiCP-ArmC-I powder compacts start to shrink at around 842°F (450 °C), which is considerably lower that the sintering start temperature of 1562°F (850 °C) for the HdH powders. This lower sintering start temperature is attributed to the high surface to volume fraction of the sponge/dendritic of the

Armstrong powder compared with the angular HdH powders. At around 1652°F (900 °C), the shrinkage rate increases. However, at around 1832°F (1000 °C) the shrinking of the samples slowed considerably, and the dilatometer curve turned horizontal. After the sintering, we saw that there were a lot of small bubbles on the surface of the sintered compact. The bubbles indicate that some form of gas was boiling off after the porosity was starting to close, causing small explosions on the surface. Because the **TiCP-ArmC-I** powder sample had a high level of sodium (470 ppm), we believe that the high sodium content impeded the sintering process.

Figure VII-7 below shows the comparative metallography of the sintered compacts.

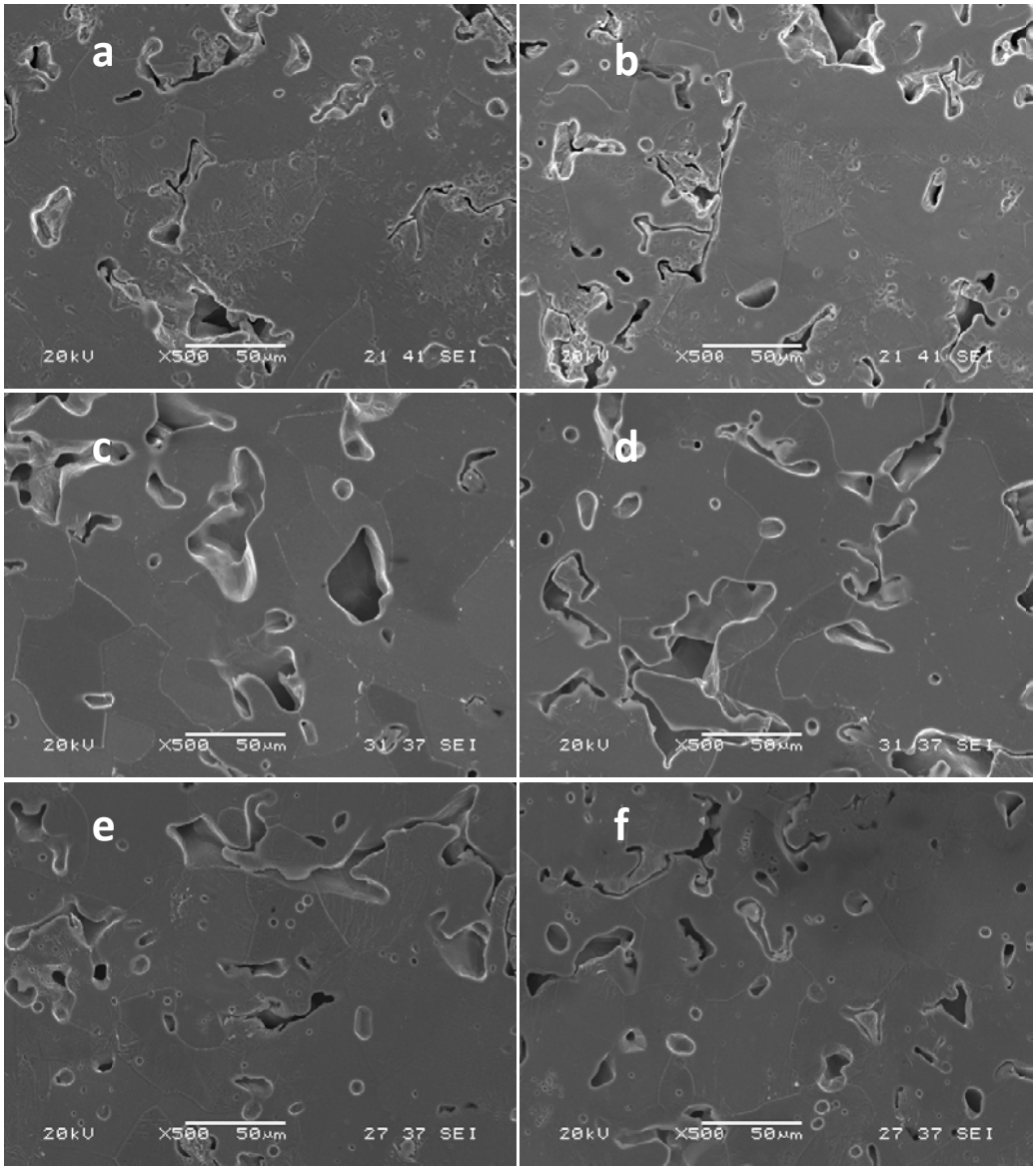


Figure VII-7 SEM metallographic images show pores and grain boundaries: (a) **TiCP-HdHS-R wZN-D** specimen sintered at 2150°F (1177°C) (b) **TiCP-HdHS-R +1%EN-I** specimen sintered at 2150°F (1177°C) (c) **TiCP-HdHW-T wZN-D** specimen sintered at 2300°F (1260°C) (d) **TiCP-HdHW-T +1%EN-I** specimen sintered at 2300°F (1260 °C) (e) **TiCP-SoRC-D wZN-D** specimen sintered at 2300°F (1260°C) (f) **TiCP-SoRC-D +1%EN-I** specimen sintered at 2300°F (1260°C). specimens etched with Kroll`s reagent.

SEM metallographic images are given in Figure VII-7. From the images, the die wall lube (ZN-D) specimens and internal lube (EN-I) specimens did not show much difference. Comparing Figure VII-7(a) with Figure VII-7(c) and Figure VII-7(e), 2300°F (1260°C) sintered specimens show more rounded pores and straight boundaries. That is because higher sintering temperature

can accelerate the diffusion and increase the neck growth rate driving the structure faster toward equilibrium [3]. So the specimens sintered at 2300°F (1260°C) densify more than the 2150°F (1177°C) ones. The powder morphology affects pore shape after sintering. **TiCP-SoRC-D** powder shows more irregular shapes than the other two powders, and has more angular shape, and smaller pores. That explains why **TiCP-SoRC-D** specimens have lower tensile strength (as we will see in the next section). Grain size can be roughly estimated, and for all of the specimens above, the grain size is about 50μm, and did not vary much. From Figure VII-7(a) and VII-7(b), we can see the large irregular regions, which contain packets of small almost parallel α plates. This region is massive martensite, which occurs only in pure titanium, or very dilute alloys [4].

Ti64 Sintering

For Ti64, we used different powders and powder blends to achieve the final alloy (90%Ti, 6%Al, and 4%V). Each of these powders and powder blends sinters differently. The powders and blends we tested are as follows:

Pre-alloyed Powders

1) **Ti64-HdHW-R** – pre-alloyed hydride de-hydride powder from wrought
2) **Ti64-HydW-R** – pre-alloyed hydride powder from wrought
3) **Ti64-ArmC-I** – pre-alloyed powder via Armstrong process

Blended Powders

1) **90%TiCP-HdHS-G + 10%Ma64-AtmM-R** – Ti64 formed from TiCP + Master alloy (60%Al + 40%V)
2) **50%Ti64-ArmC-I + 45%TiCP-HdHS-G + 5%Ma64-AtmM-R** – Ti64 formed from pre-alloyed Armstrong powder plus TiCP HdH powder blended with Master Alloy (60%Al + 40%V)
3) **50%Ti64-ArmC-I + 50%Ti64-HdHW-R** – Ti64 formed from blending pre-alloyed Armstrong and pre-alloyed HdH powders.

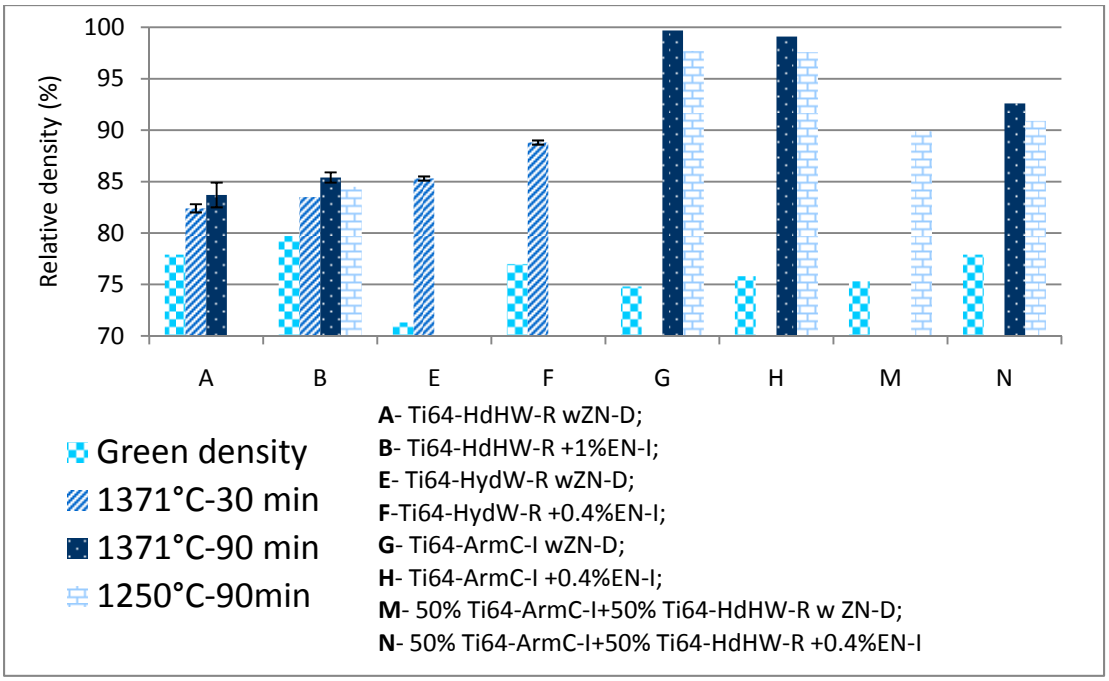


Figure VII-8 Green and sintered relative density for different pre-alloyed Ti64 powder compacts sintered at 2282°F (1250°C) or 2500°F (1371°C) for 30 min or 90 min.

Figure VII-8 shows the differences of the sintered density of pre-alloyed Ti64 powder and the blended powders at 2282°F(1250°C) or 2500°F(1371°C) for 30 min or 90 min sintering times. The Green and sintered density obtained from the two kinds of lubricant methods: die wall lube (ZN-D) and internal lube (EN-I) are also compared in Figure VII--8.

For pre-alloyed powders we see a dramatically higher sintered density (99.7%) of the Armstrong powders **Ti64-ArmC-I** versus the hydride de-hydride powders (85%), even though the starting green density of the Armstrong powders were lower (75%). This difference will be identified in the dilatometer curves to follow, and is attributed to the morphology of the powders. When we compare **Ti64-HdHW-R** (A and B) with **Ti64-ArmC-I** (G and H) compacts, **Ti64-ArmC-I** powder samples can provide higher sintered density, even though they have lower green density. For 2500°F (1371°C) -90min sintered sample, **Ti64-ArmC-I** has reached 99.7% sintered density, while **Ti64-HdHW-R** only obtained 85.4%.

The mixture **50% Ti64-ArmC-I+50% Ti64-HdHW-R** provides intermediate sintered density between **Ti64-ArmC-I** and **Ti64-HdHW-R** sample compacts, which is 92.6% after sintered at 2500°F (1371°C) for 90 min.

We also note that for the hydride de-hydride powders, adding internal lubrication improves both the green density and the final sintered density, whereas for the Armstrong powders, internal lube increases the green density but reduces the final sintered density. This effect can be attributed to the difference in the morphology of the powders. For **Ti64HdHW-R** powders at the same pressing, de-lube and sintering conditions, the internal lube (EN-I) compact provides higher green density and after sintering, and the internal lube (EN-I) compact can reach a higher sintered density. Sample **Ti64-HdHW-R +1%EN-I** (B) shows clearly 2500°F (1371°C) -90 min can obtain higher density (85.4%) than 1371°C-30 min (83.5%) and 2282°F (1250°C) -90 min (84.5%).

We also see that extending the sintering time and increasing the sintering temperature result in higher sintered densities.

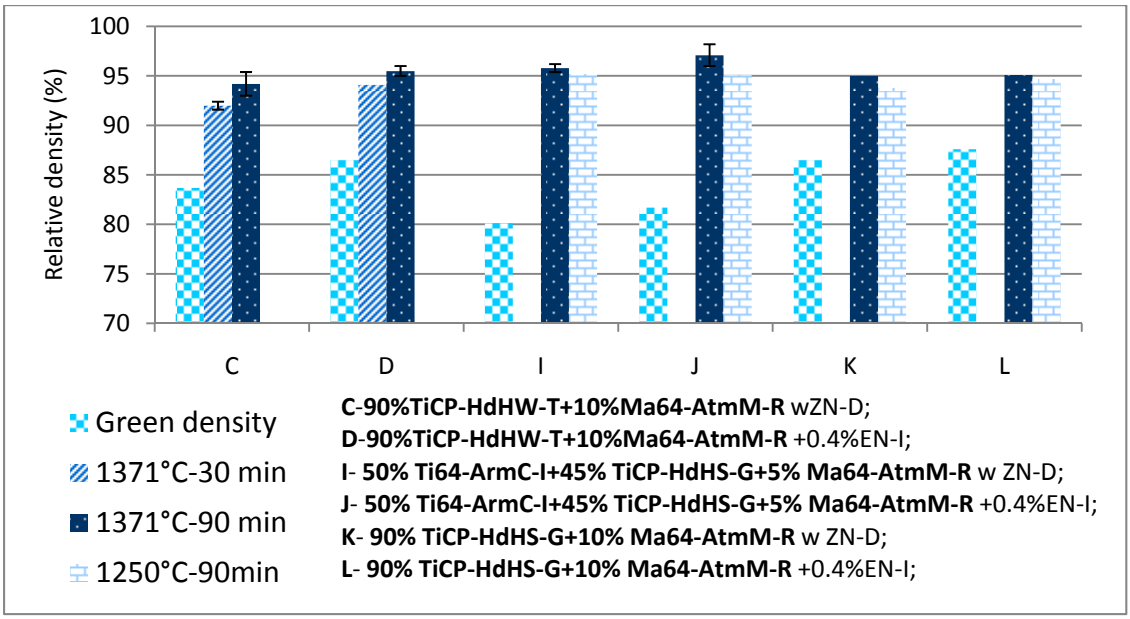


Figure VII-9: Green and sintered relative density for Ti64 Blended Powder compacts sintered 2282°F (1250°C) or 2500°F (1371°C) for 30 min. or 90 min.

Figure VII-9 shows the differences of the green and sintered density for Ti64 compacts blended from TiCP powders and Master Alloys at 2282°F (1250°C) or 2500°F (1371°C) for 30 or 90 min sintering time. The only difference between powder C (**90%TiCP-HdHW-T+10%Ma64-AtmM-R**) and powder K (**90% TiCP-HdHS-G+10% Ma64-AtmM-R**) is that they use different TiCP powder manufacturer. After sintered at 2500°F (1371°C) for 90 min in vacuum, they all obtain around 95% sintered density. Sample J (**50% Ti64-ArmC-I+45% TiCP-HdHS-G+5% Ma64-AtmM-R +0.4%EN-I**) provides highest sintered density 97.1% after sintering at 2500°F (1371°C) for 90min.

Comparing Figures VII-8 and VII-9, we see that the highest sintered density was achieved by **Ti64-ArmC-I** (97.7% to 99.7%) even though the starting green density was the lowest (74.8%). The lowest sintered density was achieved by **Ti64-HdHW-R** (84.5%).

The blended powders achieved sintered densities between these two, with **50%Ti64-ArmC-I + 45%TiCP-HdHS-G + 5%Ma64-AtmM-R** reaching (95% to 97%). From the figures VII-8 and VII-9, we see that for the HdH blended and pre-alloyed powders, adding internal lubrication (0.4%EN-I) does not affect the sintered density. However for the Armstrong powder **Ti64-ArmC-I**, adding internal lubrication reduces the final sintered density. This affect may be attributed to the previously noted problem of ineffective de-lubrication of the Armstrong green compacts.

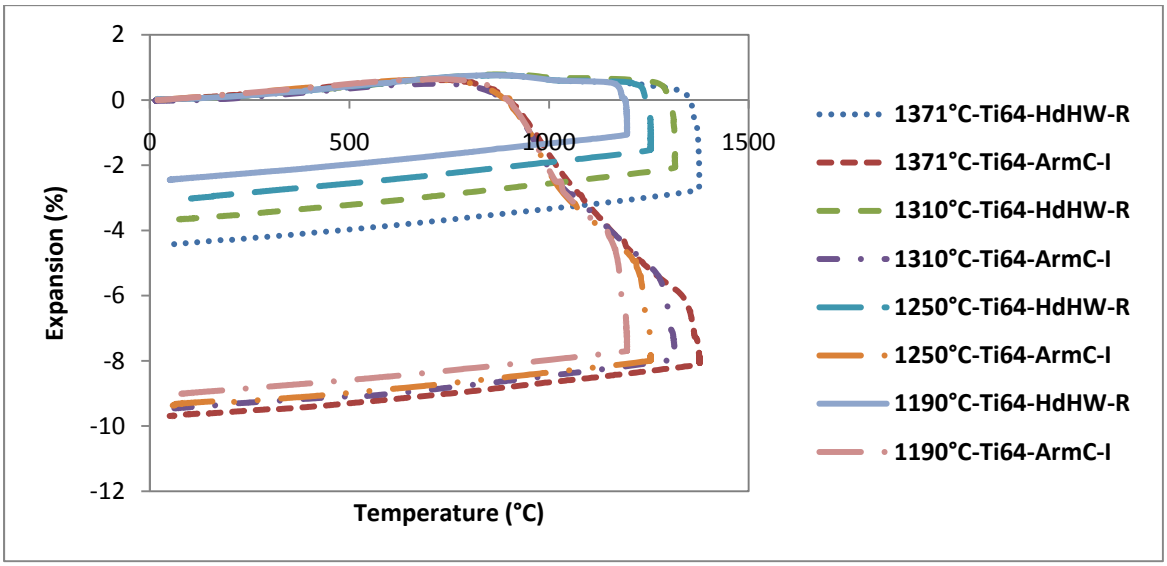


Figure VII-10 Shrinkage versus temperature of **Ti64-HdHW-R** and **Ti64-ArmC-I** at 2175°F(1190°C), 2282°F(1250°C), 2390°F(1310°C) and 2500°F(1371°C) for 90min with 20°C/min heating rate.

Thermal dilation is the process of measuring the length change caused by a physical or chemical process. In the case of sintering, we use thermal dilation to measure the shrinkage versus the temperature. Before 1292°F (700°C), thermal expansion occurs, and the compact expands. For **Ti64-HdHW-R** powder compacts, shrinkage starts at around 1652°F (900°C), while **Ti64-ArmC-I** powder compact starts to sinter at a lower temperature, around 1292°F (700°C).

To investigate which factors affect the sintering behavior of Ti64 pre-alloyed powders (HdH versus Armstrong), the dilatometer was used to determine the shrinkage of the compacts at different target temperatures and different heating rates. Figure VII-10 shows the shrinkage curves of the **Ti64-HdHW-R** and **Ti64-ArmC-I** powder compacts with different target temperatures. The holding time is 90 min with a heating rate of 20°C/min. From Figure VII-10, we can see that when the target temperatures are increased from 2175°F(1190°C) to 2500°F(1371°C), the shrinkage of the Ti64-ArmC-I only increased from 9.0% to 9.7%. So for **Ti64-ArmC-I** we can obtain a relatively high sintered density even when sintering the compact at lower temperature. For the **Ti64-HdHW-R** powder, the shrinkage can increase from 2.4% to 4.4% when the sintering temperature increases from 2175°F (1190°C) to 2500°F (1371°C. That indicates that the sintered temperature affects the **Ti64-HdHW-R** powder (90% relative change) more than **Ti64-ArmC-I** powder (8% relative change).

To determine if heating rate has an effect on the sintering process and the final sintered density, we ran a series of experiments with different heating rates (from 5°C/min. up to 20°C/min.). The dilatometer chart is shown in Figure VII-11.

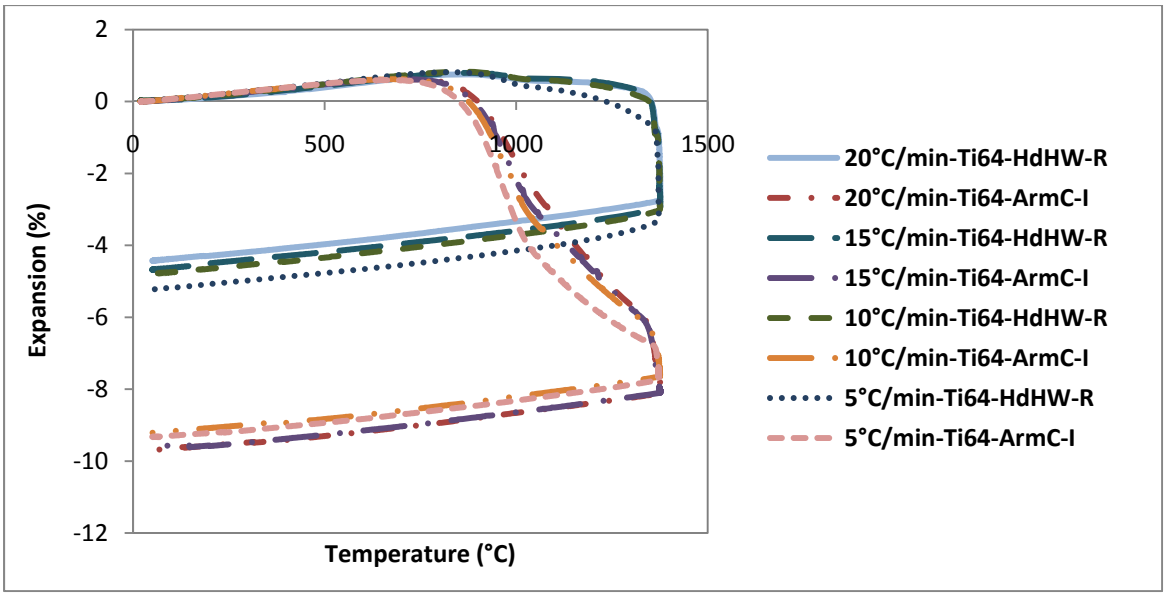


Figure VII-11 Shrinkage versus temperature of **Ti64-HdHW-R** and **Ti64-ArmC-I** at 2500°F (1371°C) for 90 min, with 20°C/min, 15°C/min, 10°C/min and 15°C/min heating rate.

Figure VII-11 shows how the heating rate (5°C/min, 10°C/min, 15°C/min and 20°C/min) affects the sintering behavior, when the target temperature 2500°F(1371°C) and holding time (90 min) is the same. For both powders, the change in heating rate had virtually no effect on the final sintered density. There is only a minor difference in that the slower heating rate allowed slightly longer overall sintering time, since the hold time at temperature was 90 min. For **Ti64-HdHW-R** powder, the slower heating rate of 5°C/min. shows a slightly larger shrinkage.

To get a better comparison of the sintering process for both pre-alloyed and blended powder mixtures, we ran the dilatometer curves for the 5 powders/blends listed below:

1) 100% **Ti64-HdHW-R**
2) **90%TiCP-HdHS-G + 10%Ma64-AtmM-R**
3) **50%Ti64-ArmC-I + 50%Ti64-HdHW-R**
4) **50%Ti64-ArmC-I + 45%TiCP-HdHS-G + 5%Ma64-AtmM-R**
5) 100%**Ti64-ArmC-I**

These 5 powders/blends were selected because they have shown the greatest potential for Press and Sinter applications. All samples were compacted at 50 TSI, and sintered at 2500°F (1371°C) for 90 min. with a heating rate of 20°C/min.

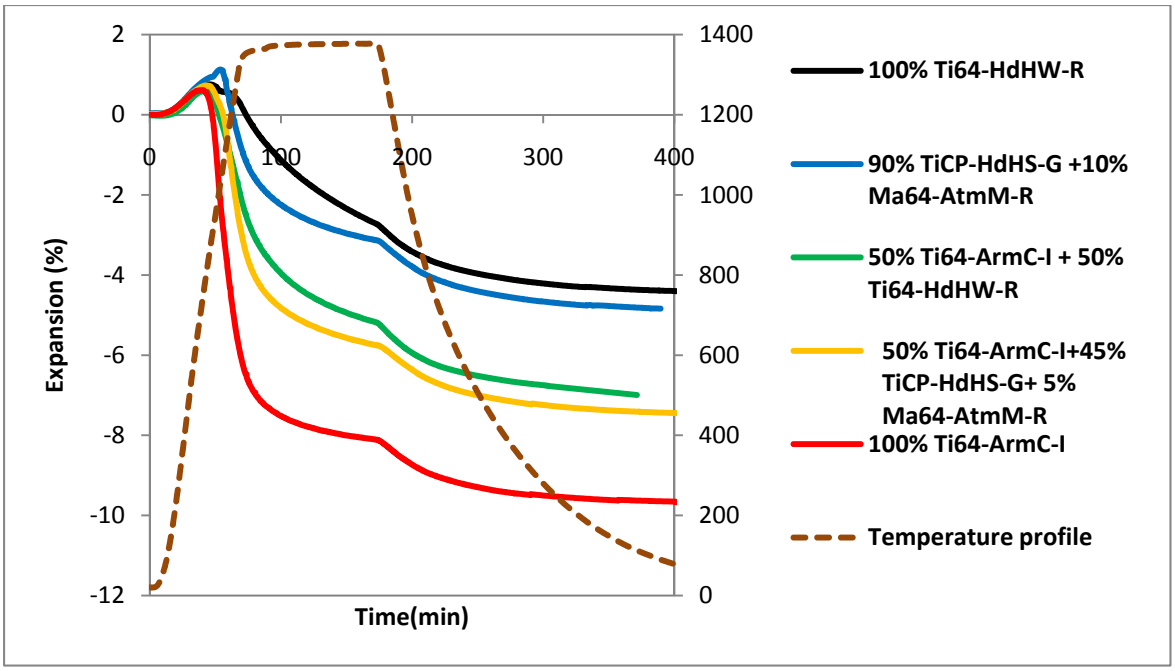


Figure VII-12 Shrinkage versus time curves of different powder mixtures. Specimens were sintered at 2500°F (1371°C) for 90 min with 20°C/min.

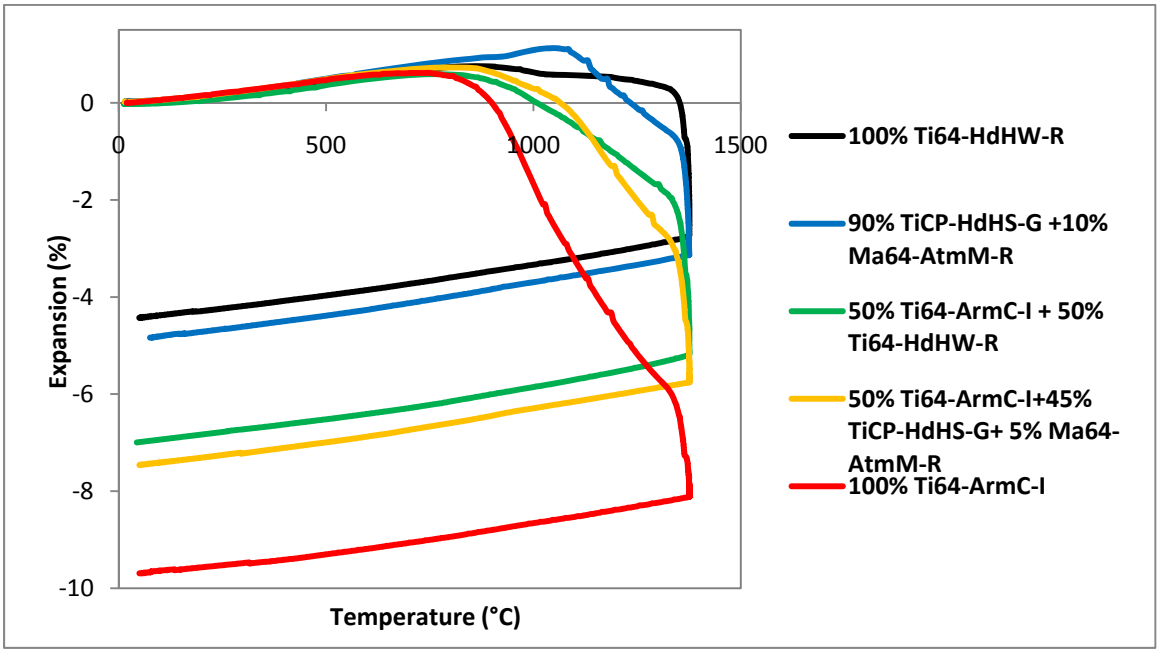


Figure VII-13 Shrinkage versus temperature curves of different powder mixtures. Specimens were sintered at 2500°F(1371°C) for 90 min with 20°C/min.

Due to the different powder characteristics of the **Ti64-HdHW-R** and **Ti64-ArmC-I** powder, they behave distinctly differently during sintering. The different blended powder compacts were all pressed at 50 TSI (690 MPa) with ZN-D and EN-I. Dilatometer experiments were conducted by heating to 2500°F (1371°C) and holding for 90 min with argon flow through the chamber. Figure VII-12 shows the shrinkage versus time curves for the five kinds of powders/blends.

Figure VII-13 shows the shrinkage versus temperature curves for the five kinds of powders. When we compare **Ti64-HdHW-R** and **90% TiCP-HdHS-G +10% Ma64-AtmM-R** compacts, we can see that **Ti64-HdHW-R** shrinkage is less than the **90% TiCP-HdHS-G +10% Ma64-AtmM-R** compact. **Ti64-HdHW-R** shrinks about 4.5% and **90% TiCP-HdHS-G +10% Ma64-AtmM-R** shrinks around 5%, while **Ti64-ArmC-I** compact can reach almost 10% shrinkage. The **Ti64-ArmC-I** also shows a lower sintering start temperature at around 1292°F (700°C) than the **Ti64-HdHW-R** and **90% TiCP-HdHS-G +10% Ma64-AtmM-R** compacts.

The sintering mechanism is the main reason why the sintering behavior is so different for the five different powders. For the **Ti64-ArmC-I**, **Ti64-HdHW-R** and their mixed powder compacts, only solid state sintering takes place. Because of the large specific surface area of the **Ti64-ArmC-I** powder, the **Ti64-ArmC-I** powder start to shrink at a low temperature, around 1292°F (700°C), while **Ti64-HdHW-R** starts to shrink at around 1652°F (900°C). Looking at the green curve of Figure VII-13, **50% Ti64-ArmC-I+ 50% Ti64-HdHW-R** powder, the shrinkage is just between the **Ti64-HdHW-R** and **Ti64-ArmC-I** powders. This powder starts to shrink at around 1472°F (800°C), and the final shrinkage is 7%.

The **90% TiCP-HdHS-G +10% Ma64-AtmM-R** powder compact shows different sintering behaviors than the pre-alloyed **Ti64-ArmC-I** and **Ti64-HdHW-R** powders, because both solid state sintering and transient liquid phase sintering occurs during the sintering. At first, Al and V both diffuse into the Ti particles and Ti diffuses into the Al-V particles. When the temperature reaches around 2012°F (1100°C), the blended compact showed rapid shrinkage. During this period of time, the initial stage of transient liquid phase sintering occurs. The mechanism of the shrinkage in this period is rearrangement of the particles. The liquid phase of the master alloy is formed and the wetting liquid spreads throughout the matrix via capillarity force [5]. The capillary force and liquid then cause rearrangement of titanium particles, and results in the rapid shrinkage of the compact. Next, liquid master alloy becomes a carrier for the Ti atoms, wherein the Ti atoms in smaller grains will dissolve into the liquid and precipitate on the larger grains due to the diffusion. This solution re-precipitation mechanism also causes densification by grain growth and shape accommodation, and then pore elimination. At the same time, liquid state Al and V also diffuse into the titanium solid skeleton. After that, Al and V atoms continue diffusing into the grains and form $\alpha+\beta$ phase. A homogeneous Ti64 alloy microstructure is obtained through solid state diffusion of V and Al in Ti.

We also mixed the **90% TiCP-HdHS-G +10% Ma64-AtmM-R** powder with **Ti64-ArmC-I**, which is the **50%Ti64-ArmC-I +45% TiCP-HdHS-G +5% Ma64-AtmM-R** powder compact (yellow curves). The shrinkage of this powder blend is between the shrinkage of **90% TiCP-HdHS-G +10% Ma64-AtmM-R** powder and the shrinkage of **Ti64-ArmC-I** powder, which yields a final shrinkage of 7.4%.

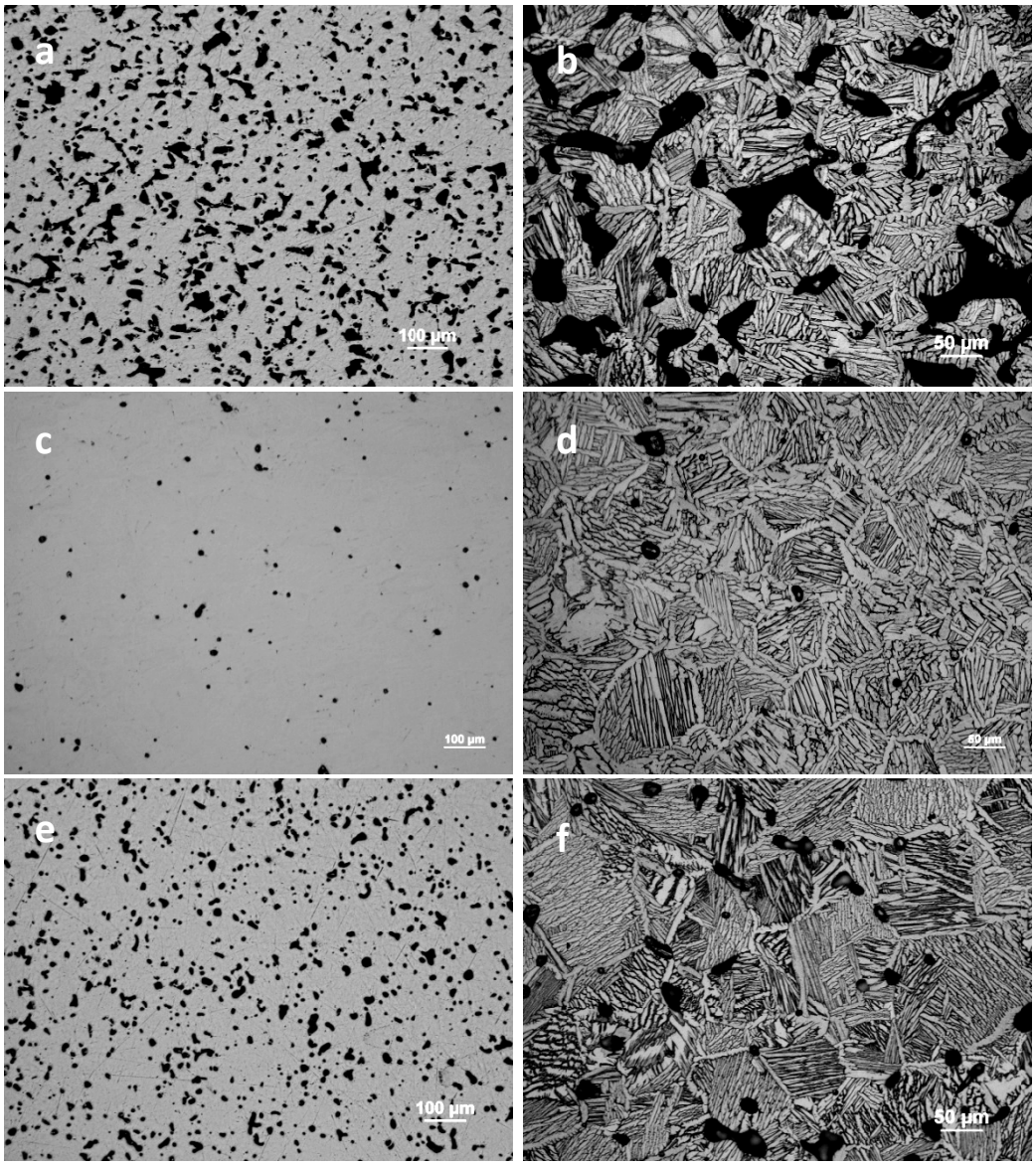


Figure VII-14 Un-etched and etched optical images of three compacts showing their microstructures. The specimens were compacted at 50 TSI, and sintered at 2282°F (1250°C) for 90 min: (a) un-etched microstructure of **Ti64-HdHW-R** ; (b) etched microstructure of **Ti64-HdHW-R**; (c) un-etched microstructure of **Ti64-ArmC-I**; (d) etched microstructure of **Ti64-ArmC-I**; (e) un-etched microstructure of **90%TiCP-HdHW-T+10%Ma64-AtmM-R**; (f) etched microstructure of **90%TiCP-HdHW-T+10%Ma64-AtmM-R**.

The hydride de-hydride pre-alloyed Ti64 (**Ti64-HdHW-R**) has a large volume of pores shown in Figure VII-14 (a), and most of the pores are irregular shape, some quite angular. The large porosity and irregular pore structure are the main reasons for the poor mechanical properties (as we will see in the next section). Figure VII-14 (c) shows the pore structure of the Armstrong pre-alloyed Ti64 powder compact (**Ti64-ArmC-I**). All of the pores are round and smooth, and most of the pores are spherical. This reduces the stress concentration under load compared with the angular pore structure. This image is clear evidence that the high sintered density and good mechanical properties of the Armstrong pre-alloyed Ti64 powder compact result from the superior microstructure. Figure VII-14 (e) and VII-14 (f) shows the etched and un-etched optical images of the blended powder compacts (**90%TiCP-HdHW-T+10%Ma64-AtmM-R**). Most pores were well rounded, some pores show irregular shape, and some pores are spherical in shape. The level of porosity is between the hydride de-hydride pre-alloyed Ti64 (**Ti64-HdHW-R**) and Armstrong pre-alloyed Ti64 (**Ti64-ArmC-I**).

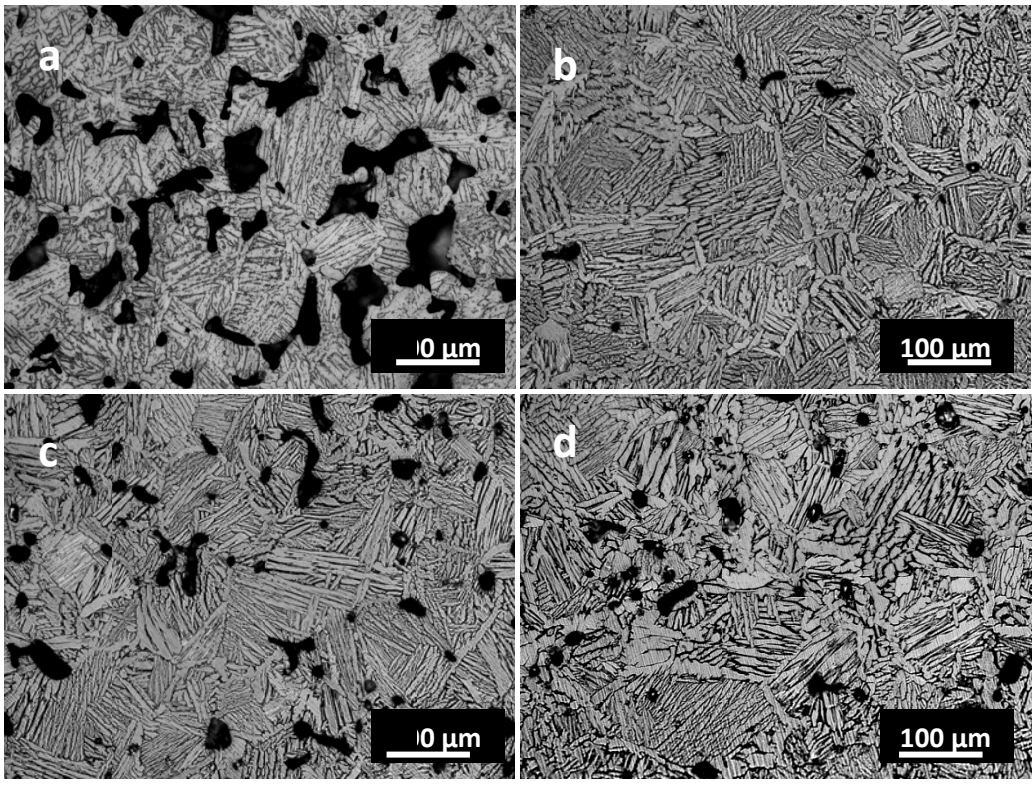


Figure VII-15 Optical images of Ti64 powders/blends compacted at 50 TSI and sintered at 2282°F (1250°C) for 90 min.: (a) **Ti64-HdHW-R** specimen; (b) **Ti64-ArmC-I** specimen; (c) **50%Ti64-ArmC-I+50%Ti64-HdHW-R** powder specimen; (d) **50%Ti64-ArmC-I+45%TiCP-HdHS-G+5%Ma64-AtmM-R** specimen.

Optical microscopy was used to observe the etched microstructures. Figure VII-15 (a) and VII-15 (b) show the images of **Ti64-HdHW-R**, **Ti64-ArmC-I** powder compacts sintered at 1250°C for 90 min. The microstructure of **Ti64-HdHW-R** clearly shows much more porosity than the **Ti64-ArmC-I** powder sample. The **Ti64-ArmC-I** sample shows well distributed, round and small sized pores and much finer spherical pores. On the other hand, the **Ti64-HdHW-R** sample contains a large volume of big angular pores. Figure VII-15 (c) and VII-15 (d) show the etched optical microstructures of **50%Ti64-ArmC-I+50%Ti64-HdHW-R** and **50%Ti64-ArmC-I+45%TiCP-HdHS-G+ 5%Ma64-AtmM-R**. The microstructures of Figure VII-15 (c) and VII-15 (d) show the improvement in pore morphology over Figure VII-15 (a) by either adding **Ti64-ArmC-I** or using blended master alloy powder resulting in transient liquid phase sintering. Both of the mixed powder samples show fewer pores and more rounded pore structure than **Ti64-HdHW-R** Figure VII-15 (a). The **50%Ti64-ArmC-I+50%Ti64-HdHW-R** compact shows fewer pores than **Ti64-HdHW-R** compact and pores were rounded. Some of the pores in the image are elongated rather than round pores. The **50%Ti64-ArmC-I+45%TiCP-HdHS-G+ 5%Ma64-AtmM-R** microstructure shows well rounded pores, but a greater fraction of pores compared with **Ti64-ArmC-I** powder compacts.

Summary

The pre-alloyed **Ti64-ArmC-I** powder achieved the highest sintered density with the best microstructure. The blended powder **50%Ti64-ArmC-I + 45%TiCP-HdHS-G + 5%Ma64-AtmM-R** also showed very good density and microstructure. We expect these powders to demonstrate good mechanical properties.

## VIII. Mechanical Properties

The engineer designing systems with metal components will need the mechanical properties of the prospective materials to properly design the component. The list of mechanical properties of interest to the designer is:

Tensile Properties

1) Ultimate Tensile Strength (UTS)
2) Yield Strength (YS)
3) Elongation (E)

Elastic Constants

1) Young's Modulus
2) Poisson's Ratio

Transverse Rupture Strength

1) Transverse Rupture Strength (TRS)

Hardness

1) Apparent Hardness
2) Micro Hardness

Compressive Strength

1) Compressive Yield Strength (CYS)

Shear Strength

1) Shear Modulus

Impact Energy

1) Impact Energy

Fatigue Properties

1) Fatigue Strength
2) Fatigue Limit

The definitions of these mechanical properties are shown in the glossary (from the MPIF Standard 35 [2]). The design team from Oshkosh Corporation requested we provide the following properties for his evaluation, Ultimate Tensile Strength, .2% Yield Strength, Elongation, Apparent Hardness, and Young's Modulus. We have therefore focused on these parameters for our analysis.

TiCP

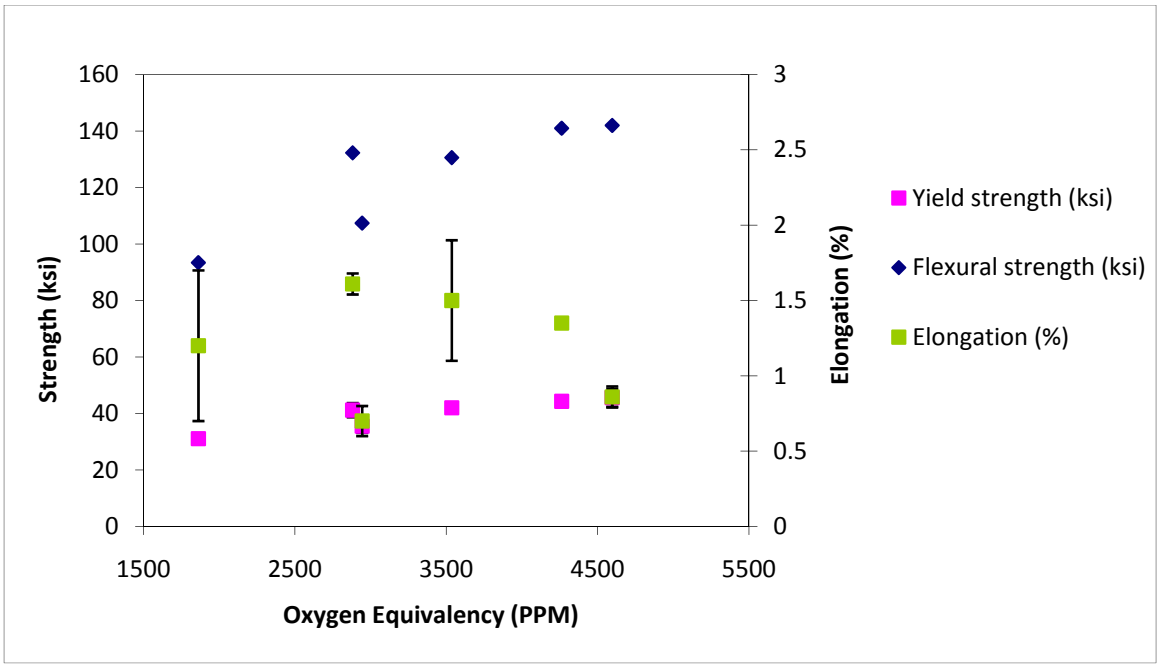


Figure VIII-1 Strength (Flexural and Yield) and Elongation versus Oxygen Equivalency for different specimens of TiCP.

The interstitial oxygen, nitrogen, and carbon which are found in the interstices of the titanium crystal structure have a strong effect on the mechanical properties. At small concentrations and properly controlled, interstitials improve strength [4]. The relationship of the oxygen equivalency and mechanical properties for the three different powders are given in Figure VIII-1. The strength (both Flexural and Yield) show an increase with increasing oxygen equivalency. The elongation decreases as the oxygen equivalency increases. If elongation is important for the design, then controlling oxygen equivalency is important.

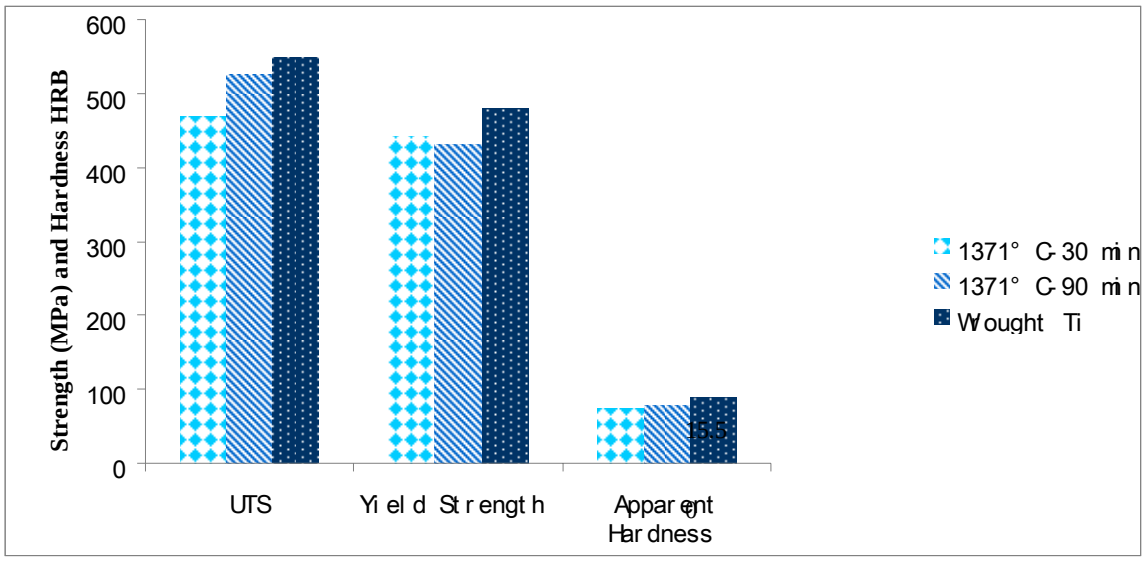


Figure VIII-2 Mechanical properties (UTS, Yield Strength, and Apparent Hardness) of **TiCP-HdHS-G +0.4%EN-I** sintered at 2500°F (1371°C), with hold times of 30 min. and 90 min.

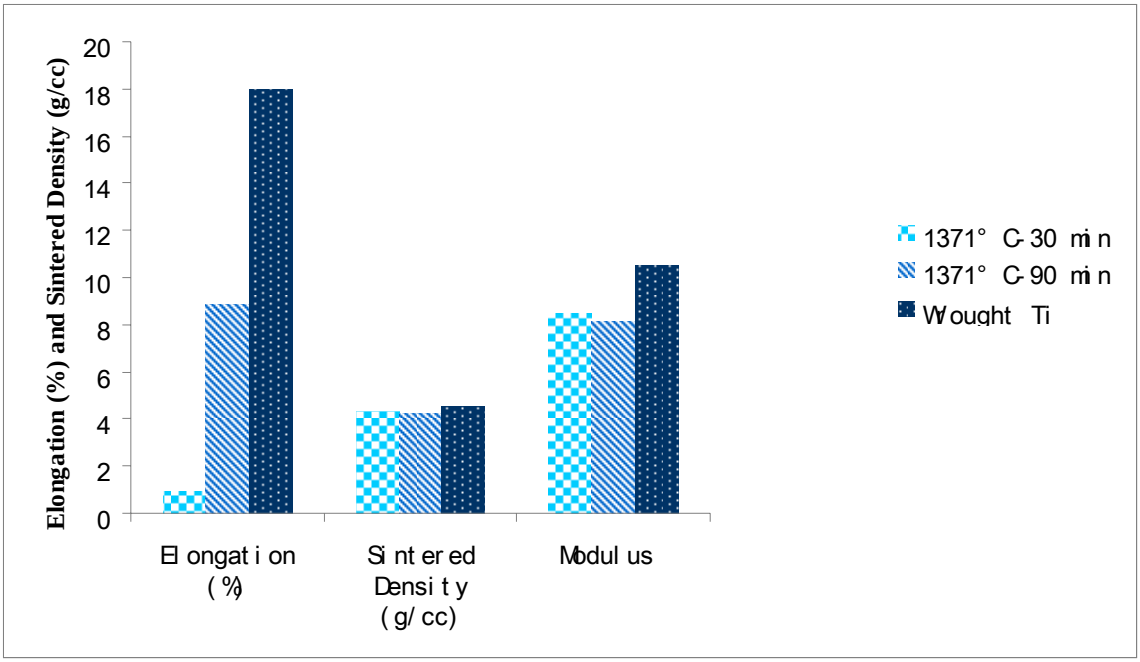


Figure VIII-3 Mechanical properties of Elongation **(%)**, Sintered Density **(g/cc)** and Young's Modulus **(.1Gpa)** of **TiCP-HdHS-G +0.4%EN-I** specimens sintered at 2500°F (1371°C ), with hold times of 30 min. and 90 min.

The data from tensile testing specimens of **TiCP-HdHS-G + 0.4%EN-I** is shown in figures VIII-2 and VIII-3 above. The samples were sintered at 2500°F (1371°C), for 30 min. and 90 min. The properties are compared with wrought TiCP [6].

From Figure VIII-2, we can see that the UTS of the 90 min sample is close to that of wrought titanium, which is around 524 MPa (76 KSI). The 90 min sintered sample shows slightly lower (but not significant) yield strength.

From Figure VIII-3, we can see that the 90 min sintered specimen has significantly greater ductility than the 30 min specimen. The wrought Titanium has an elongation about twice that of the best sintered material. The Young's modulus values are similar for the sintered samples but about 20% lower than for wrought titanium.

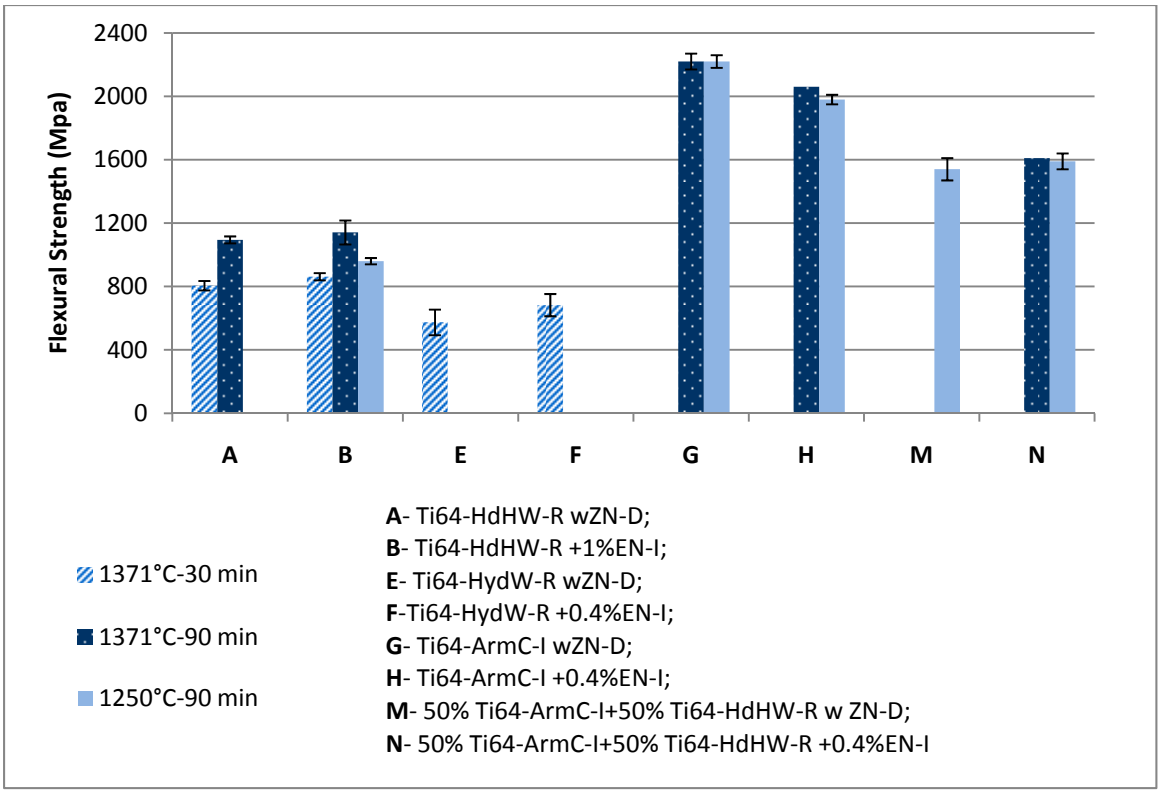


FigureVIII-4 Flexural strength (from three point bending tests) of different pre-alloyed samples of Ti64 sintered at 2500°F(1371°C ) or 2282°F( 1250°C ) with holding times of 30 min and 90 min.

Figure VIII-4 shows the differences of the flexural strength at 30 and 90 min sintering time at 2500°F(1371°C) and 2282°F(1250°C) for the pre-alloyed Ti64 powder and their blends. For **Ti64-HdHW-R**, it is clear that extending the sintering time promotes the densification of the compact and in turn improves the flexural strength. Also for **Ti64-HdHW-R**, the figure shows that 2282°F(1250°C) -90min sintered samples provide less strength than the 2500°F(1371°C) -90min samples.

Figure VIII-4 also shows **Ti64-ArmC-I** samples (G and H) (2200Mpa flexural strength) provided much higher sintered density than **Ti64-HdHW-R** samples (A, B, E, and F) (1141 MPa) when sintered at 2500°F(1371°C) for 90 min. Blended samples M and N (**50% Ti64-ArmC-I+50% Ti64-HdHW-R**) are pre-alloyed Ti64 mixtures. N obtained 1610 MPa when sintered at 2500°F(1371°C) for 90 min, which is between **Ti64-ArmC-I** and **Ti64-HdHW-R** powder.

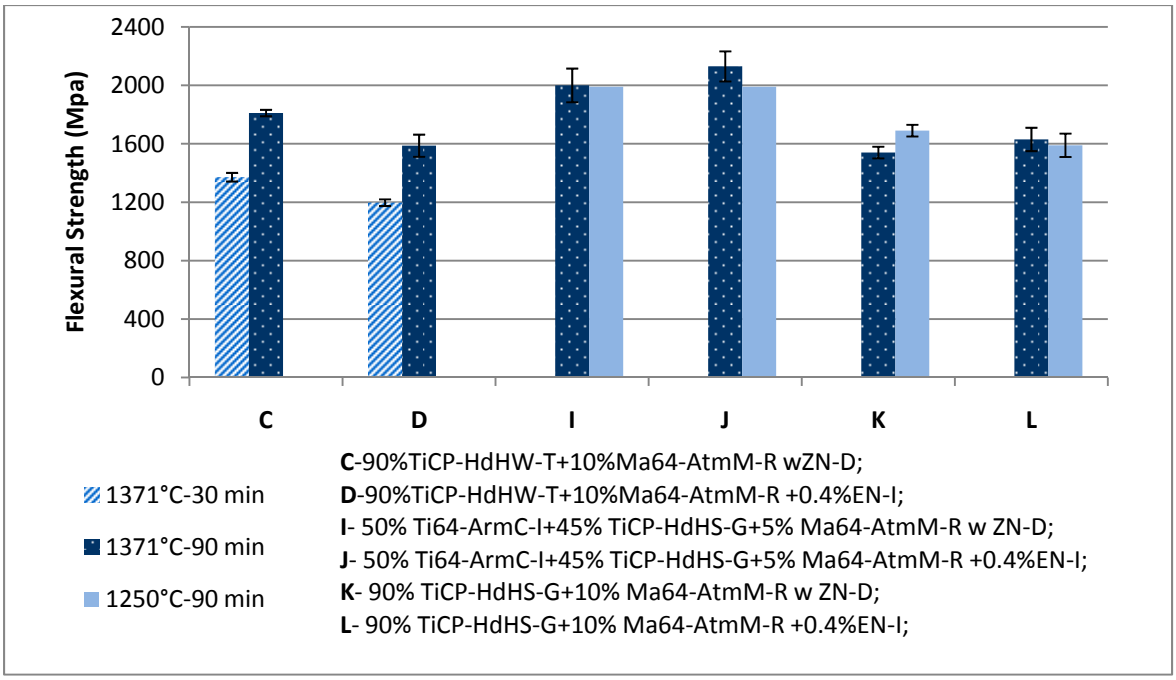


Figure VIII-5 Flexural strength (from three point bending tests) of different Blended samples of Ti64 sintered at 2500°F(1371°C) or 2282°F(1250°C) with holding times of 30 min and 90 min.

Figure VIII-5 shows the differences of the flexural strength at 30 and 90 min sintering time at the temperatures 2500°F(1371°C) and 2282°F(1250°C) for the blended Ti64 powders and their mixtures. It is also shows that extending the sintering time will improve the flexural strength. The figure shows **50%Ti64-ArmC-I+45% TiCP-HdHS-G+5% Ma64-AtmM-R** samples (I and J) with 2130 MPa flexural strength, achieved higher flexural strength than other blended samples (C, D, K and L) when sintered at 2500°F( 1371°C ) for 90 min. The blended powder mixtures all provide higher flexural strength than **TiCP-HdHW-T** powder compacts, but slightly lower flexural strength than **Ti64-ArmC-I** powder compacts.

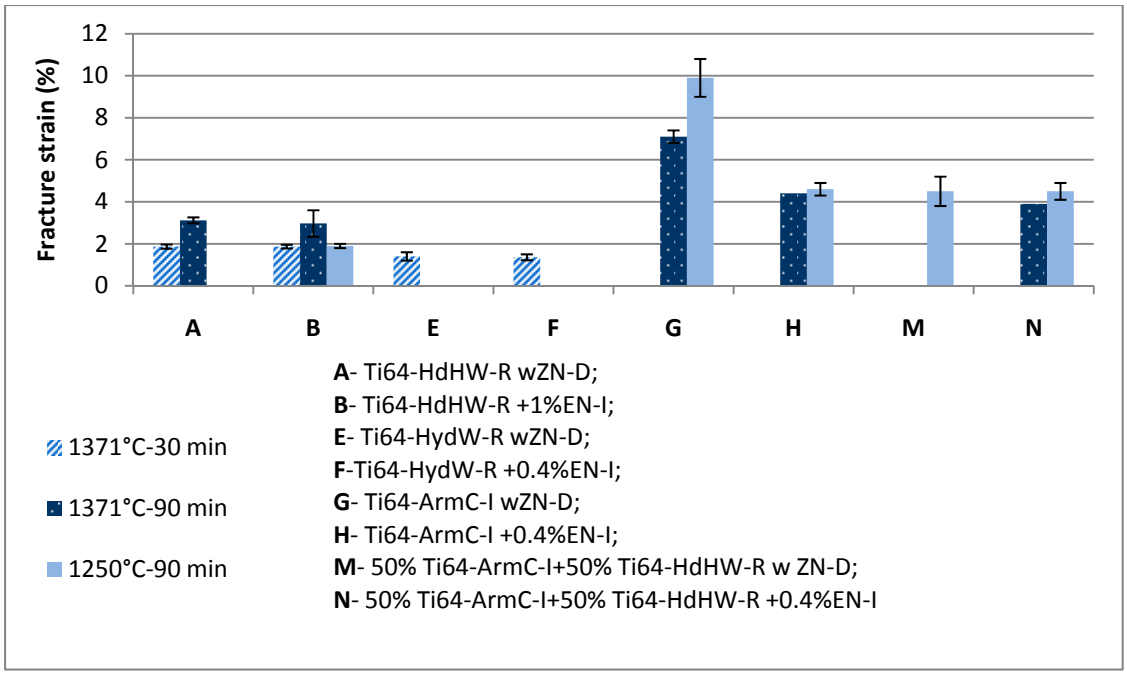


Figure VIII-6 Fracture Strain (from three point bending tests) of different pre-alloyed samples of Ti64 sintered at 2500°F(1371°C) or 2282°F(1250°C) with holding times of 30 min and 90 min.

Figure VIII-6 shows the differences of the fracture strain at 30 and 90 min sintering time at 2500°F(1371°C) and 2282°F(1250°C) for the pre-alloyed Ti64 powder and their mixtures. From sample A and B, we can see the 2500°F91371°C) -30 min. sintered specimens have lower fracture strain than the 90 min ones. The figure also shows **Ti64-ArmC-I** samples (G and H) (7.1% fracture strain) provided much higher fracture strain than **Ti64-HdHW-R** samples (A, B, E, and F) (around 3% fracture strain) when sintered at 2500°F(1371°C) for 90 min. The admixed samples M and N (**50% Ti64-ArmC-I+50% Ti64-HdHW-R**) obtain around 4% fracture strain. The **Ti64-ArmC-I** powder with die wall or 0.4%EN-I obtain almost the same sintered density but show a large difference in Fracture Strain. The **50%Ti64-ArmC-I+50%Ti64-HdHW-R** specimens show only a small difference in fracture strain between ZN-D and 0.4%EN-I when sintered at 2282°F(1250°C) for 90 min. The **Ti64-ArmC-I** die wall lube 2282°F(1250°C) /90 min specimens show the best combination of strength (322 KSI) and fracture strain (10%). One reason is the relatively high sintered density and rounded pores, the other is the ZN-D specimens possess a lower oxygen equivalency compared with the 0.4%EN-I specimens, because there is an increase in impurities when internal lube is added. Most of the lubricant will burn off during the de-lube process, but due to the sensitivity of the ductility of Ti to interstitial content, internal lubrication can be a problem to the mechanical properties. The internal lube specimens for **Ti64-ArmC-I** compacts have almost half the ductility compared with the ZN-D specimens.

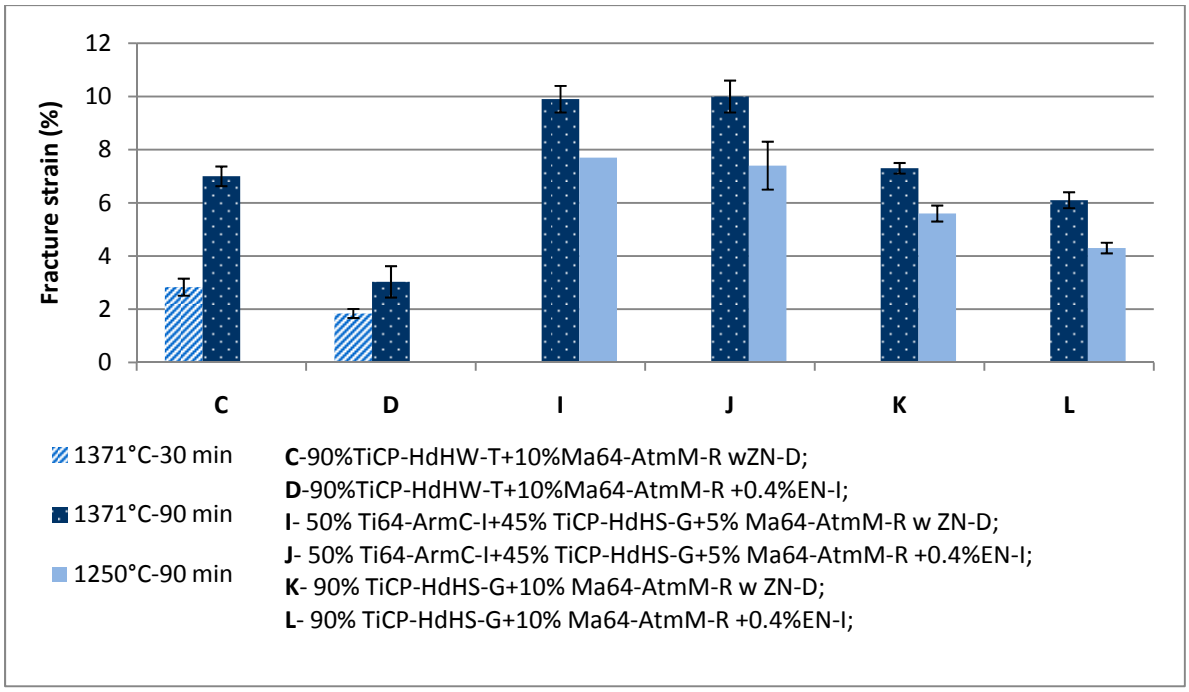


Figure VIII- 7 Fracture Strain (from three point bending tests) of different Blended samples of Ti64 sintered at 2500°F(1371°C) or 2282°F(1250°C) with holding times of 30 min and 90 min.

Figure VIII-7 shows the differences of the fracture strain with 30 and 90 min sintering times at 2500°F(1371°C) and 2282°F(1250°C) for the blended Ti64 powders. Powder Blends I and J (**50% Ti64-ArmC-I+45% TiCP-HdHS-G+5% Ma64-AtmM-R**) obtained the highest fracture strain (10%) when the samples were sintered at 2500°F(1371°C) for 90 min. In this figure VIII-7, it is obvious that 2282°F(1250°C) -90 min sintered sample and 2500°F(1371°C) -30 min sintered samples both have lower fracture strain than the 2500°F(1371°C) -90min samples.

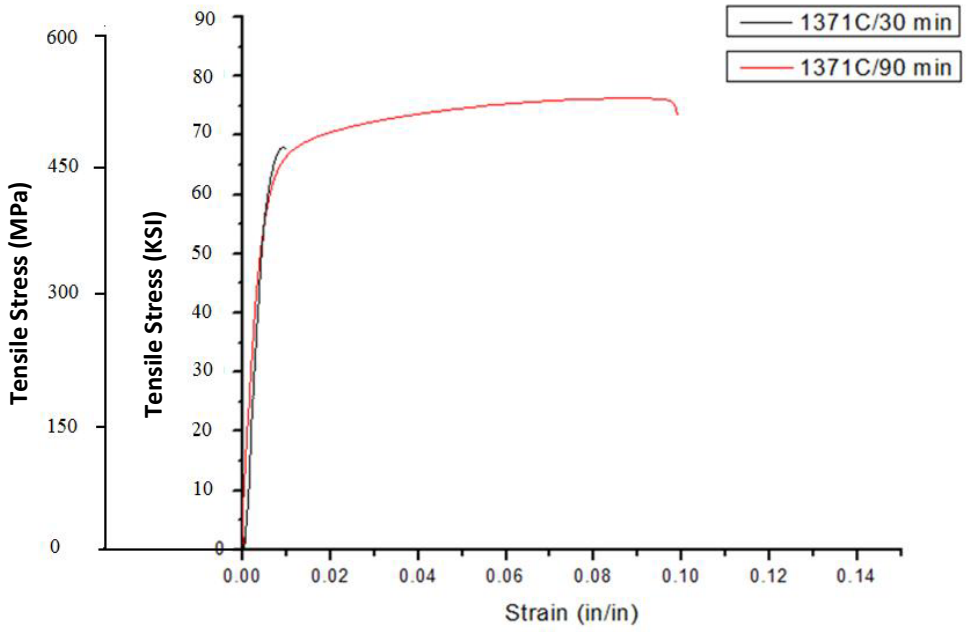


Figure VIII-8 Fracture stress-strain curves of **TiCP-HdHS-G +0.4%EN-I** specimens for different sintering times at 2500°F(1371°C)

Figure VIII-8 shows the effect of sintering hold time on the fracture stress strain curve of a sample **TiCP-HdHS-G + 0.4%EN-I**.The sample sintered at 2500°F(1371°C) for 90 min. showed a much higher fracture strain (about 10%) versus the 30 min. sample. This difference is caused by the extensive rounding of the pores and higher density of the 90 min. sample.

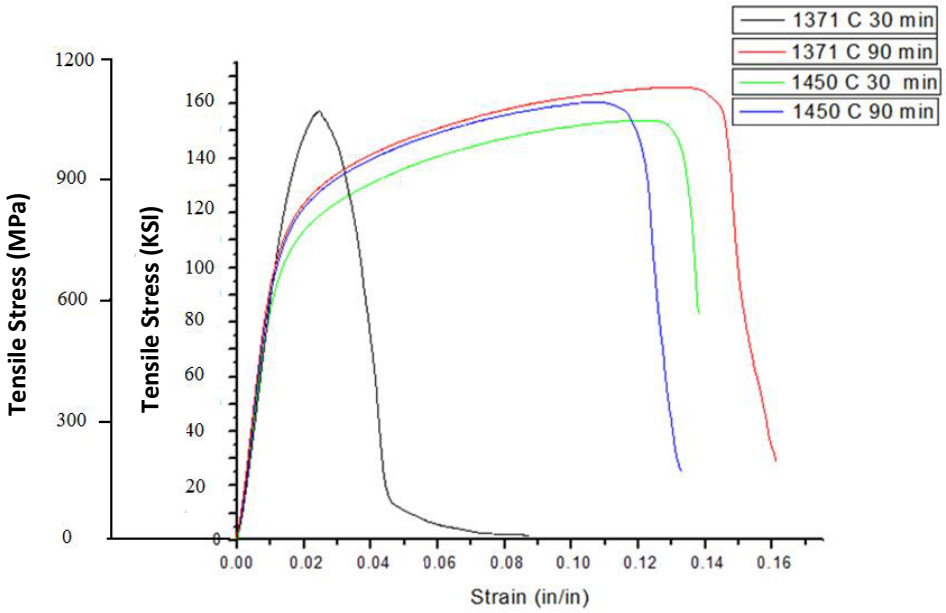


Figure VIII- 9 Fracture stress strain curve of **TiCP-HdHS-G +0.4%EN-I** specimens for different sintering temperatures (2500°F(1371°C) and 2642°F(1450°C)) and hold times (30 min. and 90 min.).

Figure VIII-9 shows the effect of sintering hold time and temperature on the fracture stress strain curve of a sample **TiCP-HdHS-G + 0.4%EN-I**. Two temperatures (2500°F(1371°C) and2643°F(1450°C) and two hold times (30 min. and 90 min.) are used. From Figure VIII-9, we can see that the best stress strain curve is achieved at 2500°F(1371°C) and 90 min. hold time. Even though the 2642°F(1450°C) and 90 min. hold time achieved a higher density, the fracture strain falls short of the 2500°F(1371°C) 90 min. curve. The lower fracture stain is probably caused by grain coarsening at the higher temperature. For these samples sintering becomes rapid around the alpha-beta transformation temperature but most shrinkage occurs during the hold at the sintering temperature.

Ti64

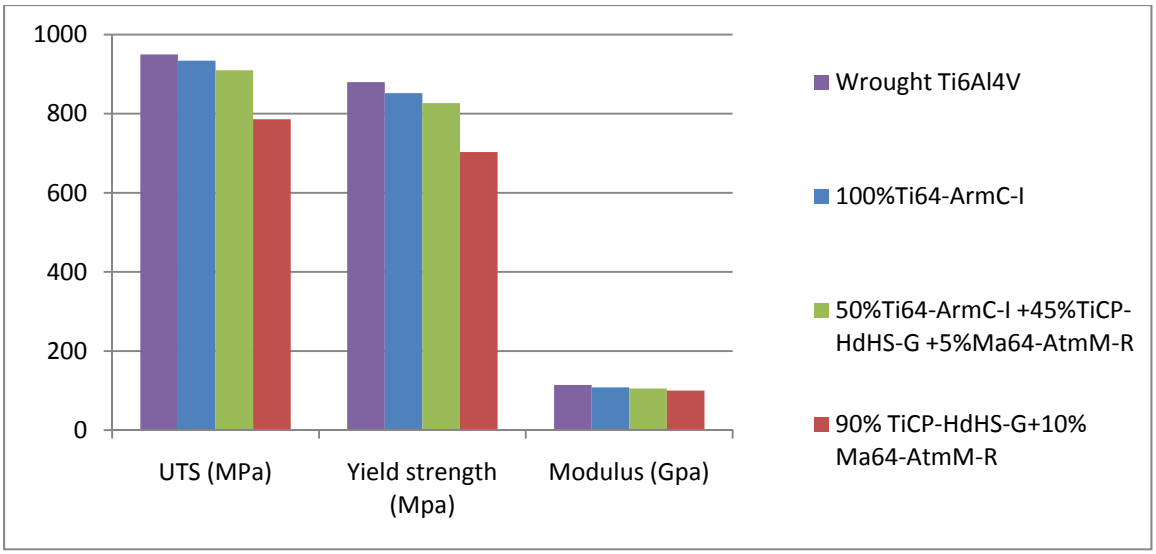


Figure VIII-10: UTS, Yield strength, and Young's modulus of Wrought Ti64 with **Ti64-ArmC-I**, **90% TiCP-HdHS-G+10% Ma64-AtmM-R** and **50%Ti64-ArmC-I+45%TiCP-HdHS-G+5%Ma64-AtmM-R** specimens.

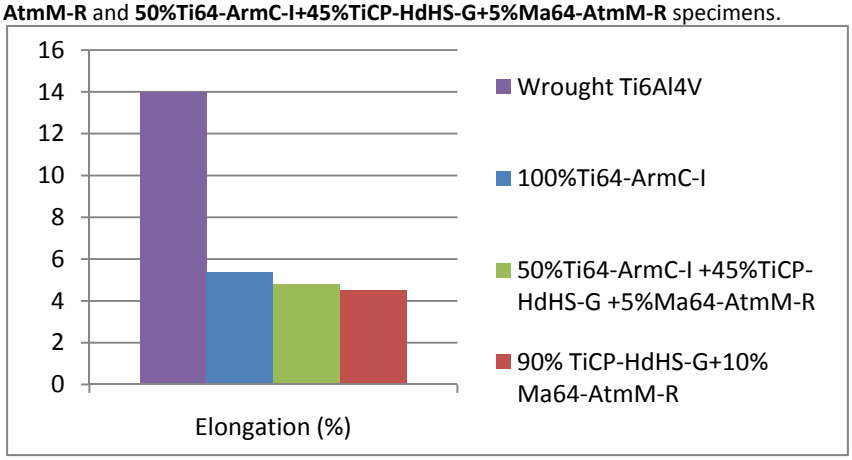


Figure VIII-11 Elongation of Wrought Ti64 with **Ti64-ArmC-I**, **90% TiCP-HdHS-G+10% Ma64-AtmM-R** and **50%Ti64-ArmC-I+45%TiCP-HdHS-G+5%Ma64-AtmM-R** specimens.

In figures VIII-10 and VIII-11, we see the comparison of the Tensile Properties for wrought Ti64 with **Ti64-ArmC-I**, **50%Ti64-ArmC-I+45%TiCP-HdHS-G+5%Ma64-AtmM-R**, and **90%TiCP-HdhS-G+10%Ma64-AtmM-R** titanium powders and blends. We can see from the figures VIII-10 and VIII-11, that all 3 of the powder samples and blends come within 10% of the UTS and Yield Strength, however the elongation is only about 35% of Wrought Ti64 [7]. The primary difference in the Elongation is caused by the higher porosity and the interstitials of the Ti64 P/M samples.

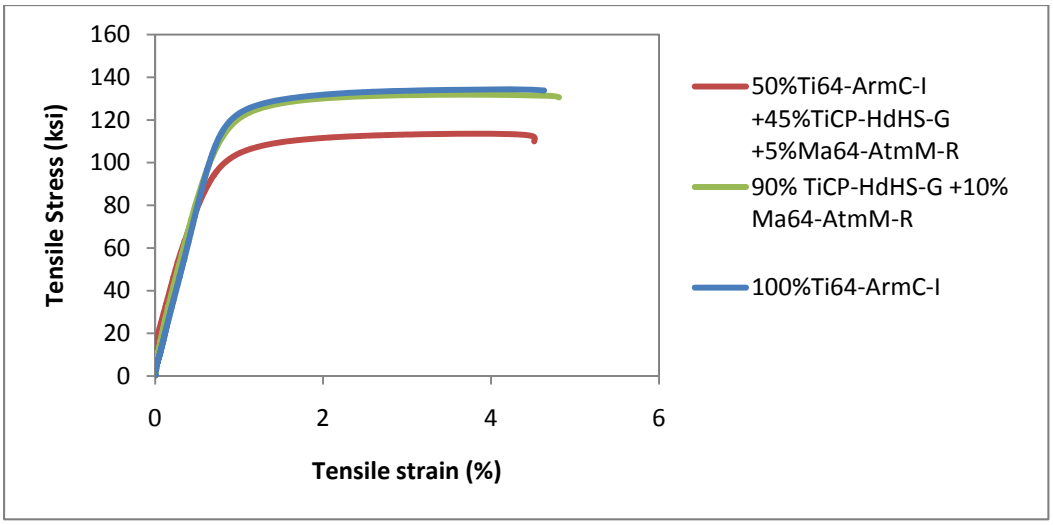


Figure VIII-12 Tensile stress strain curves of **Ti64-ArmC-I**, **90% TiCP-HdHS-G+10% Ma64-AtmM-R** and **50%Ti64-ArmC-I+45%TiCP-HdHS-G+5%Ma64-AtmM-R** specimens.

Figure VIII-12 shows the stress strain curves for **Ti64-ArmC-I**, **90%TiCP-HdHS-G+10%Ma64-AtmM-R** and **50%Ti64-Armc-I+45%TiCP-HdHS-G+5%Ma64-AtmM-R** sintered compacts. Of the 3 samples in Figure VIII-12, **Ti64-ArmC-I** has the highest Young's Modulus (108 GPa) and UTS (934 MPa), which compares favorably with wrought Ti64's Young's Modulus of 114GPa and UTS of 950 MPa. The other powder blends come close, but are not as high as the **Ti64-ArmC-I** sintered compact. The Elongations for all 3 sintered compacts are around 5%.

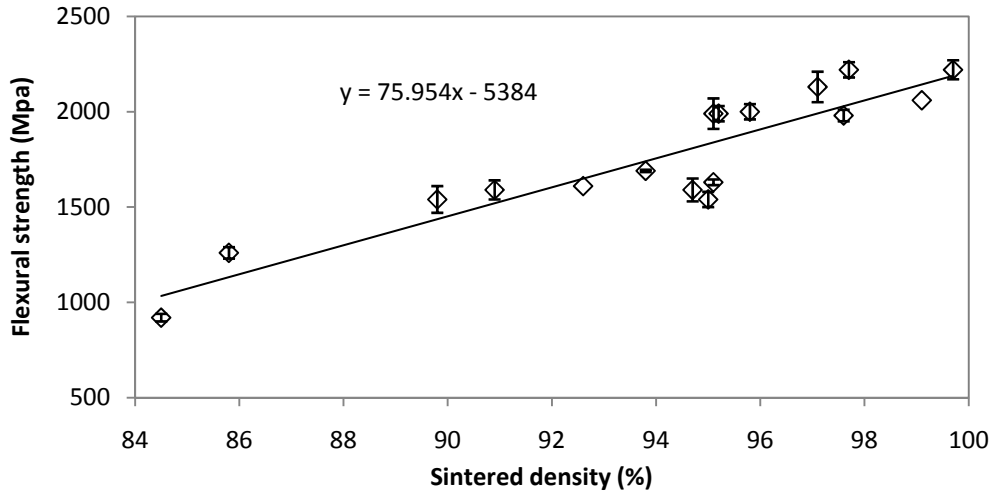


FigureVIII - 33: Flexural Strength versus Sintered Density of Ti64 sintered compacts (all kinds).

Using existing data from many different sintered compacts, in Figure VIII-13 we plotted the average flexural strength versus density. The curve turns out to be very linear. Flexural strength shows good correlation (linear relationship) with the sintered density regardless of the kind of powder mixture and kind of lubricant used. Flexural strength shows a linear relationship with sintered density, which can be fitted as: $y = 74.406x - 5243.1$, where x is sintered density in %, and y is flexural strength in Mpa. From this relationship we can conclude that the main determinant of Flexural Strength of Ti64 sintered compacts is the sintered density.

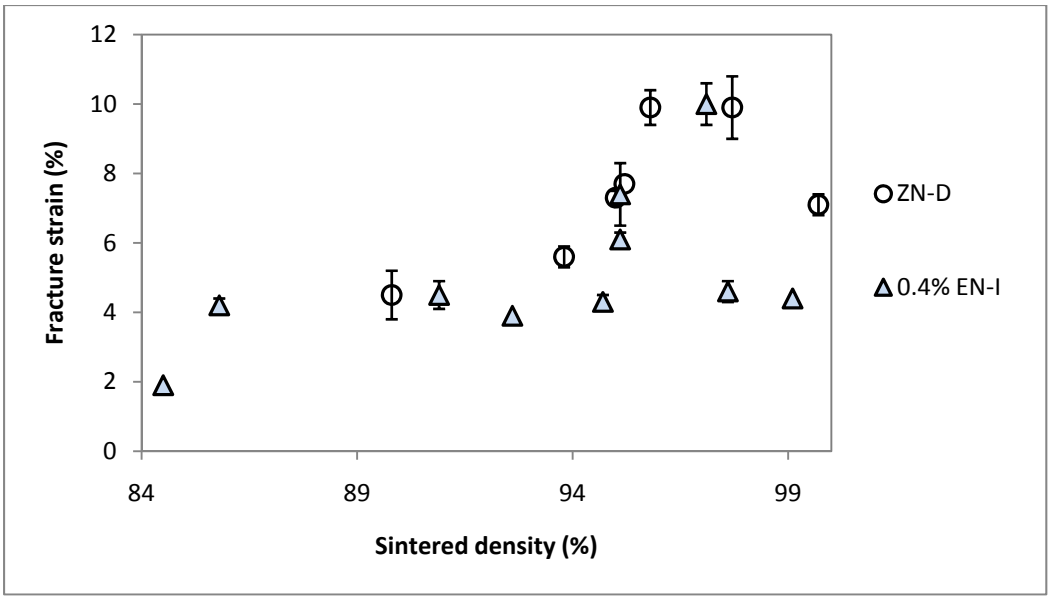


Figure VIII-14: Fracture Strain versus Sintered Density of Ti64 sintered compacts (all kinds).

Using existing data from many different sintered compacts, in Figure VIII-14 we plotted the average fracture strain versus density. In this case, the fracture strain shows considerable scatter in the range of 4% to 10% with no clear relationship to sintered density. The lubrication method (internal (EN-I) versus die wall (ZN-D)) appears to be the reason for the variation of the fracture strain. So the Internal Lube (EN-I) samples and the die wall lube (ZN-D) samples are identified separately in the plot. Even after separating the data into internal lube (En-I) samples and die wall lube samples (ZN-D), there is no clear correlation between fracture strain and sintered density for each of these samples. Most of the internal lube (EN-I) specimens' fracture strain is around 4%, because the EN-I likely adds impurities to the specimens, especially to the Armstrong powder.

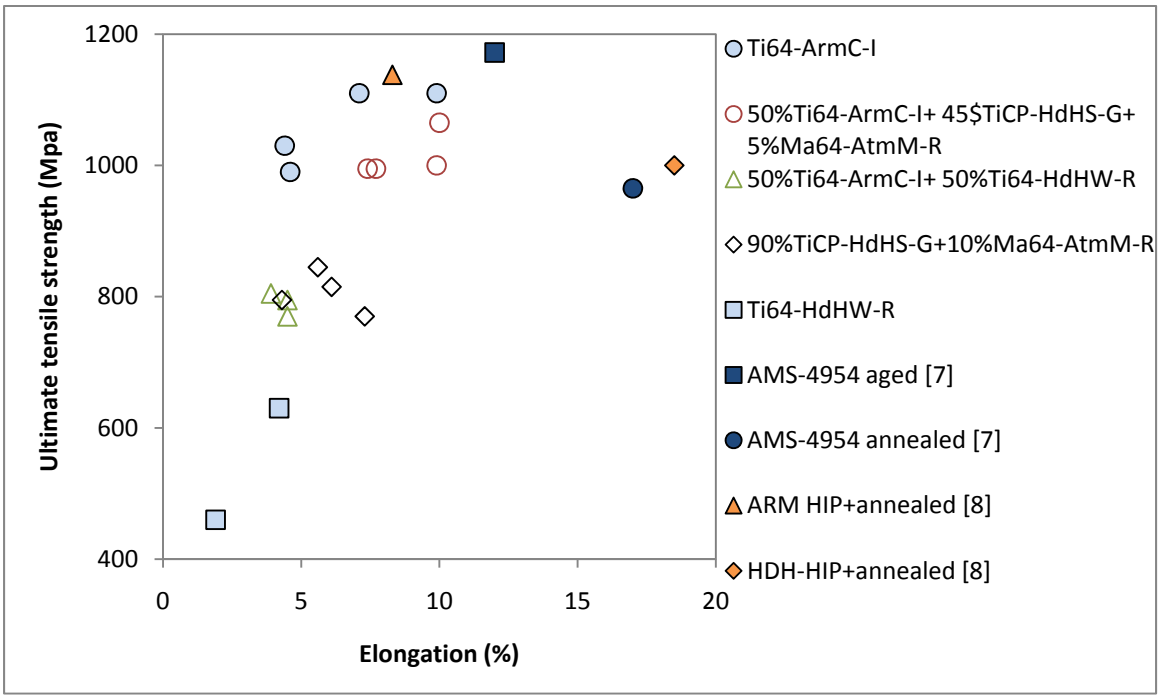


Figure VIII-15 UTS versus elongation of wrought Ti64, Hipped Ti64 and sintered powder compact

Another way to look at the Tensile Properties of Ti64 materials is to plot the UTS versus Elongation on a graph. In the case of Figure VIII-15, using our existing data for sintered compacts of **Ti64-Armc-I**, **50%Ti64-ArmC-I+50%Ti64-HdHW-R**, **50%Ti64-ArmC-I+45%TiCP-HdHS-G+5%Ma64-AtmM-R**, **90%TiCP-HdHS-G+10%Ma64-AtmM-R**, with other powder data and wrought data.

To compare our results with wrought Ti6/4 (AMS-Aerospace Material Specification) and other PM Ti6/4, we converted flexural strength to ultimate tensile strength by assuming it is 50% of the flexural strength (based on our experiments). The HIP data are from published literature [8] which also used **Ti64-ArmC-I** powder. The HIP'ed samples were pressed, sintered, Hot Iso-static Pressed (HIP) and annealed. Wrought Ti6Al4V (ASM-4954) mechanical data either aged or annealed are taken from published literature [7]. Although, wrought Ti6Al4V and HIP Ti6Al4V provide higher ductility than our single press and sinter specimens, the comparative results for the press and sinter only samples are very good, with UTS values as high as 1100 MPa and Elongation as high as 10%.

In summary, press and sinter Titanium technology can come very close to achieving the properties of wrought Ti materials.

## IX. Summary of Process Results

Having completed a major study of the available Titanium Powders and the results of our press and sinter processing evaluations, what conclusions can we begin to draw from these studies? Also how can we use this information to assist us in designing a process for a specific application or part. I have prepared a summary chart that includes the powder characteristics and the key processing results for TiCP and Ti64 press and sinter materials. These are the 4 (1 TiCP and 3 Ti64) powders that performed the best in press and sinter applications.

| Powder/Process of Interest | Apparent Density g/cc | Hall Flow Sec. | Green Density at 50 TSI g/cc | Sintered Density 2500F(1371C) g/cc | UTS KSI | Yield Strength KSI | Elongation % |
|---|---|---|---|---|---|---|---|
| TiCP-HdHS-G | 1.62 | 34 | 85% | 96% | 76 | 65 | 9 |
| Ti64-ArmC-I | 0.67 | Non-flow | 75% | 99% | 134 | 123 | 5.50% |
| 50%Ti64-ArmC-I + 45%TiCP-HdHS-G + 5%Ma64-AtmM-R | 1.01 | 40 | 81% | 97% | 130 | 119 | 5% |
| 90%TiCP-HdHS-G + 10% Ma64-AtmR | 1.61 | 30 | 83% | 95% | 113 | 101 | 4.50% |

Table X-1 Properties of TiCP and Ti64 powders and processing

As you can see in the table X-1, all of the powders give respectable results for Tensile properties, with the Armstrong powders generally giving the highest properties for Ti64 due to their high sintered densities. We were not able to process Armstrong TiCP powder due to availability of powder. We believe it should give results similar to the **Ti64-ArmC-I** powder when it is available.

When designing a press and sinter process for an application or a part, the choice of powder will be based on the geometry of the part. As a general rule of thumb, if the part is tall (greater than 1.0”) then a powder with a low apparent density will be a handicap for part compaction. Therefore we would probably choose a hydride de-hydride powder (**TiCP-HdHS-G**) to simplify the tool design.

However, if we had a fairly thin part, with a simple geometry, the Armstrong powder would do quite well.

The good news is that there are several powders available, and we can choose the best powder and properties to meet the objective of the part or the application.

## X. - Application to a vehicle part – Oshkosh Corporation

Our first objective in developing a part for a vehicle application was to find a vehicle manufacturer who would be willing to work with us on the development of a Titanium part for a vehicle application. This would require a manufacturer who had the interest, was willing to commit internal resources for testing, and had the metallurgical capabilities to evaluate our results. The Webster-Hoff sales and marketing team were able to find a good match for the project, and we reached agreement with the management of Oshkosh Corporation to proceed with the project. The agreement was that Webster-Hoff would provide sample Titanium parts and Oshkosh Corporation would test the parts in the application. The Oshkosh Corporation project manager assigned to the team was Chad Johnson – Project Materials Engineer.

A. Selection/design of a part

The process involved reviewing several parts suggested by Oshkosh Corporation for potential design with Titanium. Oshkosh Corporation wanted to find a part where strength to weight is an important consideration, where the benefits of Titanium could be realized. After several rounds of discussion, we settled on the "Pillow Block", which is shown in Figure X-1 below. The criteria for selecting this part was based on the fact that the part is used in the suspension where weight is critical, and attempts to convert the part from steel to aluminum were not successful because Aluminum did not have the required strength. The part is manufactured by machining the part from a block of steel or aluminum.

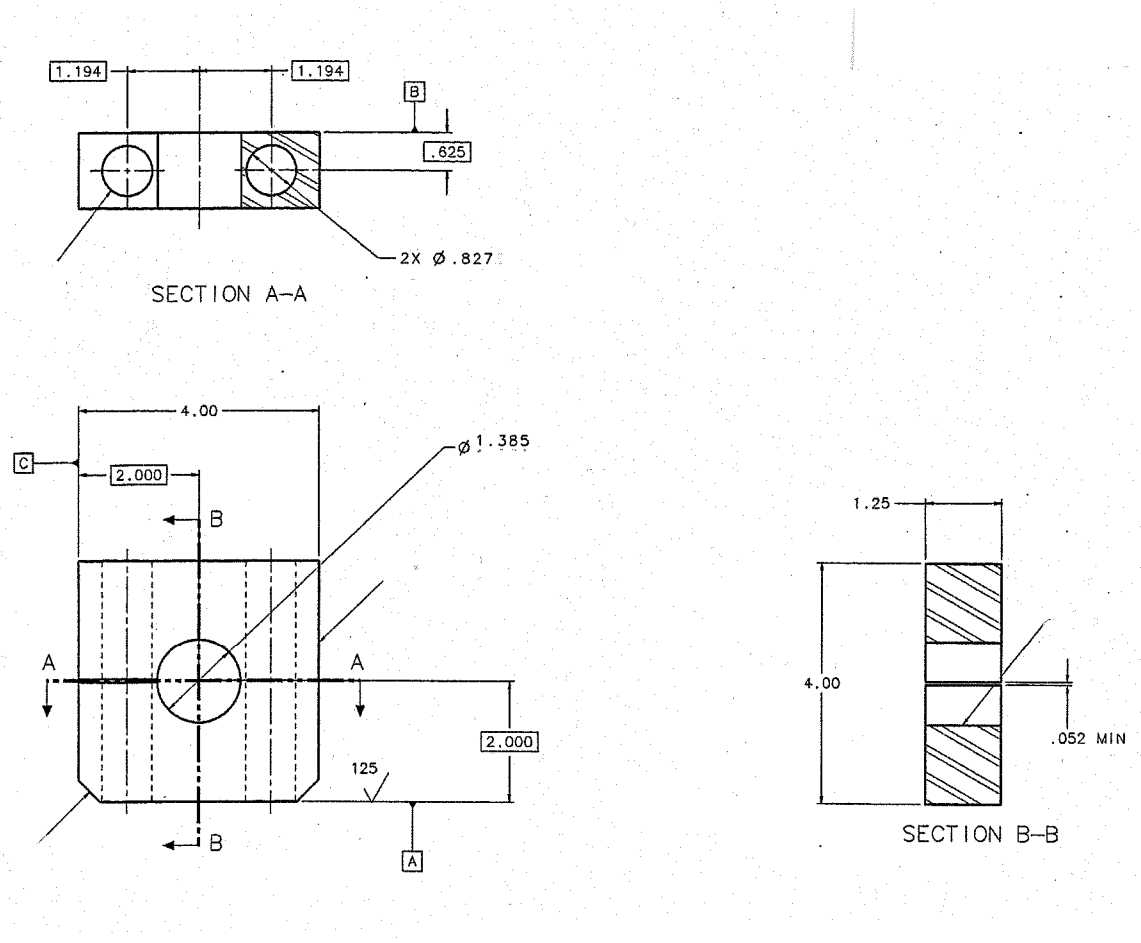


Figure X-1 Original Part Design Pillow Block cross section

One of the major benefits of the Powder Metallurgy process is to manufacture the part net shape (with no machining operations). This is particularly important for Titanium, since Titanium is very difficult to machine. The part as shown in Figure X-1 cannot be manufactured via Powder Metallurgy to a net shape, it has to be machined.

Webster-Hoff proposed changing the design to a 2 piece construction. The result of that design effort is shown in Figure X-2, Pillow Block for PM Processing. In this case, there are 2 parts, a long version (2.0" tall), and a short version (1.38" tall). With appropriate tool design, both parts can be manufactured from the same tool, thereby saving tool cost. The parts are assembled prior to use on the truck suspension

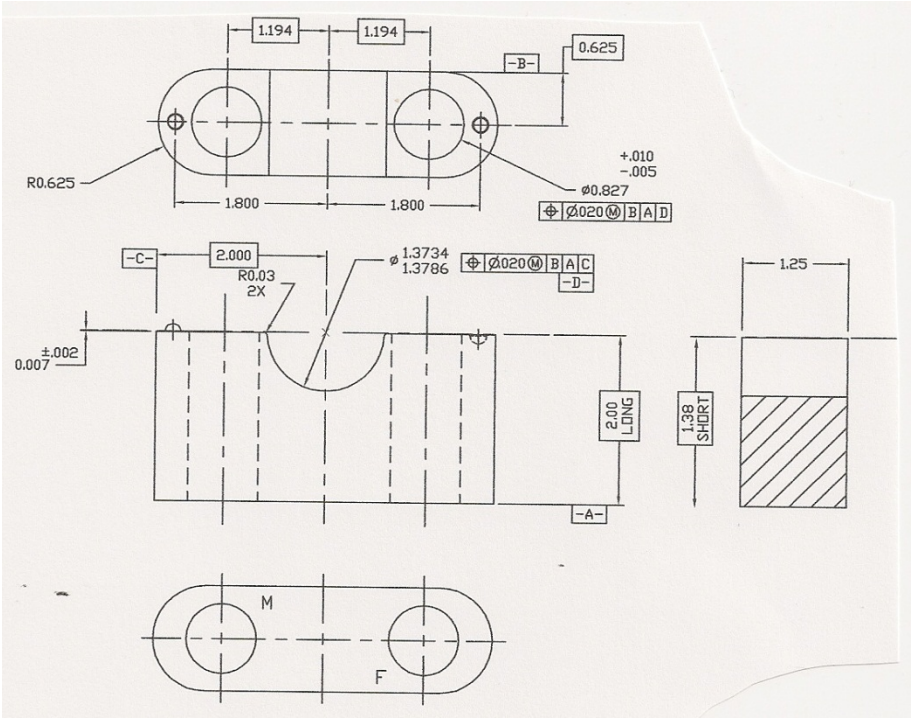


Figure X-2 Webster-Hoff version of Pillow Block for PM Net Shape Processing

B. Design of the process

The process for manufacturing the parts from Titanium would be the Press and Sinter process as evolved from the work done previously with sample powders and processes. The powder would be compacted in a tool to achieve the highest possible green density, and then sintered in a vacuum. This seems simple enough, but again the physical aspects require that the proper selection of powder and tooling be chosen to be able to manufacture the part.

The long part is 2.0" tall after sintering, therefore the die fill height must be based on the compaction ratio of the powder (the apparent density of the powder). If we were to choose **TiCP-ArmC-I** powder for this application, with an apparent density of .68 g/cc (fill ratio of approximately 5:1), then the die depth would have to be more than 10.0" deep. This 10" die depth is totally impractical for a tool design on Webster-Hoff presses. The die would be so large that it would not fit in the press. The maximum fill on our largest press is 7.0". So for this application we chose to use **TiCP-HdHS-G** powder which has an apparent density of 1.67 g/cc, with a fill ratio of 2.1:1. We also determined that internal lubrication would be required to enable ejection of the part from the tooling. So the powder chosen was **TiCP-HdHS-G + 1.0%EN-I**, which includes 1.% internal lubrication.

To evaluate the part with Ti64 material, we chose to use a blended master alloy material, **90%TiCP-HdHS-G + 10%Ma64-AtmM-R + 1.0%EN-I**. This material also included 1.0% internal lubrication to facilitate part ejection.

C. Tool Design

The tool drawings for the Oshkosh Part are shown in the Appendix (includes the die, upper punch, lower punch and core rods). We designed the tool for a compaction ratio (fill ratio) of 3:1. This will allow us some flexibility in the choice of powder for the application. The selection of material for the die and core rods was carbide. The Titanium powder is very abrasive, and from experience we chose the hardest tool material (Carbide tool steel) for wear resistance. To achieve the net shape of the part, the part is oriented vertically in the die so that the cored holes could be included. Drilling those holes in Titanium material would be very costly. To provide a smooth form for the clamp radius (1.380/1.385) the shape was included on the face form of the lower punch. We would later add a die splash form on the die to compensate for the different fill heights (to achieve even density).

## XI. - Processing the part – Oshkosh Corporation

Having completed the design and build of the tool for the Oshkosh Corporation Part, we proceeded to manufacture the prototype parts based on our designed process. We initially worked with several different powders to determine which would work best in the tooling we designed. We also made changes to the tooling to improve the die filling and ejection of the parts. Our build of prototype parts for testing at Oshkosh Corporation included 2 materials TiCP (**TiCP-HdHS-G + 1.0%EN-I**) and Ti64 (**90%TiCP-HdHS-G + 10%Ma64-AtmM-R + 1.0%EN-I**). Our goal was to provide the 2 basic alloys for testing at Oshkosh Corporation.

### A. Powder Blending

The powders were blended in a small Patterson V-Blender for 30 minutes. Because of the pyrophoric nature of the powder, they were blended in small lots (about 10 lbs.) with appropriate safety devices on hand in case of a fire. After thorough blending the powder was checked for its characteristics and found to have the following properties. For the **TiCP-HdHS-G + 1.0%En-I** the apparent density was 1.67 g/cc, and the hall flow rate was 35 sec. For the **90%TiCP-HdHS-G + 10%Ma64-AtmM-R + 1.0%EN-I** the apparent density was 1.61 g/cc, and the hall flow rate was 39 sec.

### B. Compaction

The 2 powders were compacted in the Oshkosh Corporation tool using the Webster-Hoff 250 Ton Hydraulic press forming both the short and long versions of the part. For the short versions of the part, were able to achieve a green density of 3.45 g/cc for both TiCP and Ti64 materials. For the long versions of the parts were able to achieve a green density of 3.23 g/cc. The difference in density between short and long parts is due to the difference in overall height and the density gradient from top to bottom of the part.

### C. De-Lubrication

The removal of lubricant from the green part was completed using the partial vacuum method developed by Webster-Hoff and IIT. The parts contain 1.0% internal lubricant, which was removed and verified by weight reduction. An additional de-lubrication step was included at sintering by holding the parts at 750°F(400°C) for 30 min. in a vacuum.

### D. Sintering

Because of the size of the parts, we had to sinter them in a large commercial furnace. The photos in the Figure XI-1 shows the parts in the furnace and orientation on the sintering plates. As you can see, the capacity of the furnace is quite large and will process at least 100 parts at a time.

Figure XI-1 DSH Sintering Photos

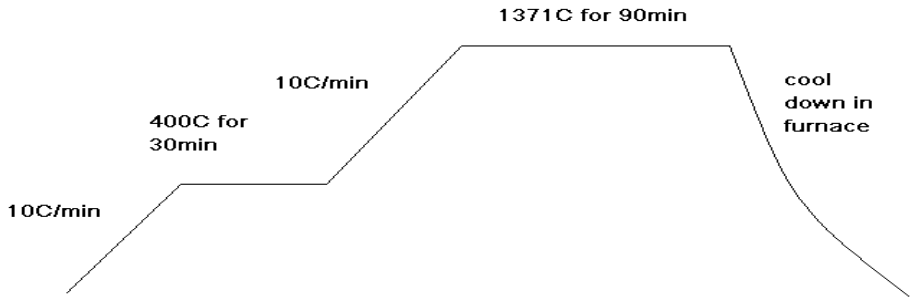


Figure XI-2 DSH Sintering Profile

The sintering temperature profile is shown in Figure XI-2. Note the hold at 400 C for 30 min. was used as an extra de-lube process and temperature stabilization for the large furnace.

| Sample | Green Density | | Sintered Density | | Density Change |
|---|---|---|---|---|---|
| | g/cc | % | g/cc | % | % |
| TiCP-S | 3.44 | 76% | 3.94 | 87% | 11% |
| TiCP-L | 3.23 | 72% | 3.81 | 85% | 13% |
| Ti64-S | 3.46 | 78% | 4.04 | 91% | 13% |
| Ti64-L | 3.23 | 73% | 3.9 | 88% | 15% |

Table XI-2 Density Changes

The density changes from green to sintered is shown in Table XI-2. In general, you will see that the increase in density for the long parts (TiCP-L and Ti64-L) is about 2% greater than the short parts (TiCP-S and Ti64-S). This seems to be a result of the starting lower green density. You will also notice that the Ti64 parts increase density by about 2% more than the TiCP parts for both sizes (S & L). This is a result of the accelerated sintering caused by the liquid phase sintering of the Master Alloy addition.

Note that both TiCP and Ti64 start with the same base powder **TiCP-HdHS-G**. The difference is the 10% addition of the master alloy **Ma64-AtmM-R** for the Ti64 parts.

## XII. - Test of part in application – Oshkosh Corporation

The proof of the pudding is in the eating, so the true test of our prototype parts in the application. Oshkosh Corporation agreed to build a test fixture to compare the loading of the Titanium prototype parts and compare the results with steel and aluminum parts. The engineering test report from Oshkosh Corporation is included in this report. However to understand the report requires a bit more narrative, since the report was written for engineers very familiar with the design and its application.

The pillow block is used as a mounting mechanism for a control arm on the suspension of the wheel.

Figure XIII-1 Pillow Blocks Mounting the Control Arm to the Frame

The control arm is clamped to a pin (not visible in the picture), allowing rotation, and the pin is clamped to the frame with screws through the pillow block. When the pillow block is tightened to the pin, a preload is applied, which is controlled by the gap in the bore of the pillow block and the torque on the screws. The load is transmitted through the pin and the pillow block to the frame of the truck.

The test report in the appendix simulates this loading process. The testing process utilizes a strain gage mounted on the top surface of the pillow block between the mounting bolts (see report). Using Young's Modulus of the material, the movement of the strain gage can be converted to a stress load on the part. Young's Modulus is the ratio of Stress to Strain in the elastic region as the sample is loaded.

The test report has two sets of graphs for each material, "Stress during Torque up" (application of pre-load by tightening the screws on the pin), and the "Stress and Force Graph" which is the application of a maximum load that is normal to the pin and pillow block assembly using the Hydraulic Press. Because the physical geometry of the PM Pillow Blocks is different than the machined blocks, the actual loading graphs appear different. The Geometry of the PM Pillow blocks can be adjusted to provide the desired preload during "Torque up" and the effective stress range during loading.

All the specimens passed the load test without failures. Further work will be required to tune the PM design for the application.

The Titanium parts were successfully applied and tested.

CORPORATE MATERIALS & PROCESS ENGINEERING
2307 OREGON ST.
OSHKOSH, WI 54903-2566
920-235-9151

To: Tom Zwitter

From: Chadwick Johnson
Date: June x, 2011
Subject: Mechanical Testing of Titanium PM TAK-4 Pillow Block
cc: R. Hathaway

The pillow block component of the Oshkosh Corporation's TAK-4 suspension system was selected for demonstrating the feasibility of a single-press/ single-sinter technique in titanium powder metallurgy. This work was sponsored by the Department of Energy through DOE Grant NT01913. Several sets of pillow blocks were successfully manufactured in this manner by the Webster-Hoff Corporation of Glendale Heights, IL.

The Titanium PM prototype samples were submitted to Oshkosh Corporation's Test and Development center for physical testing. Two titanium grades were selected for testing: Titanium Commercially Pure (TiCP), and Titanium alloy Ti-6Al-4V. The samples were placed in a test fixture, and stressed to a proof load of 31,000 lbs. This is the maximum load the component is subjected to in application. The traditional materials for this component were also stressed in the same test fixture for comparative purposes. Oshkosh Engineering Technical Report #063 provides the details of the physical testing (attached).

The results of the physical testing showed that the Titanium PM pillow blocks passed the proof load test without failure or permanent deformation. This testing confirms that they could be used in the TAK-4 suspension application. One performance characteristic noted during physical testing was that the preload of the Titanium PM pillow blocks (e.g. after installation) was lower than that of the incumbent materials. This essentially creates a larger stress amplitude in the Titanium PM pillow blocks when exposed to cyclic stresses up to the proof load (i.e. fatigue). The difference in preload can be attributed to the difference in mechanical design of the Titanium PM pillow blocks, which is a two-piece design vs. a one-piece design. The two-piece design currently exhibits a bore size that closely matches the mating pin diameter, with up to a 0.014-inch gap allowed for closure of the two halves. Modification of the gap dimension will alleviate the difference in stress amplitude and increase the durability of the current two-piece design.

# ENGINEERING TECHNICAL REPORT

ETR #: Components ETR 063

DATE OF INCIDENT: 3-23-2011

MODEL: TAK-4

VEHICLE S/N: N/A

VEHICLE MILEAGE: N/A

VEHICLE OPERATING HOURS: N/A

PROJECT #: 5064

REQUESTED BY: Chad Johnson

SUBJECT: Pivot Block Stress Measurement; Test Request 189


Executive Summary

Loads (with a shop press) were placed on four pivot blocks made of different materials (aluminum, steel, TiCp and Ti-6-4) to evaluate each material. The aluminum and steel blocks exhibited a lower stress increase when the load was applied versus the Ti. This is desirable since this would lower the overall stress amplitude and make the piece more resistant to fatigue failure. However the overall geometry of the pieces and the fitment of the pin in the bore will influence this characteristic as well.


Table of Contents



TECHNICIAN: Mark White

REPORTED BY: Matt Zietlow

TIME TAKEN: One day

DISTRIBUTION: Rob Anderson, Don Knurr, Chad Johnson

Objectives: To evaluate pivot blocks made of 4 different materials: Aluminum, Steel, TiCp and Ti-6-4.

Setup/Procedures:

1. Strain gages were applied to the 4 pivot block material samples (Figure 1).

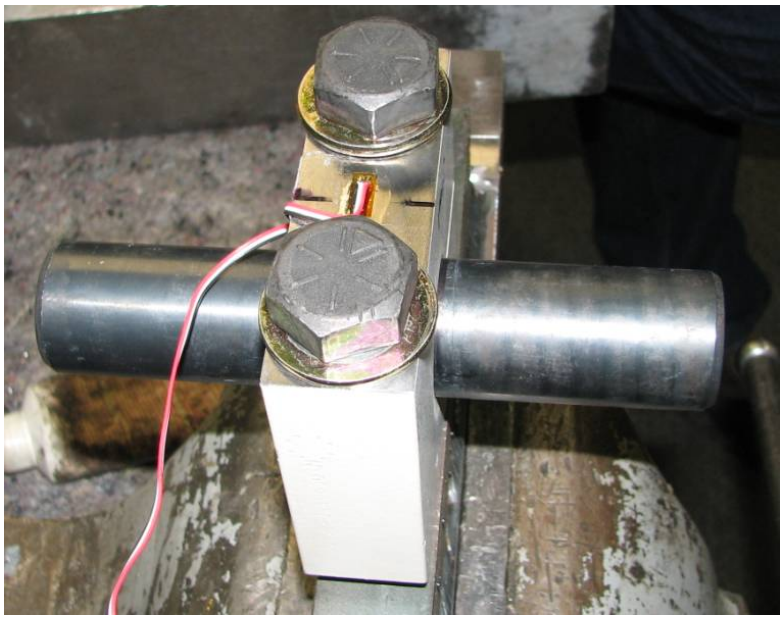

Figure 4

2. A fixture and push block (using other pivot blocks to apply force to the pin) was fabricated to allow load to be placed on the pivot block in the shop press. Mounting and fixture assembly shown in Figures 2, 3 and 4.

Figure 5

Figure 6

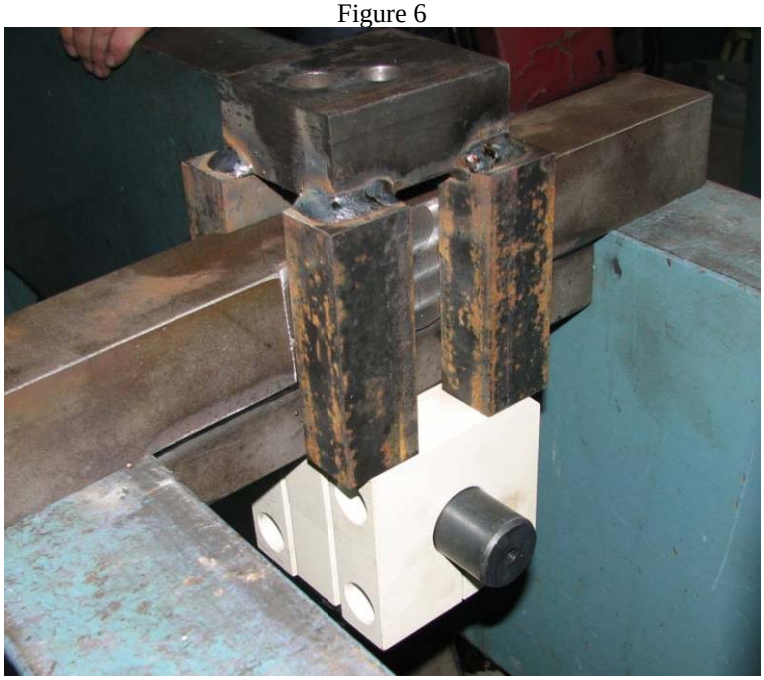

Figure 7

3. The fixture was secured in a vise and the strain gage was connected to data acquisition sampling at 10 Hz. The pivot block bolts where then torqued to 280 ft-lbs in a crossing pattern (Figure 5)

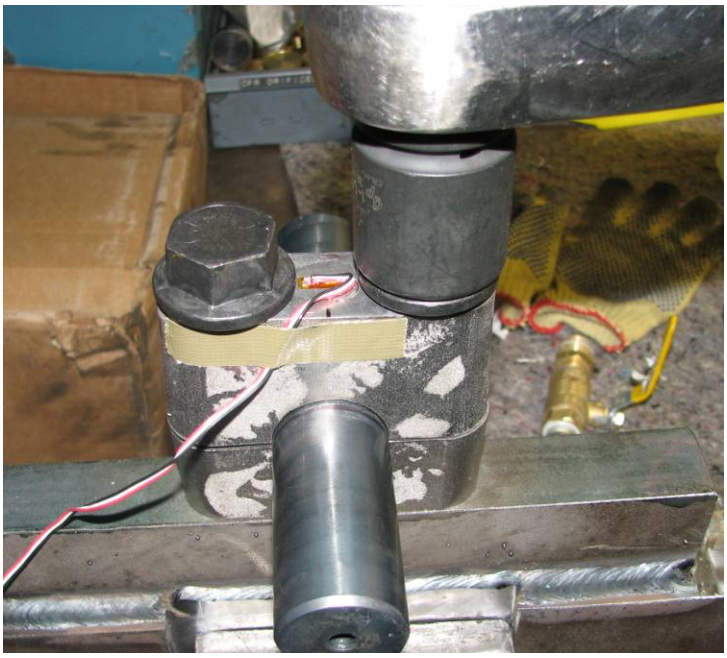

Figure 8

4. The fixture was then placed in the 100 ton shop press (Figure 4) and a pressure transducer (for press hydraulic pressure) was connected to the data acquisition sampling at 10 Hz.

   Note: hydraulic pressure was logged instead of a load cell due to the lack of a large enough compressive load cell

5. The press pressure was increased slowly until 1500 PSI was reached (~ 31,000 lbs)
6. This procedure was repeated for the 4 materials (aluminum, steel, Ti-6-4, TiCp)

Test Results:

Torque Up Results:

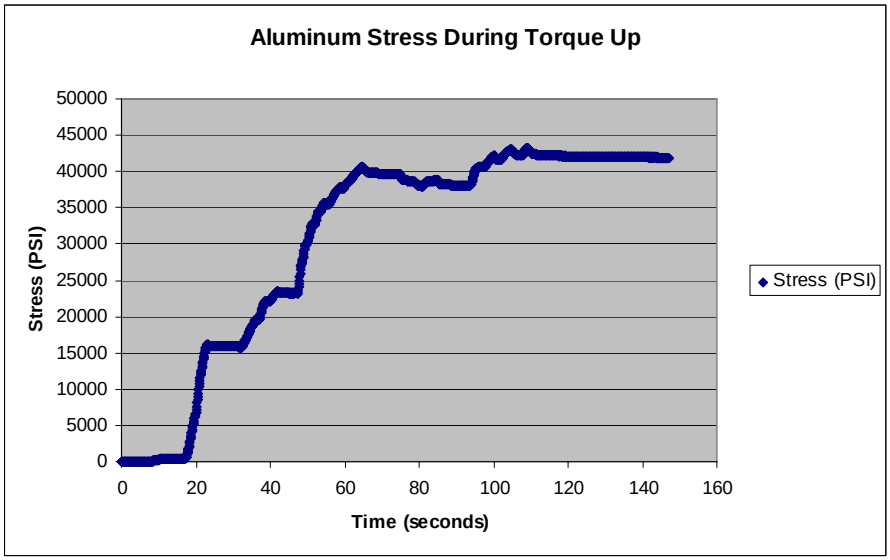

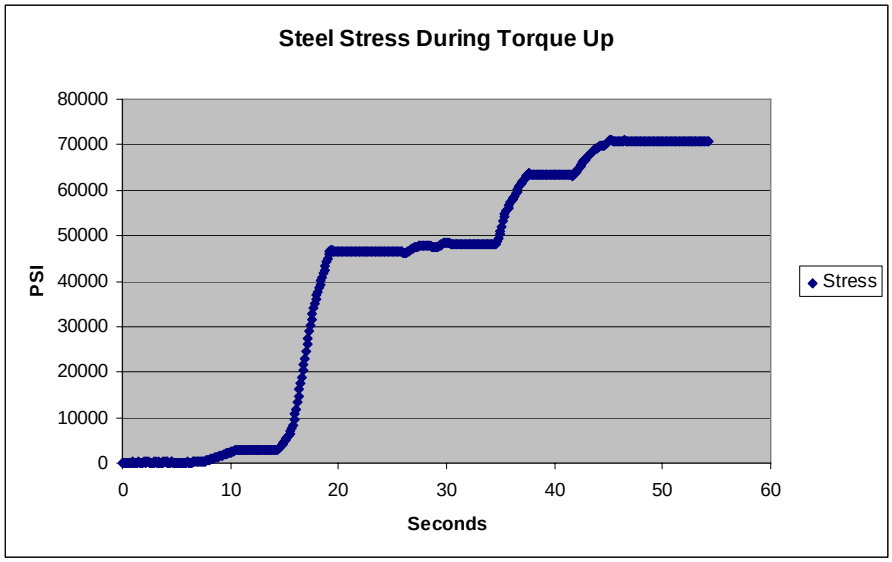
Steel Stress During Torque Up
80000
70000
60000
50000
40000
30000
20000
10000
0
PSI
0
10
20
30
40
50
60
Seconds
Stress

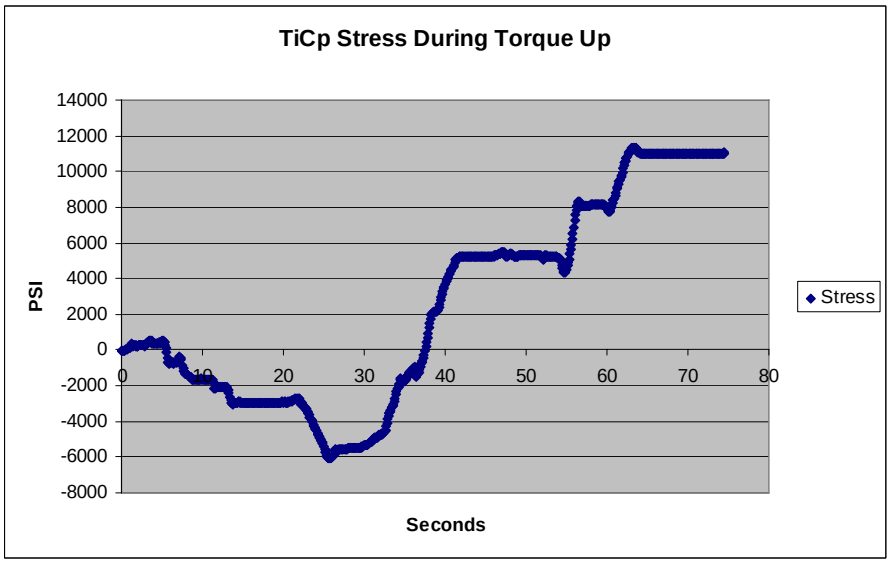
TiCp Stress During Torque Up
14000
12000
10000
8000
6000
4000
2000
0
-2000
-4000
-6000
-8000
PSI
0
10
20
30
40
50
60
70
80
Seconds
Stress

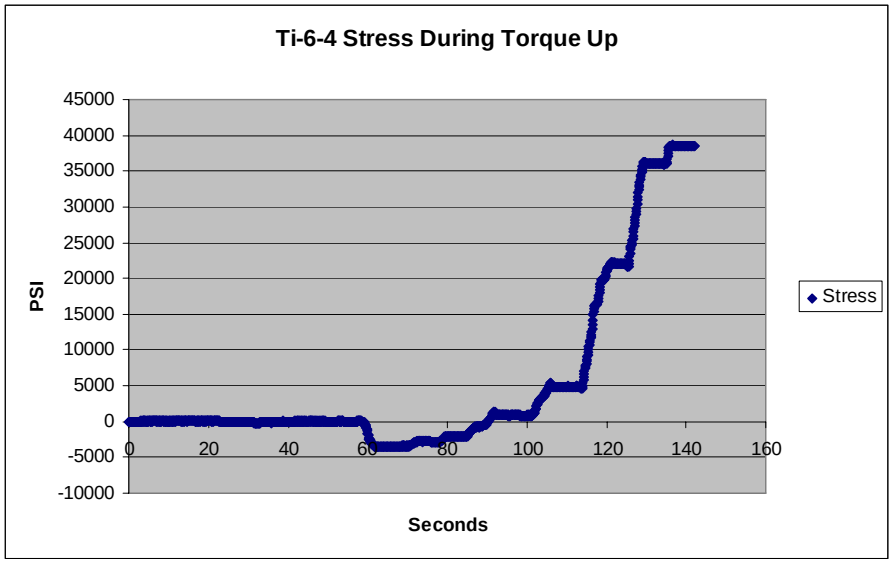


Press Results:

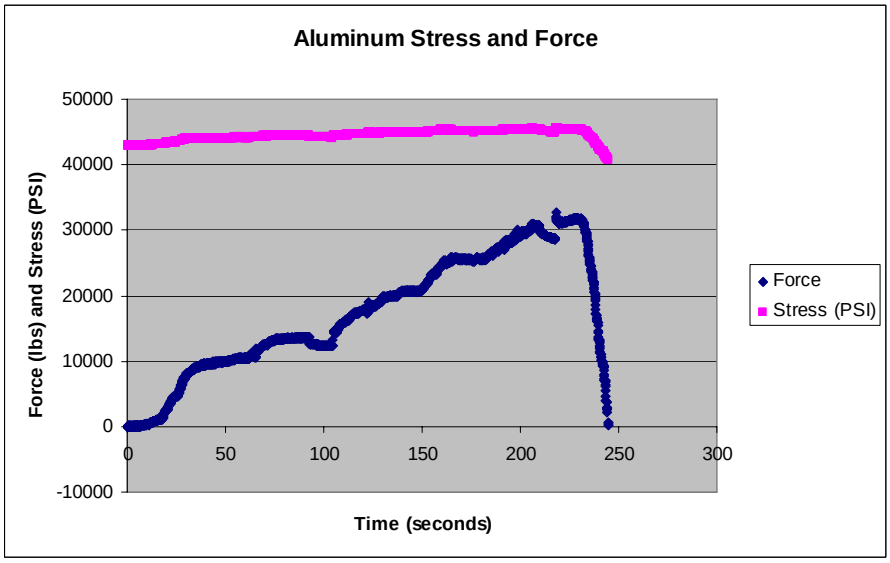

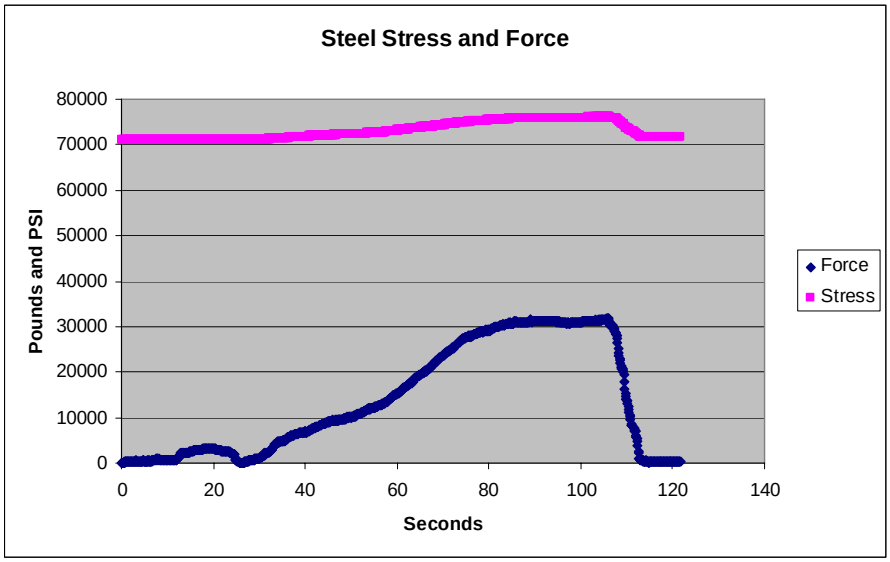


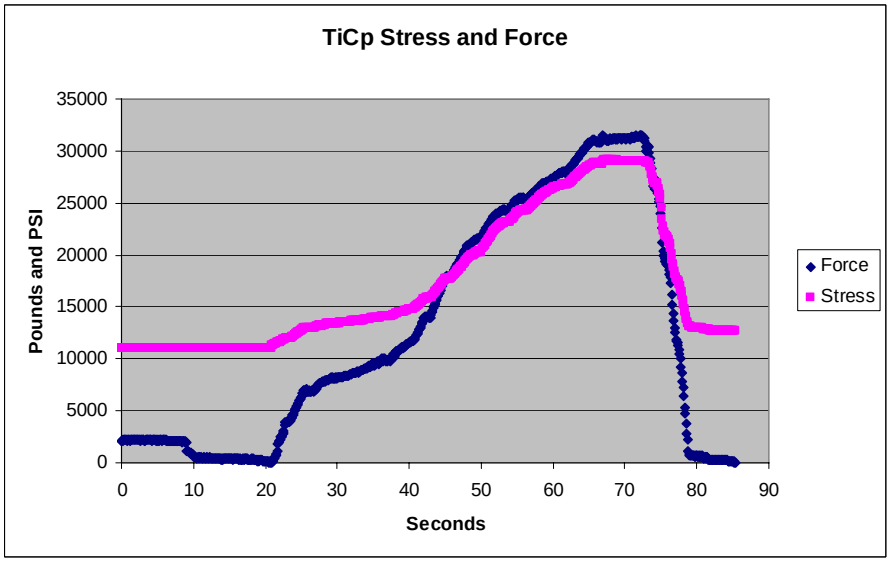


Note 1: The Ti blocks had a different geometry than that of the steel and aluminum blocks; shown in Figures 2 and 5. Dimensions for the Ti blocks are listed in print 3818364.
Note 2: The Ti-6-4 press data is not useable due to instrumentation issues.

Conclusion:

The aluminum and steel blocks exhibited a lower stress increase when the load was applied versus the Ti. This is desirable since this would lower the overall stress amplitude and make the piece more resistant to fatigue failure. However the overall geometry of the pieces and the fitment of the pin in the bore will influence this characteristic as well.

## XIV. – Conclusions

**Project Objective:** Titanium has been identified as one of the key materials with the required strength that can reduce the weight of automotive components and thereby reduce fuel consumption. Working with newly developed sources of titanium powder, Webster-Hoff will develop the processing technology to manufacture low cost vehicle components using the single press/single sinter techniques developed for iron based powder metallurgy today. Working with an automotive or truck manufacturer, Webster-Hoff will demonstrate the feasibility of manufacturing a press and sinter titanium component for a vehicle application. The project objective is two-fold, to develop the technology for manufacturing press and sinter titanium components, and to demonstrate the feasibility of producing a titanium component for a vehicle application.

This final report provides the details of our efforts to develop press and sinter process technology for Titanium Powder applications and demonstrate the capability of press and sinter for a vehicle component application. The original Statement of Project Objectives is included in the Appendix. This report speaks for itself regarding the accomplishment of the project objectives.

In addition, my general conclusions from the project are as follows:

1) With a properly executed process, starting with quality Titanium powder, Titanium components (both TiCP and Ti64) can be readily manufactured via the press and sinter process.
2) The press and sinter process for Titanium Components can achieve very high densities (up to 99%), and therefore yield properties very close to wrought Titanium
3) Based on the component and its mechanical property requirements, there are several different types of powders that can be utilized to optimize the final sintered component for the application.
4) If the new Titanium powder manufacturing processes are successful in reducing the cost of Titanium Powder, we will see Titanium components become common place in future vehicles.

## XV. Appendix

Webster-Hoff version of Pillow Block

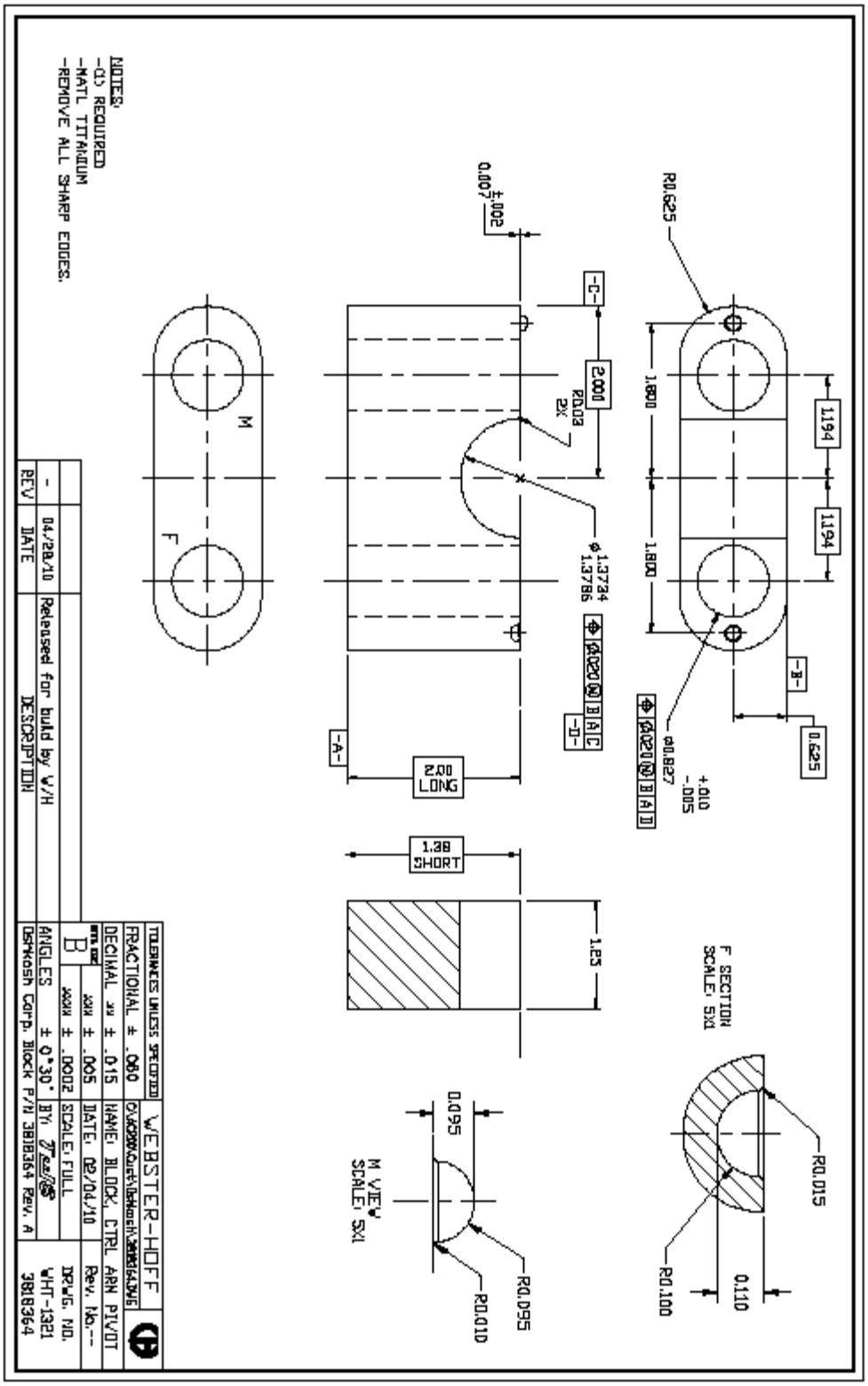

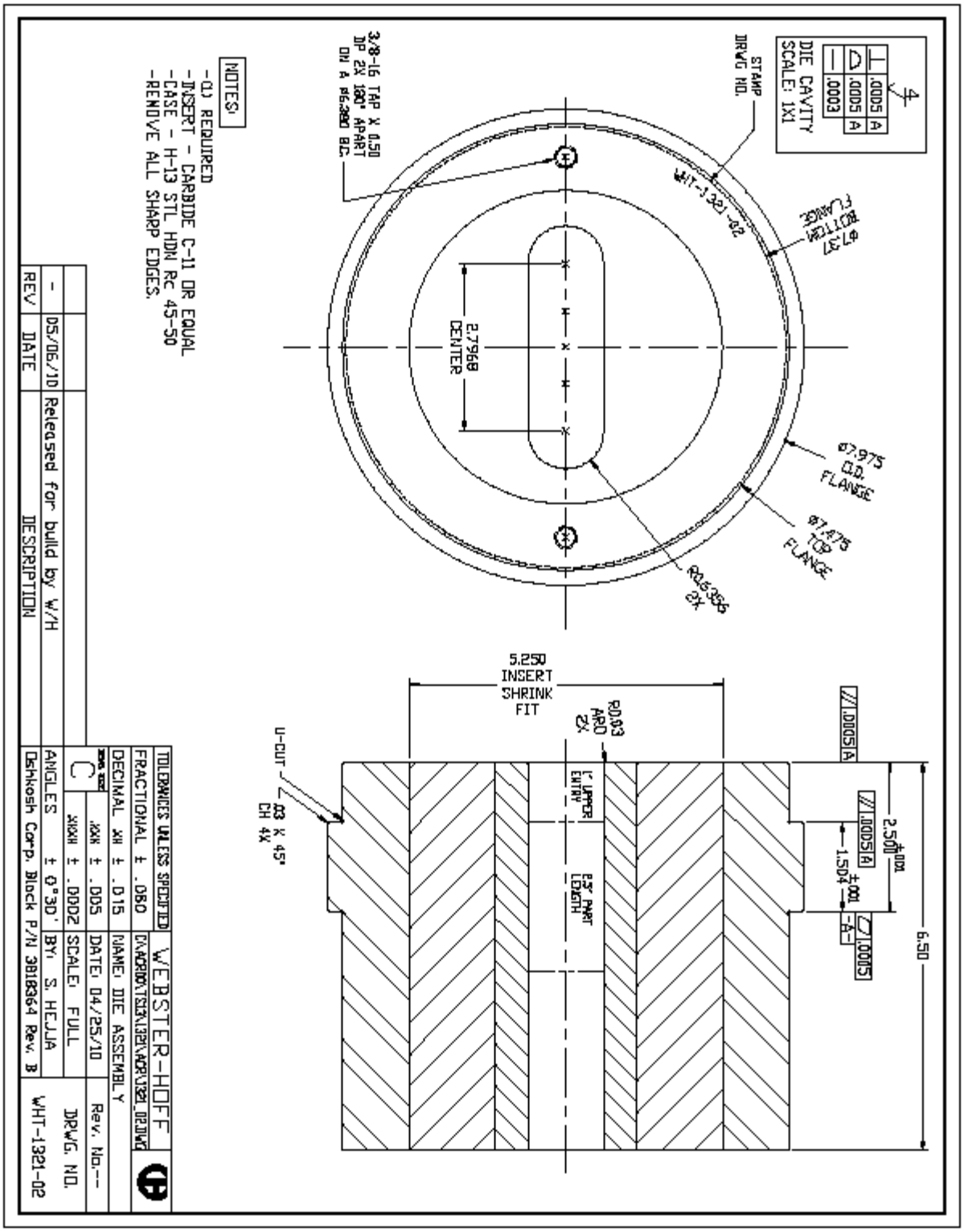
DIE CAVITY
SCALE: 1X1
STAMP DRWG NO.
WHT-1321-02
3/8-16 TAP X 0.50 DP 2X 180° APART ON Ø6.000 BC.
2.7968 CENTER
Ø7.975 O.D. FLANGE
Ø7.475 TOP FLANGE
R0.250 2X
5.250 INSERT SHRINK FIT
R0.03 ARO 2X
U-CUT
.03 X 45° CH 4X
2.500 ±.001
1.504 ±.001
6.50
.0005 A
.0005 A
.0005 A
NOTES:
-CL) REQUIRED
-INSERT - CARBIDE C-11 OR EQUAL
-CASE - H-13 STL HDN Rc 45-50
-REMOVE ALL SHARP EDGES.
REV
DATE
DESCRIPTION
-
05/06/10
Released for build by W/H
TOLERANCES UNLESS SPECIFIED
FRACTIONAL ± .060
DECIMAL XX ± .015
XXX ± .005
ANGLES ± 0°30'
XXXX ± .0002
WEBSTER-HOFF
DRAWING SIZE
NAME: DIE ASSEMBLY
DATE: 04/25/10
SCALE: FULL
BY: S. HEJJA
Oshkosh Corp. Block P/N 3816364 Rev. B
Rev. No.--
DRWG. NO.
WHT-1321-02

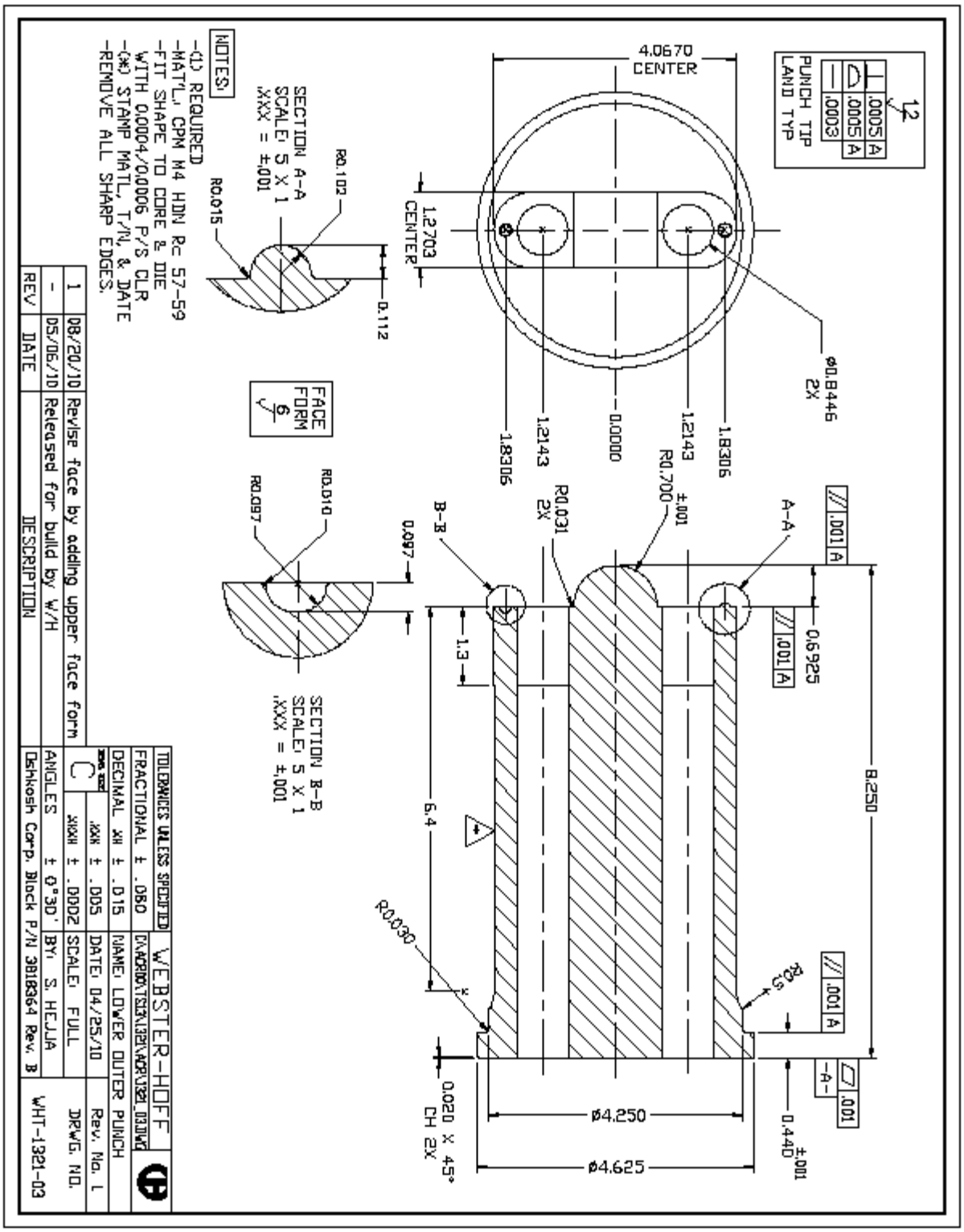
12
.0005 A
.0005 A
.0003
PUNCH TIP
LAND TYP
4.0670
CENTER
1.2703
CENTER
ø0.8446
2X
1.8306
1.2143
0.0000
1.2143
1.8306
R0.700 ±.001
R0.031
2X
.001 A
.001 A
A-A
B-B
0.6925
8.250
1.3
6.4
ø0.030
M
0.020 X 45°
CH 2X
ø4.250
ø4.625
.001 A
.001
-A-
0.440 ±.001
FACE
FORM
6
SECTION A-A
SCALE: 5 X 1
.XXX = ±.001
R0.102
R0.015
0.112
SECTION B-B
SCALE: 5 X 1
.XXX = ±.001
R0.097
R0.010
0.097
NOTES:
-(1) REQUIRED
-MATL: CPM M4 HDN Rc 57-59
-FIT SHAPE TO CORE & DIE
WITH 0.0004/0.0006 P/S CLR
-(*) STAMP MATL, T/N, & DATE
-REMOVE ALL SHARP EDGES.
1
08/20/10
Revise face by adding upper face form
-
05/06/10
Released for build by W/H
REV
DATE
DESCRIPTION
TOLERANCES UNLESS SPECIFIED
FRACTIONAL ± .060
DECIMAL .XX ± .015
.XXX ± .005
ANGLES ± 0°30'
.XXXX ± .0002
WEBSTER-HOFF
DRAWING TITLE: LOWER OUTER PUNCH
NAME: LOWER OUTER PUNCH
DATE: 04/25/10
SCALE: FULL
BY: S. HEJJA
Rev. No. 1
DRWG. NO.
Oshkosh Corp. Block P/N 3818364 Rev. B
WHT-1321-03

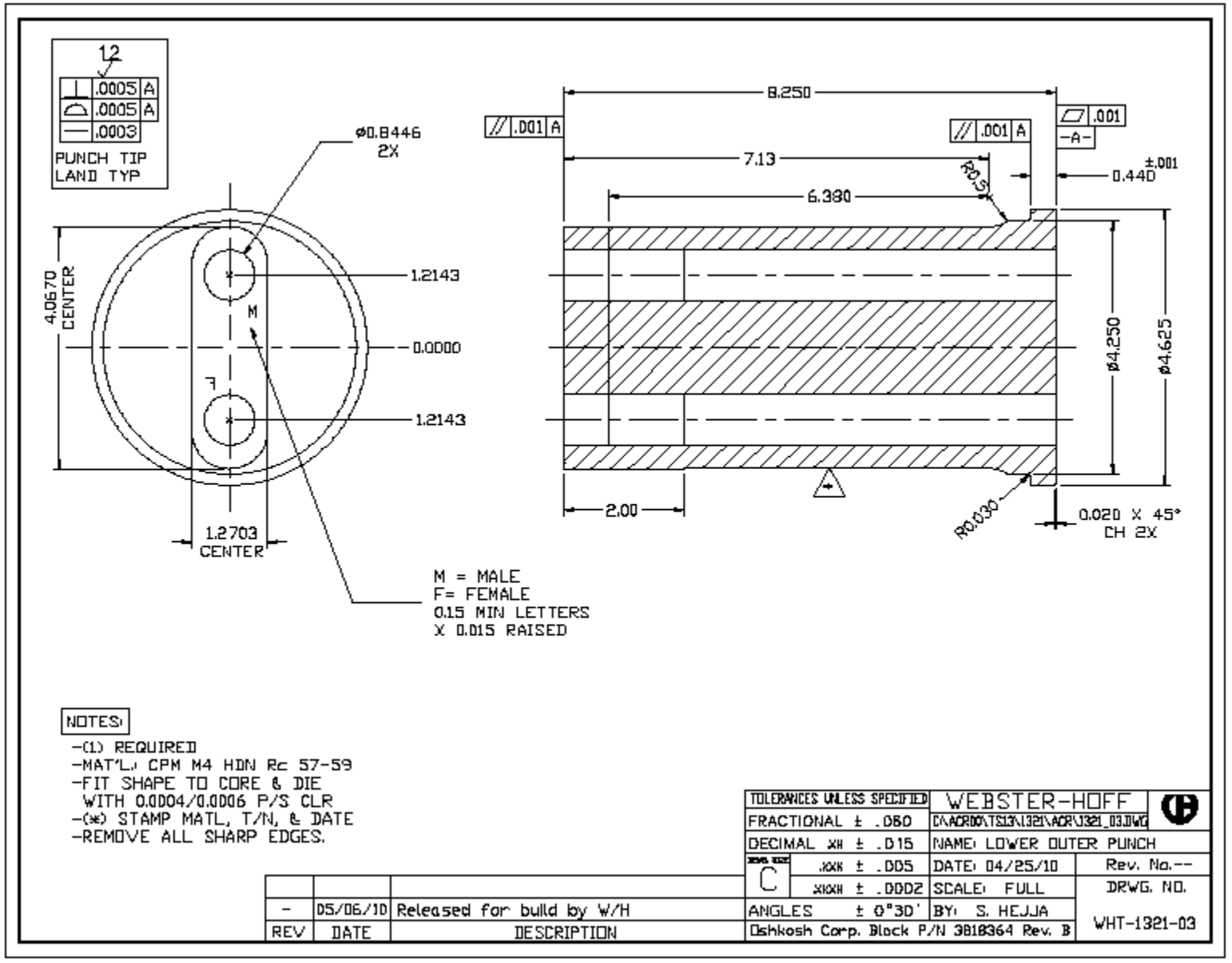
12
.0005 A
.0005 A
.0003
PUNCH TIP
LAND TYP
ø0.8446
2X
4.0670
CENTER
1.2143
0.0000
1.2143
1.2703
CENTER
M
F
M = MALE
F= FEMALE
0.15 MIN LETTERS
X 0.015 RAISED
8.250
.001 A
7.13
6.380
.001 A
.001
-A-
±.001
0.440
R0.50
ø4.250
ø4.625
2.00
R0.030
0.020 X 45°
CH 2X
NOTES:
-(1) REQUIRED
-MAT'L: CPM M4 HDN Rc 57-59
-FIT SHAPE TO CORE & DIE
WITH 0.0004/0.0006 P/S CLR
-(※) STAMP MATL, T/N, & DATE
-REMOVE ALL SHARP EDGES.
TOLERANCES UNLESS SPECIFIED
FRACTIONAL ± .060
DECIMAL XX ± .015
.XXX ± .005
.XXXX ± .0002
ANGLES ± 0°30'
C
WEBSTER-HOFF
C:\ACR00\TS13\1321\ACR\1321_03.DWG
NAME: LOWER OUTER PUNCH
DATE: 04/25/10
Rev. No.--
SCALE: FULL
DRWG. NO.
BY: S. HEJJA
WHT-1321-03
Oshkosh Corp. Block P/N 3818364 Rev. B
REV
DATE
DESCRIPTION
-
05/06/10
Released for build by W/H

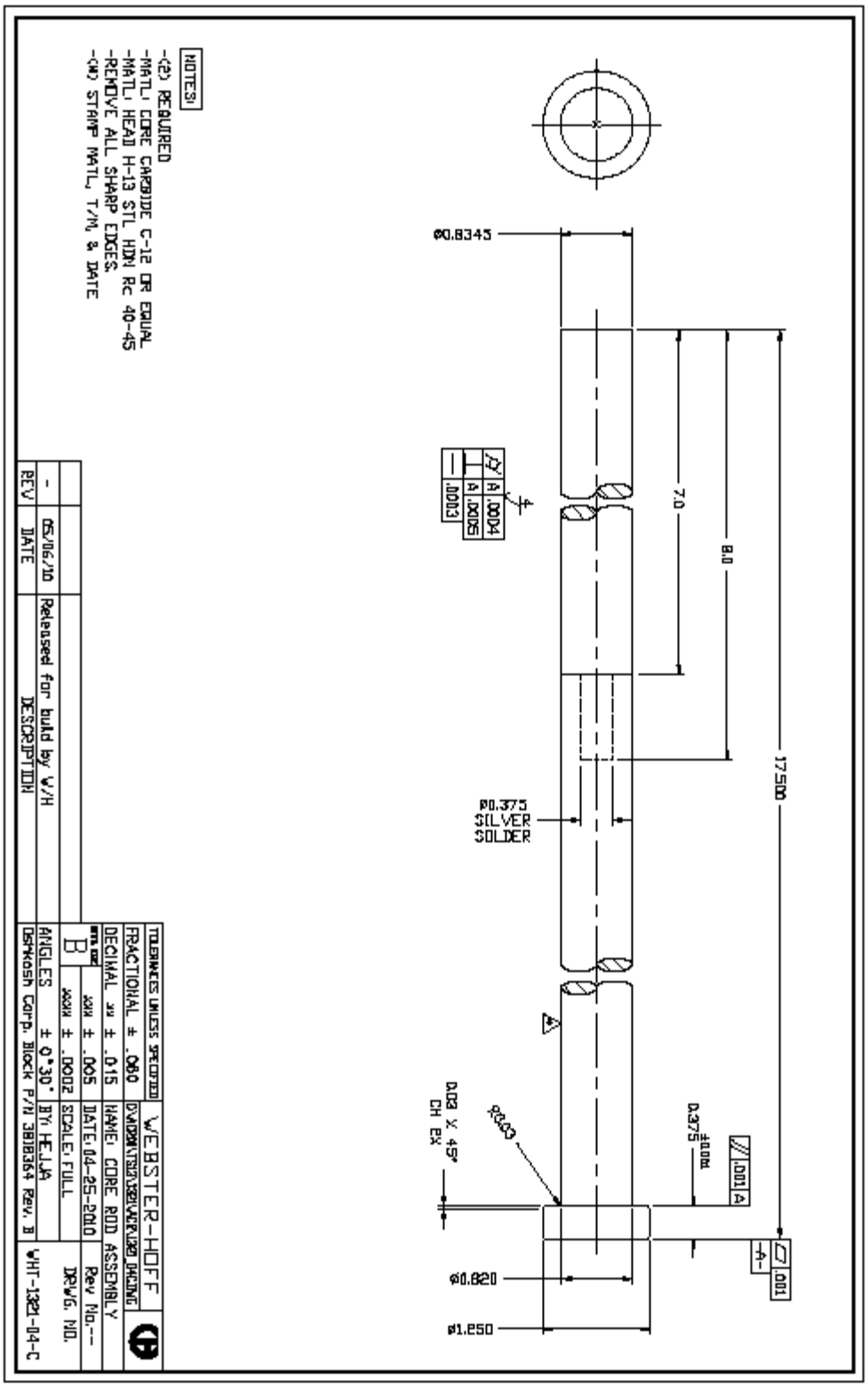
NOTES:
-(2) REQUIRED
-MATL: CORE CARBIDE C-12 OR EQUAL
-MATL: HEAD H-13 STL HDN Rc 40-45
-REMOVE ALL SHARP EDGES
-(M) STAMP MATL, T/M, & DATE
Ø0.8345
7.0
8.0
17.500
Ø0.375 SILVER SOLDER
.003 X 45° CH EX
Ø0.820
Ø1.250
0.375 ±.004
.001 A
.001
A .0004
A .0005
.0003
WEBSTER-HOFF
TOLERANCES UNLESS SPECIFIED
FRACTIONAL ± .060
DECIMAL .XX ± .015
.XXX ± .005
.XXXX ± .0002
ANGLES ± 0°30'
NAME: CORE ROD ASSEMBLY
DATE: 04-25-2010
SCALE: FULL
Rev No.--
DRWG. NO.
BY: HEJA
Oshkosh Corp. Block P/N 3818364 Rev. B
WHT-1321-04-C
REV
DATE
DESCRIPTION
-
05/06/10
Released for build by W/H

Statement of Project Objectives
Webster-Hoff Corporation

Energy Efficient Press and Sinter of Titanium Powder for Low-Cost Components in Vehicle Applications

A. Project Objectives

Titanium has been identified as one of the key materials with the required strength that can reduce the weight of automotive components and thereby reduce fuel consumption. Working with newly developed sources of Titanium powder, Webster-Hoff will develop the processing technology to manufacture low cost vehicle components using the single press/single sinter techniques used for Iron Based Powder Metallurgy today. Working with an automotive or truck manufacturer Webster-Hoff will demonstrate the feasibility of manufacturing a press and sinter Titanium component for a vehicle application.

The project objectives are therefore two-fold, to develop the technology for manufacturing press and sinter Titanium components, and to demonstrate the feasibility of producing a Titanium component for a vehicle application.

B. Project Scope

This project falls under the Aegis of the DOE, NETL, for the development of technologies for energy efficient vehicle systems. The scope of this project is to develop the technology for low weight, high strength components to increase the energy efficiency of vehicle systems.

C. Task to be Performed

a. Technology Issues to be resolved

i. Evaluation of Sources of Titanium Powder – To characterize commercially available sources of Titanium powder for Powder Metal compaction applications. Various processing techniques such as attrition and sieving will be developed as necessary to achieve the powder characteristics necessary for efficient compaction of these Titanium Powders.

ii. Development of Powder Lubrication Systems – All powder compaction techniques require a lubricant in the powder to achieve even compaction of the powder, and ejection of the powder compact from the tool. Current lubrication systems available for steel powders have not worked effectively with Titanium powders in our initial tests. A new lubrication system will have to be developed, to provide proper lubrication of the powders and proper lubricant removal prior to sintering.

iii. Compaction Tests – Compaction tests will have to be completed to determine the capability and characteristics of the green compacts formed from Titanium powders. In this case we will test the compaction process on our standard production presses and evaluate the properties of the green compacts.

iv. Lubrication Removal – Prior to sintering, the lubricant must be removed from the green compact. We will be using a variety of de-lubing techniques to determine the best technique for removal of the lubricant without increasing oxygen or carbon in the Titanium matrix.

v. Sintering Process – Solid State sintering is the process that forms the metallurgical bonds between the powder particles in the green compact. For Titanium green compacts, this must be done in a vacuum. We will be evaluating both convection and microwave thermal techniques to achieve proper metallurgical bonding.

vi. Mechanical Properties – After completing our development of the press and sinter process, we will use special tooling to press tensile test bars, process the bars, and test the bars to generate the tensile strength, elongation properties, and hardness (apparent and micro) to provide our

potential customers the material properties they will need to evaluate the material for potential applications.

vii. Identify Production Applications – using the mechanical properties and the cost structure for producing parts work with Vehicle Manufactures to identify potential applications for Titanium P/M.

viii. Build Prototype tooling for specific application – We will build a prototype tool for at least one application and produce prototype parts for testing and evaluation by the Vehicle manufacturer.

b. Order of Tasks Phase I

i. Task 1.0 – Preparation for testing Powder, Lube and Compaction

1. Task 1.1 Complete Titanium Safety Training
    a. Hold a safety training class for the project team regarding safe handling of Titanium powder (high pyro-phoric), and emergency reactions to a fire.
2. Task 1.2 Build Dog Bone Compaction tool for Tensile Testing
    a. Design and build a dog-bone compaction tool for calibrated tensile testing of compacted samples.
3. Task 1.3 Acquire Titanium powders and V-Al master mix
    a. Based on supplier specifications for apparent density, morphology, purity (oxygen content), acquire Titanium CP, pre-alloyed Titanium 6-4, and V-AL master alloy powders for testing.
4. Task 1.4 Acquire sample lubrications for testing
    a. Based on supplier specifications, and previous work, acquire the appropriate powder lubrication system for use with the Titanium powders. The lubrication system must be designed to allow proper ejection of the compact from the tooling without leaving carbon and oxygen in the Titanium matrix after the de-lubing process.
5. Task 1.5 Test powder for Oxygen/Carbon/Pollutant levels
    a. A. Send the pure Titanium powders to a chemistry lab for verification of purity levels (oxygen and carbon should be kept to as low a level as possible).
6. Task 1.6 Adjust the powder to the appropriate apparent density for compaction
    a. Test the powders for apparent density – the target is an apparent density of 1.3 g/cc to 1.9 g/cc.
    b. If necessary, send powder out for Jet Milling in an Argon atmosphere. (If Jet Milled, then retest Oxygen and Carbon content of powder.
7. Task 1.7 Blend powder with sample lubrications.
    a. Test each sample for Hall flow rate and apparent density.

ii. Task 2.0 – Compaction testing

1. Task 2.1 Press samples of selected powders with blended lubrication to determine compressibility of powders, ejection forces in tooling, and green densities achieved.
    a. Determine the compressibility (ratio of final density to TSI), ejection cracks and final density
2. Task 2.2 Evaluate the green dog bones for green density, green strength.
    a. Check green density and green strength of the compacted tensile bars.

iii. Task 3.0 – De-lubrication testing

1. Task 3.1 De-lube the samples using a variety of temperatures and atmospheres.
    a. Process the parts through the de-lubing furnace at a variety of temperatures and atmospheres.
2. Task 3.2 Check the de-lubed samples to determine the extent of carbon removal and oxygen pickup in the de-lubing process.
    a. The critical action required in the de-lubing process is to remove the lubrication material with a low vapor point from the Titanium without leaving any carbon behind, or introducing oxygen into the matrix.

b. The parts will be sent to a lab for evaluation of carbon and oxygen content.

c. Order of Tasks Phase 2.
    i. Task 4.0 – Sintering Testing
        1. Task 4.1 – Sinter samples of each type in a standard vacuum furnace, at a range of temperatures and times.
            a. The parts which have been successfully de-lubed, will be sintered in a vacuum furnace at Illinois Institute of Technology.
        2. Task 4.2 – Sinter samples of each type in a Microwave vacuum furnace at a range of temperatures and times.
            a. Another group of parts that have been successfully de-lubed will be sintered in a vacuum microwave furnace at Spheric Technologies in Phoenix Arizona.
        3. Task 4.3 – Evaluate the sintered samples for final density, mechanical properties, chemistry (oxygen/carbon pickup), and metallographic data. This work would be done at Illinois Institute of Technology.
            a. Check final density of sintered samples.
            b. Check mechanical properties of the samples (tensile strength, elongation, and 2% yield strength).
            c. Check the samples for metallurgical bonding, grain boundaries, and metallurgical properties.
            d. Check the samples for chemistry – including % impurities (oxygen, carbon, etc.)

d. Order of Tasks Phase 3.
    i. Task 5.0 – Distribute the properties to potential vehicle manufactures for target application testing
        1. Prepare a specification for the properties achieved with the process.
        2. Compare the properties with wrought titanium.
    ii. Task 6.0 – Determine a compatible application for prototype tooling and testing
        1. Based on the process capabilities (green strength, density, tool abrasion, etc.) determine the best part applications for the process.
    iii. Task 7.0 – Build prototype tooling for application testing
        1. Based on negotiations with vehicle manufactures, determine a prototype part suitable for the desired application.
        2. Design a build a tool for the application

e. Order of Tasks Phase 4.
    i. Task 8.0 – Process the prototype parts based on the agreed process.
        1. Using the tool and process developed above, manufacture prototype parts for the application.
    ii. Task 9.0 – Submit samples to vehicle manufacturer for application testing
        1. The vehicle manufacturer selected will have the ability to full test the parts in the application.
    iii. Task X.0 – Prepare and submit final report.
        1. Submit the final report on process, and applications for the Titanium press and sinter process.

## XVI. Glossary

Powder Mnemonic Definitions – **AAAA-BBBB-C**

Where **AAAA** is the powder alloy

1) **TiCP** – commercially pure Titanium
2) **Ti64** – 90% Titanium. 6% aluminum, 4% Vanadium
3) **Ma64** – Master alloy 60% Aluminum, 405 Vanadium

Where BBBB is the manufacturing process

1) **HdHW** – hydride crushed de-hydride from wrought
2) **HdHS** – hydride crushed de-hydride from sponge fines
3) **HdHP** – hydride crushed de-hydride from scrap wrought
4) **HydW** – hydride crushed, but not de-hydrided
5) **ArmC**- Armstrong process from chlorides
6) **SoRC** – Batch Sodium Reduction from chlorides
7) **AtmM** – atomized from melt

Where C is the manufacturer

1) **R** – Reading Alloys
2) **D** – DuPont
3) **G** – Global Titanium
4) **T** – TIPRO
5) **I** – International Titanium Corp.

For example **TiCP-HdHW-R** is commercially pure titanium powder manufactured from wrought by Reading Alloys.

Tensile Properties

1) Ultimate Tensile Strength - Ultimate tensile strength, expressed in KSI (MPa), is the ability of a test specimen to resist fracture when a pulling force is applied in a direction parallel to its longitudinal axis. It is equal to the maximum load divided by the original cross-sectional area.
2) Yield Strength - Yield strength, expressed in KSI (MPa), is the load at which a material exhibits a 0.2% offset from proportionality on a stress-strain curve in tension divided by the original cross-sectional area. (See *MPIF Standard 10* for additional details.)
3) Elongation - Elongation (plastic), expressed as a percentage of the original gauge length (usually 1.0 in.) (25.4 mm), is based on measuring the increase in gauge length after the fracture, providing the fracture takes place within the gauge length. Elongation can also be measured with a breakaway extensometer on the tensile specimen. The recorded stress strain curve displays total elongation (elastic and plastic). The elastic strain at the 0.2% yield strength must be subtracted from the total elongation to give the plastic elongation.

Elastic Constants

1) Young's Modulus (E) - Young's modulus, expressed in $10^6$psi (GPa), is the ratio of normal stress to corresponding strain for tensile or compressive stresses below the proportional limit of the material. We have used a strain gage to obtain the accurate data from three point bend test. And we use clip gage to measure the accurate deflection data.


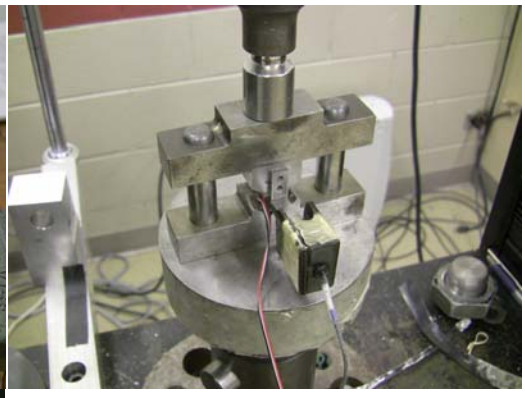
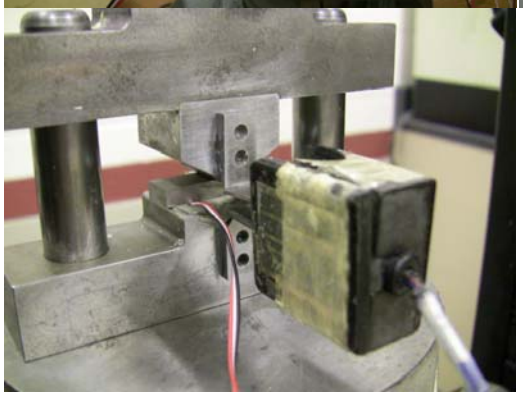

2) Poisson's Ratio - Poisson's ratio is the absolute value of the ratio of transverse strain to the corresponding axial strain resulting from uniformly distributed axial stress below the proportional limit of the material

Transverse Rupture Strength

1) Transverse Rupture Strength - Transverse rupture strength, expressed in KSI (MPa), is the stress, calculated from the bending strength formula, required to break a specimen of a given dimension. The specimen is supported near the ends with a load applied midway between the fixed centerline of the supports. From the value of the break load, the transverse rupture strength can be calculated as follows:
   $S = 3*P*L/(2*T^2*W*1000)$
   Where:
   a. S = transverse rupture strength, in KSI (MPa),
   b. P = break load in pounds (N),
   c. L = distance between the supporting members of the test fixture, in inches (mm) (usually 1.000 inch)(25.4 mm),
   d. T = thickness of the piece in inches (mm), and
   e. W = width of the piece, in inches (mm).

   This strength formula is strictly valid only for non-ductile materials; nevertheless, it is widely used for materials that bend before fracture, and is useful for establishing comparative strengths. Data for such materials are included as *typical* properties in this Standard.
   (See *MPIF Standard 41* for additional details.)

Hardness

1) Apparent Hardness - The hardness value of a PM part when using a conventional indentation hardness tester is referred to as "apparent hardness" because it represents a combination of matrix hardness plus the effect of porosity. Apparent hardness measures the resistance to indentation or brinelling. Following is a recommended procedure for measuring the apparent hardness of a PM material:
   a. A. Specify a region for evaluation.
   b. B. Remove any burrs that might affect the indentation hardness reading both on indentor and support surfaces.
   c. C. Obtain a minimum of five hardness readings per part, eliminating gross anomalies.
   d. D. Average the readings.

e. E. Report the average results to the nearest whole number.

Because of possible density variations in a finished PM part, the location of critical apparent hardness measurements should be specified on the engineering drawing of the purchased part. The manufacturer and purchaser should agree on the hardness, the measuring procedure, and the hardness scale, e.g., HRB or HRC, for each part tested. Also, because of the effect of possible void closure as a result of polishing or machining, on hardness readings, the surface condition should be specified and agreed upon by the manufacturer and purchaser.
(See *MPIF Standard 43* for additional details.)

2) Micro Hardness – Micro-indentation hardness is determined by utilizing Knoop (HK) or Vickers (HV) indentors with a micro-indentation hardness tester. It measures the true hardness of the structure by eliminating the effect of porosity, and thus is a measure of resistance to abrasive and adhesive wear. Micro-indentation hardness measurements are convertible to equivalent Rockwell hardness values for comparison with other materials. Care should be taken in converting Knoop to HRC because the conversion chart listed in ASTM E 140 is based on a 500 gf load, while the recommended load for a PM material is 100 gf. A description of the microstructure must be reported. The specimen shall be polished to reveal the porosity and lightly etched to view the phases in the microstructure and to determine where to place the hardness indentation. If the indentor strikes an undisclosed pore, the diamond mark will exhibit curved edges and the reading must be discarded. Since the data tend to be scattered compared with pore-free material, it is recommended that a minimum of 5 indentations be made, anomalous readings discarded, and an average taken of the remainder.
(See *MPIF Standard 51* for additional details.)

Compressive Strength

1) Compressive Yield Strength - Compressive yield strength, expressed in KSI (MPa), is the stress at which a material exhibits a specified permanent set. The 0.1% permanent offset was measured utilizing a clip-on extensometer on a 0.375 inch (9.53 mm) diameter by 1.05 inch (26.7 mm) long specimen. For certain heat treated steels listed in the data tables, the hardenability of the alloy is not sufficient to completely through-harden the 0.375 inch (9.53 mm) diameter test specimen. Due to variation in hardenability among the heat treated steels listed in the data tables, the compressive yield strength data are appropriate only for 0.375 inch (9.53 mm) sections. Typically, smaller cross sections have higher compressive yield strengths and larger sections somewhat lower strengths due to the hardenability response. Since the cross section of the tensile yield test specimen is smaller than the compressive yield specimen a direct correspondence between tensile and compressive yield strength data is not possible.

Shear Strength

1) Shear Strength - The yield strength in shear for a limited number of PM steel alloys (both sintered and heat treated) was determined using a hollow torsional specimen. The results found the shear yield equal to 55% of the tensile yield for these materials, confirming the established ratio for wrought steels.

Impact Energy

1) Impact Energy - Impact energy, measured in foot-pounds (J), is a measurement of the energy absorbed in fracturing a specimen with a single blow. The unnotched Charpy specimen is most commonly used in powder metallurgy.
(See *MPIF Standard 40* for additional details.)

Fatigue Properties

1) Fatigue Strength - Fatigue strength, expressed in units of KSI (MPa), is the maximum alternating stress that can be sustained for a specific number of cycles without failure, the stress being reversed with each cycle unless otherwise stated. The number of cycles survived should be stated with each strength listed.
2) Fatigue Limit - The fatigue limit is the stress sustainable for an indefinite number of cycles, and no cycle number is given. For PM ferrous materials, like wrought ferrous materials, fatigue strengths of $10^7$ cycles duration using smooth, unnotched specimens on R. R. Moore testing machines are considered to be sustainable indefinitely and are therefore stated as fatigue limits (also termed endurance limits). By contrast, nonferrous PM materials do not have $10^7$cycle maximum fatigue strengths sustainable for indefinite times and therefore these stress limits remain as simply the $10^7$cycle fatigue strengths. The fatigue limits in this standard were generated through statistical analysis of rotating bending fatigue strength data. Due to the limited number of data points available for the analysis, these fatigue limits were determined as the 90% survival stress, i.e. the fatigue stress at which 90% of the test specimens survived $10^7$ cycles.

## XVII. Bibliography

References:

[1] Dennis D. Harwig, Mai Ittiwattana, and Harvey Castner, “Advances in oxygen equivalent equations for predicting the properties of titanium welds”, Welding journal, 2001.

[2] Standard Test Method for Metal Powders and Powder Metallurgy Products, published at 2010, by MPIF, Princeton, New Jersey.

[3] Randall M. German: *Powder metallurgy and particle materials processing*, Metal powder industries federation, Princeton, New Jersey, 2005.

[4] Gerd Lutjering, and James C. Williams, *Titanium*, Springer-Verlag Berlin Heidelberg 2003.

[5] Randall M. German, *Liquid phase sintering*, Plenum Press, New York, 1985.

[6] Titanium CP Ti (Grade 3), Annealed, MatWeb material property data, Automation Creation, Inc.

[7] Structural alloy handbook, wrought titanium selector chart, June, 1982.

[8] Yukinori Yamamoto, William H. Peter and Adrian S. Sabau, “Low cost titanium near-net –shape manufacturing using Armstrong process CP Ti and Ti6Al4V powders”, PowderMet 2010 MPIF conference, 2010, p.03-24.